TRAIL: A novel atheroprotective mechanism in the vasculature

Pradeep Manuneedhi Cholan

Faculty of Medicine and Health

The University of Sydney

2019

A thesis submitted to fulfil requirements for the degree of Doctor of Philosophy

Statement of Original Authorship

The work contained in this thesis has not been previously submitted to meet requirements for an award at this or any other higher education institution. To the best of my knowledge and belief, the thesis contains no material previously published or written by another person except where due reference is made.

Signature: 

Date: _10/1/2019_

Acknowledgement

I am really thankful to each and everyone who have supported me for last few years and helped me achieve the crazy dream of undertaking a PhD. Firstly, I would like to thank my supervisors Dr Mary Kavurma and Dr Sian Cartland for guiding and mentoring me throughout my PhD. It would have been impossible without their help, sacrifice and support. I have learnt a great deal from them both professionally and personally. From the bottom of my heart I would once again like to thank them for putting up with me.

I would like to thank all the past and present members of Vascular Complications group especially Scott Genner, Dhanya Ravindran, Manisha Patil and Lauren Boccanfuso for creating a safe, helpful and friendly environment for me to work in.

I will be forever grateful for Pat Pisansarakit, for helping me with tissue culture and imparting his vast knowledge. My animal experiments wouldn't have been a success without the help of Biological Facilities, both Jessica Toolan and Katja Humphry for taking good care of all my animals. I would also like to thank the Heart Research Institute, for providing me the opportunity and the scholarship to undertake my PhD.

I would like to thank my collaborators, A/Prof Shane Thomas and Dr Lei Dang from University of New South Wales, for providing information, support and samples in regard to Chapter 3 and Chapter 4. I would also like to acknowledge the contributions of clinical samples from A/Prof Sanjay Patel of Cell Therapeutic group at the Heart Research Institute.

I have been fortunate to be surrounded by great friends without whom this PhD would have left me mentally scarred. Dhanya Ravindran and Leila Reyes, thank you both for being my best friends, confidant and metal health counsellors. Thank you for sharing your PhD journey with me. I would also like to thank my friends Scott Genner, Katja Humphry, Anisyah Ridiandries

and Brad Pearson for making me forget the hardships of PhD. My relationship with each and every one of you has made me a better person and for that I am forever grateful.

It was scary moving to Sydney all alone to start my PhD. But along the way I found friends who have now become my family. I would like to thank Sheryl, Venkat, Shandilya, Kiran and Thena for being there for me throughout the highs and lows, smiles and tears. Thank you once again for being the support I needed. I would also like to thank my landlord/house mates, Archi and Sudhir for being the best. They made sure I wasn't home sick and took care of me when I was actually sick. I would like to thank them both from the bottom of my heart.

Finally, I would like to thank the two most important people who have always showered me with unconditional love and support along each and every step of the way. Amma and Appa thank you so much for everything. I truly hope I make you proud.

Table of Contents

Acknowledgement 3

Table of Contents 5

Publications arising from this thesis 10

Chapter 1: Introduction 17

1.1 Atherosclerosis 17

1.2 Endothelial cells 20
1.2.1 Anti-inflammatory/ pro-inflammatory state of endothelium 21
1.2.2 Anti-atherogenic endothelium 25
1.2.3 Anti-thrombotic endothelium 27

1.3 Vascular smooth muscle cells 27
1.3.1 Phenotypic switching of VSMCs 28
1.3.2 Extracellular matrix 30

1.4 Oxidative stress 31
1.4.1 Mitochondria and oxidative stress 33
1.4.2 NADPH oxidase and oxidative stress 35
1.4.3 Nitric oxide and oxidative stress 39
1.4.4 Oxidative stress and atherosclerosis 41

1.5 TNF-related apoptosis inducing ligand 43
1.5.1 TRAIL receptor interaction 43
1.5.2 Clinical relevance of TRAIL 46
1.5.3 TRAIL role in *in vivo* studies 47
1.5.4 TRAIL and *in-vitro* studies 51

1.6 Research Hypothesis 53

1.7 Resesarch Aims 53

Chapter 2: Methods 55

2.1 Materials 55
2.1.1 Buffers 55

2.2 Human studies 57
2.2.1 Blood collection and ethics 57
2.2.2 Human TRAIL ELISA 57
2.2.3 8-isoprostane purification 58
2.2.4 8-isoprostane ELISA 58

2.3 Cell Culture 58
2.3.1 Propagation 58
2.3.2 Cell culture media 59
2.3.3 RNA extraction of cells 59
2.3.4 cDNA synthesis from total RNA 60
2.3.5 Quantitative real time PCR 61
2.3.6 Primer sequences 62
2.3.7 BCA protein assay 62

2.3.8 Western blotting 63
2.3.9 Monocyte adhesion assay 64
2.3.10 DHE staining of cells 64
2.3.11 Mitosox staining of cells 66
2.4 Animal studies 67
2.4.1 Animal housing 67
2.4.2 Genotypes of mice 67
2.4.3 Animal ethics 68
2.4.4 Cell-specific TRAIL gene deletion mice 69
2.4.5 High fat feeding study 72
2.4.6 Blood pressure measurement 72
2.4.7 Glucose and insulin tolerance 73
2.4.8 RNA extraction of mouse aorta 74
2.4.9 Primer sequence 74
2.4.10 Myography 75
2.4.11 Vessel Permeability 76
2.4.12 Cholesterol assay 77
2.4.13 Insulin assay 77
2.4.14 Nitrate/nitrite assay 77
2.4.15 DHE staining of aortas 78
2.4.16 Histology 78
2.5 Statistical analysis 83
Chapter 3: TRAIL's role against oxidative stress in clinical and pre-clinical models 85
3.1 Introduction 85
3.2 brief methods 86
3.2.1 Human TRAIL and 8-iso prostaglandin F2α ELISA 86
3.2.2 Myography 86
3.2.3 DHE aortic staining 86
3.2.4 4-Hydroxyneal ELISA 86
3.2.5 Vessel permeability 87
3.2.6 Mouse aorta RNA extraction 87
3.2.7 Western blotting 87
3.3 Results 88
3.3.1 CAD patients have reduced circulating TRAIL levels that negatively correlate with 8-iso prostaglandin F2α 88
3.3.2 TRAIL deletion in mice promotes EC dysfunction 90
3.3.3 TRAIL deletion in mice promoted vascular ROS generation 92
3.3.4 TRAIL deletion increases vascular permeability and reduces VE-cadherin expression in mice 93
3.4 Discussion 95
Chapter 4: Protective role of TRAIL against AngII-induced oxidative stress 98
4.1 Introduction 98
4.2 Breif methods 99
4.2.1 DHE and MitoSOX cell staining 99
4.2.2 Drug treatments 99
4.2.3 siRNA treatment 100
4.2.4 Hydrogen peroxide assay 100
4.2.5 VE-cadherin localisation 100

4.3 Results 101
4.3.1 AngII stimulates ROS production in ECs *in-vitro* 101
4.3.2 AngII- induced ROS production involves NOX-4 104
4.3.3 AngII-induced oxidative stress is inhibited by TRAIL 105
4.3.4 TRAIL inhibits AngII-induced monocyte adhesion and alters the expression of VCAM-1 *in-vitro* 107
4.3.5 TRAIL inhibits AngII-induced VE-cadherin disruption *in-vitro* 109

4.4 Discussion 111

Chapter 5: Characterisation of EC-specific TRAIL knockout mice 114

5.1 Introduction 114

5.2 Brief methods 115
5.2.1 Animals 115
5.2.2 Mouse aortic RNA extraction 115
5.2.3 Plasma biochemistry 115
5.2.4 Glucose and insulin tolerance test 115
5.2.5 Blood pressure 116

5.3 Results 117
5.3.1 Baseline characterisation of $Trail^{EC-/-}$ mice showed reducing trend in VCAM-1 expression 117
5.3.2 Baseline characterisation of $Trail^{EC-/-}$ mice showed reduced IL-18 and MCP-1 mRNA expression 117
5.3.3 Baseline biochemical plasma analysis showed no significant difference in $Trail^{EC-/-}$ mice 120
5.3.4 Baseline characterisation of $Trail^{EC-/-}$ mice showed no significant difference in the physical structure of the vasculature 121
5.3.5 12-week HFD mice showed no significant difference in body and organ weights between $Trail^{EC+/+}$ and $Trail^{EC-/-}$ 123
5.3.6 12-week HFD mice showed no significant difference in glucose and insulin tolerance test between $Trail^{EC+/+}$ and $Trail^{EC-/-}$ 125
5.3.7 Systolic and diastolic pressure was reduced in $Trail^{EC-/-}$ mice on a 12-week HFD 126
5.3.8 Increase in nitric oxide synthase mRNA expression in aortae of 12-week HFD $Trail^{EC-/-}$ mice 128
5.3.9 No significant difference in vessel structure was observed in 12-week HFD $Trail^{EC-/-}$ mice 129
5.3.10 Plasma cholesterol levels are significantly increased in $Trail^{EC-/-}$ mice following 12-week HFD. 131
5.3.11 Changes in cell adhesion and inflammatory genes in aortic mRNA expression in $Trail^{EC-/-}$ mice following 12-week HFD 133

5.4 Discussion 135

Chapter 6: VSMC-specific TRAIL knockout mice characterisation 140

6.1 Introduction 140

6.2 Brief methods 141
6.2.1 Animals 141
6.2.2 Mouse aortic RNA extraction 141
6.2.3 Plasma biochemistry 141
6.2.4 Glucose and insulin tolerance test 141
6.2.5 Blood pressure 142

6.3 Results 143

6.3.1 Baseline characterisation *Trail*$^{VSMC-/-}$ showed changes in contractile and synthetic gene mRNA expression ... 143
6.3.2 Baseline characterisation of *Trail*$^{VSMC-/-}$ mice showed reduced VCAM-1 and IL-1β mRNA expression ... 145
6.3.3 TRAIL deletion in VSMC has no effect on plasma chemistries at baseline ... 147
6.3.4 Baseline characterisation of *Trail*$^{VSMC-/-}$ mice showed no significant difference in the physical structure of the vasculature ... 148
6.3.5 Liver weights were significantly increased in *Trail*$^{VSMC-/-}$ mice after 12 w HFD150
6.3.6 12-week HFD mice showed no significant difference in body weight, glucose and insulin tolerance test between *Trail*$^{VSMC+/+}$ and *Trail*$^{VSMC-/-}$ ... 152
6.3.7 No changes in blood pressure in *Trail*$^{VSMC-/-}$ mice and its control in a 12-week HFD model ... 154
6.3.8 No changes in plasma biochemistry of VSMC-specific TRAIL knockout mice following 12-week HFD ... 156
6.3.9 No significant difference in vessel structure was observed in 12-week HFD *Trail*$^{VSMC-/-}$ mice ... 157
6.3.10 α-tropomyosin mRNA expression was increased in *Trail*$^{VSMC-/-}$ mice in a 12-week HFD model ... 159
6.3.11 VE-cadherin mRNA expression was increased in *Trail*$^{VSMC-/-}$ mice in a 12-week HFD model ... 161

6.4 Discussion ... 163

Chapter 7: Discussion ... 167

7.1 Discussion ... 167

7.2 Future Directions ... 173

Bibliography ... 177

Authorship Attribution statement

Chapter 3 and Chapter 4 have been published in the journal "**Free Radical Biology and Medicine**", under the title **"TRAIL inhibits Angiotensin-II-induced oxidative stress and inflammation in vascular endothelial cells."**

In addition to the statements above, in cases where I am not the corresponding author of a published item, permission to include the published material has been granted by the corresponding author.

Pradeep Manuneedhi Cholan, 1/02/2019.

As supervisor for the candidature upon which this thesis is based, I can confirm that the authorship attribution statements above are correct.

Mary Kavurma, 1/02/2019.

Publications arising from this thesis

Manuneedhi Cholan P**,** Cartland, S.P, Kavurma M. **"NADPH oxidases, Angiogenesis, and Peripheral Artery disease". "*Antioxidant*" 2017.**

Manuneedhi Cholan P, Cartland S, Genner S, Dang L, Rayner B, Hawkins C, Thomas S and Kavurma M. **"TRAIL inhibits Angiotensin-II-induced oxidative stress and inflammation in vascular endothelial cells."** "**Free Radial Biology and Medicine" 2018**.

Cartland, S.P, Genner, S.W, Martínez, G.J, Robertson, S, Kockx, M, Lin, R.C, O'Sullivan, J.F, Koay, Y.C, Manuneedhi Cholan, P, Kebede, M, Murphy, A.J, Bennett, M.R, Jessup W, Kritharides, L, Geczy, C, Patel, S, Kavurma, M.M. **"TRAIL-expressing monocyte/macrophages are critical for reducing inflammation and atherosclerosis". "iScience" 2018.**

List of Abbreviations

%	**Percentage**
ANOVA	Analysis of Variance
BCA	Bicinchoninic Acid
BSA	Bovine Serum Albumin
CAD	Coronary Artery Disease
cDNA	Complimentary Deoxyribose Nucleic Acid
CFSE	Carboxyfluorescein Succinimidyl Ester
CO_2	Carbon di oxide
$CuSo_4$	Cupper (II) sulphate
DHE	Dihydroethidium
DMSO	Dimethyl sulfoxide
EC	Endothelial cells
ELISA	Enzyme-Linked Immunosorbent Assay
eNOS	Endothelial Nitric Oxide Synthase
FSC-A	Forward Scatter-Area
g	Gram
GTT	Glucose Tolerance Test
h	Hour
H&E	Haematoxylin and Eosin
HBSS	Hanks' balanced Salts
HFD	High Fat Diet
Hg	Mercury
HMEC-1	Human Microvascular Endothelial Cell-1

ICAM-1	Intercellular Adhesion Molecule -1
IL	Interleukin
iNOS	Inducible Nitric Oxide Synthase
ITT	Insulin Tolerance Test
KHB	Krebs-Henseleit Buffer
KLF	Krüppel-like Factor
MAP	Mean Arteriole Pressure
mg	Milligram
min	Minutes
mM	Millimolar
MYH	Myosin Heavy Chain
nm	Nanometer
PBS	Phosphate buffer saline
pH	Potenz-hydrogen
qPCR	Quantitative Polymerase Chain Reaction
RIPA	Radio-Immunoprecipitate Assay
RNA	Ribose Nucleic Acid
RO	Reverse Osmosis
Rpm	Rotation per minute
s	Seconds
SEM	Standard Error Mean
SNP	Sodium Nitroprusside
SSC-A	Side Scatter-Area
TNFSF10	Tumour Necrosis Factor Super Family–10

TRAIL	TNF-Related Apoptosis Inducing Ligand
UNSW	University of New South Wales
VCAM-1	Vascular Cell Adhesion Molecule-1
VSMC	Vascular Smooth Muscle Cells
α-SMA	Alpha-smooth muscle actin
µL	Microlitre
µM	Micromolar
^{o}C	Degree Celsius

Abstract

The vasculature is critical for the maintenance of cardiovascular homeostasis. Cardiovascular disease (CVD) is characterised by endothelial cell (EC) and vascular smooth muscle cell (VSMC) dysfunction, in which vascular oxidative stress is a primary cause. The mechanisms and stimuli involved in vascular dysfunction are not fully characterised. Our lab showed that TNF-related apoptosis-inducing ligand (TRAIL) is a master regulator of vascular cell function, and its deletion in *Apoe*$^{-/-}$ mice accelerated atherosclerosis and CVD. TRAIL is increasingly recognised to play a protective role in CVD, however, how it may regulate vascular function is unclear.

This thesis aimed to investigate TRAIL's protective role against oxidative stress resulting in CVDs. It studied TRAIL's role in clinical, pre-clinical and *in-vitro* models. This thesis also aimed to elucidate the mechanism of action of TRAIL in vascular cells *in vivo* using cell-specific TRAIL knockout mouse models under normal and pathological conditions.

This thesis demonstrated that:

i. Circulating plasma TRAIL and oxidative stress markers are negatively correlated in patients with coronary artery disease (CAD).

ii. Following high fat diet (HFD), mice lacking TRAIL had endothelial dysfunction, vascular inflammation and increased vessel permeability.

iii. TRAIL protected against angiotensin II (AngII)-induced oxidative stress *in vitro* in ECs. TRAIL also negated AngII-induced cell processes by reducing monocyte adhesion and improving permeability *in-vitro* in ECs.

iv. EC-specific TRAIL deleted mice challenged with an HFD, experienced high plasma cholesterol, reduced blood pressure and altered gene expression profiles for inflammatory markers compared to wild type mice.

v. VSMC-specific TRAIL deleted mice challenged with an HFD, displayed altered expression of genes regulating VSMC phenotype. These mice also had an enlarged liver compared to wild type mice in response to an HFD.

This thesis provided novel insight into the protective role of TRAIL against endothelial dysfunction via its ability to modulate oxidative stress. This thesis studied the mechanism of action of TRAIL in vascular cells. Thus, understanding the role TRAIL plays in normal physiology and disease, may lead to potential new therapies to improve vascular functions and CVDs.

Chapter 1: **Introduction**

According to the World Health Organisation (WHO), heart and blood vessel diseases, known collectively as cardiovascular disease (CVD) account for 31% of global deaths. In Australia, CVD was the main cause of hospitalisation in 2014-15 and 43963 deaths in 2016: currently killing one Australian every 11 minutes (Heart Foundation of Australia). The main cause of CVD is atherosclerosis, where damage to the endothelium results in accumulation of vascular smooth muscle cells (VSMCs), inflammatory cells, lipids, cholesterol and cellular waste producing a thickened neointima in the arterial wall. Atherosclerosis is a major risk factor for myocardial infarction, stroke, hypertension and peripheral artery disease. Understanding the functional response of the vasculature under physiological and pathological conditions, can pave way to new and improved therapeutic targets to combat CVD.

1.1 ATHEROSCLEROSIS

A normal muscular artery contains three layers (**Figure 1.1a**). The inner layer, tunica intima is made up of a monolayer of endothelial cells (ECs). This layer is in constant contact with blood overlying the basement membrane. The second layer, tunica media, consists of VSMCs embedded in an extracellular matrix (ECM). The outer most layer, tunica externa, is the adventitia containing mast cells, micro-vessels and nerve endings, anchoring blood vessels to muscle or bones [6].

Atherosclerosis is defined as a chronic disease of the arterial wall affecting loss of productive life years and death worldwide. The initial stage of atherosclerosis involves adhesion of blood leukocytes to the monolayer of damaged/activated endothelium, followed by directed migration of leukocytes into the intima. Here, leukocytes such as monocytes,

differentiate into macrophages, take up lipid, and become foam cells. Foam cells secrete multiple cytokines including growth factors and pro-inflammatory mediators. VSMCs respond to these growth factors and migrate into the intimal layer, where they accumulate and proliferate. This is followed by synthesis of ECM such as elastin, collagen and proteoglycans in the intimal layer. In the advanced lesion, the environment becomes toxic, with plaque macrophages and VSMCs undergo apoptosis or necrosis. These dead and dying cells release the extracellular lipid within them, creating a large necrotic core comprising of cholesterol crystals and micro-vessels. The more cells die, the larger the necrotic core becomes. In the final stages, the plaque's fibrous cap thins and ruptures enabling blood coagulation factors within the necrotic core to come in contact with the blood. This causes thrombus formation in the lumen of the blood vessel, impeding blood flow [5]. Because atherosclerosis is a complex chronic disease, we still do not know enough about how lesions progress and the involvement of oxidation stress, inflammation and immunity. Understanding how atherosclerosis develops could provide new strategies to therapeutically delay the progress of this disease. Progression of atherosclerosis from the initial endothelial damage to eventual plaque rupture is depicted in **Figure 1.1**.

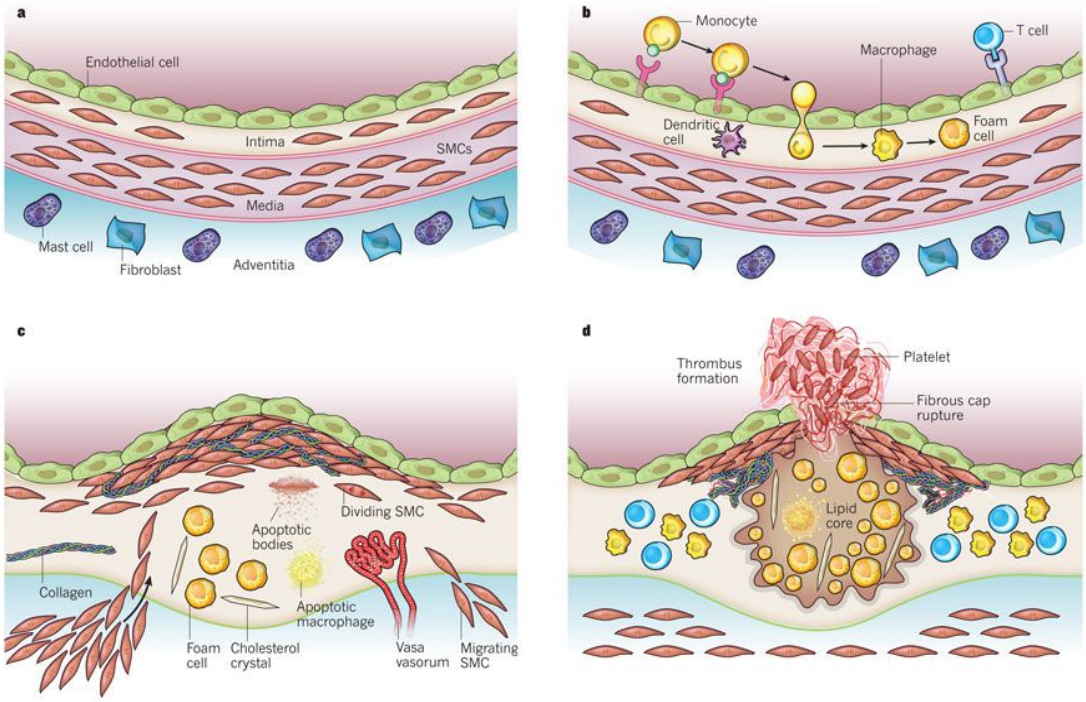

Figure 1.1 Progression of atherosclerosis. (a) A healthy vasculature, indicating tunica intima, media and adventitia. **(b)** Early stages of atherosclerosis, with endothelial damage, up-regulation of cell adhesion molecules and increase in monocyte tethering to the endothelium. These leukocytes extravasate into the sub-endothelial space, uptake ox-LDL and form foam cells. **(c)** VSMC's proliferating and migrating into the sub-endothelial space, along with increased foam cell accumulation. **(d)** Final stage of atherosclerosis, with the rupture of the thin fibrous cap and exposing the contents of the plaque to systemic circulation. This is followed thrombus formation due to platelet aggregation. Figure adapted from Libby *et al.* (2011) [5].

1.2 ENDOTHELIAL CELLS

Endothelial cells (ECs) line the lumen of the blood vessel creating a selective barrier between blood and tissues [7]. In humans the endothelial layer has an approximate surface area of 350 m^2 which makes any physiological or pathological changes occurring in the endothelium very important [8]. Apart from forming a selective barrier, ECs have autocrine, paracrine and endocrine functions, influencing VSMC, leukocyte and platelet processes. Though a singular cell type, ECs express different receptors, antigens and respond differently to the same stimulus depending on their location. At homeostasis, ECs are anti-inflammatory, anti-thrombotic and anti-coagulant.

As mentioned before, endothelial damage/dysfunction is the initial step of atherosclerosis which was originally described by Ludmer *et al.* In this study, impaired endothelial dependant vaso-relaxation in the presence of atherosclerosis was observed in mild to severe coronary artery disease (CAD) patients [9]. Endothelial dysfunction entails structural, functional and biochemical changes to this monolayer, thereby stimulating/activating the endothelium. In atherosclerotic susceptible regions, the dysfunctional endothelium changes its morphology to cuboidal morphology and disordered alignment [10,11]. These changes can upregulate transcription factors such as NF-κB, which has pathophysiological implications in the progression of this disease [12]. Effector proteins such as endothelial-leukocyte adhesion molecule-1 (e-selectin), vascular cell adhesion molecule-1 (VCAM-1), monocyte up-regulated on the damaged endothelium. Atherosclerosis can also disturb endothelial dependant regulation of vascular tone. It can cause impairment of nitric oxide (NO) production which is essential to maintain a healthy endothelium [13]. All the above changes induce an activated endothelium which is pro-inflammatory, pro-thrombotic and pro-atherogenic in nature.

1.2.1 **Anti-inflammatory/ pro-inflammatory state of endothelium**

ECs are important regulators of the inflammatory response by maintaining a steady state anti-inflammatory surface. Internal and external factors contribute to the protection of vessel wall [14]. External signals such as interleukin-10 (IL-10), transforming growth factor- β (TGF-β), IL-1 receptor antagonist, low density lipoprotein (LDL) and several other growth and angiogenic factors contribute to anti-inflammatory state of the endothelium [15-18].

The anti-inflammatory state of the endothelium is disrupted during atherosclerosis. Activation of protein kinase C and NF-κB are primary events associated with endothelial inflammation [19]. They generate inflammatory cytokines such as tumour necrosis factor–alpha (TNF-α), MCP-1, interleukin-1 beta (IL-1β), interleukin-18 (IL-18) and chemokines. These inflammatory cytokines play a central role in pathophysiology of atherosclerosis. TNF-α can trigger the interaction between invading monocytes and ECs [20], up-regulate cell adhesion molecule expression [21], increase oxidative stress in the endothelium by escalating the production of reactive oxygen species (ROS) in these cells [22], and ultimately increase production of other cytokines such as MCP-1. The impact of MCP-1 is important in the progression of atherosclerosis where it enables LDL accumulation in macrophages in the intimal layer [23]. Furthermore, interleukins such as IL-18 and IL-1β are upregulated in a clinical setting with patients who have experienced myocardial infarction, which is an indication of advanced atherosclerosis [24,25]. These inflammatory cytokines are constantly produced by a damaged endothelium and activated leukocytes, thereby aiding in various stages of atherosclerosis progression.

Following inflammation at the site of injury there is up-regulation of chemokines and cell adhesion molecules which enable monocyte recruitment, attachment and trans-endothelial migration. Chemokines are a sub-class of cytokines which are produced by the damaged endothelium. They enable monocyte recruitment to the site of injury through chemotaxis [26].

A study by Tacke *et al.* (2007) showed that chemokines such as CCR2, CCR5 and CX_3CR1 was required for monocyte recruitment, playing an important role in atherogenesis. Following leukocyte attachment, subsequent trans-migration into the sub-endothelial space is initiated by adhesion molecules present on the cell surface [27]. These molecules are part of the immunoglobulin family, trans-membrane protein and include ICAM-1, VCAM-1 and selectins. The expression of adhesion molecules present on the surface of the endothelium, plays an important role in many pathological conditions. At homeostasis, ICAM-1 (CD54) is constitutively expressed and is important in adaptive and innate immunity, leukocyte extravasation to site of injury and interacts with antigen presenting cells and T cells [28]. On the other hand, VCAM-1 expression is induced by factors such as cytokine production in tissues, high levels of ROS, oxidized-LDL (ox-LDL), turbulent shear stress and high glucose.

After the initial stage of endothelial damage, the inflammatory environment causes upregulation of cell adhesion molecules. The interaction between circulating leukocytes and endothelium is facilitated by these adhesion molecules [29]. Research has shown that ICAM-1 is strongly expressed on the endothelium near the developing plaque in human coronary and carotid arteries [30]. Furthermore, the soluble or cleaved ICAM-1 is increased in a cardiovascular setting [31]. ICAM-1 is seen as a molecule which works in collaboration with VCAM-1 and selectins such as P-selectin and E-selectins. Several studies have shown that VCAM-1 was not expressed at baseline, however, it was rapidly induced by proatherogenic conditions in mice and humans [32,33]. Up-regulation of these cell adhesion molecules increase monocyte tethering on to the activated endothelium.

Another family of adhesion molecules involved in atherosclerosis are selectins. P and E-selectins are present on the activated endothelium. P-selectins enable rolling of leukocytes on the endothelium, which in turn facilitate leukocyte recruitment to the vessel wall. Deletion of P-selectin in animal models have resulted in delaying the recruitment of monocytes to the

site of lesion and thereby reducing the lesion formation [34,35]. P-selectins can also be released from the endothelium as a soluble form creating a pro-coagulant environment, which during later stages of atherosclerosis can have a damaging impact on the body [36,37]. Similar to P-selectin, E-selectin is also expressed on human atherosclerotic plaque [38,39]. Combined deletion of E-selectin with P-selectin and LDL receptor in mice reduced plaque size in response to a high fat diet [40]. The two families of adhesion molecules facilitate lesion progression in atherosclerosis and are crucial for attachment and transmigration of leukocytes such as monocytes into the sub-endothelial space.

Once monocytes have trans-migrated into the sub-endothelial space, they take up LDL, and undergo differentiation to form macrophages [41]. The differentiation of monocytes to macrophage is aided by regulators such as macrophage-colony stimulating factor (M-CSF) [42]. At homeostasis, attracted monocytes/macrophages are involved in clearance of apoptotic cells in the vasculature, thereby preventing any excessive inflammation. However, during atherosclerosis, there is increased recruitment of circulating monocytes to the site of inflammation. They are initially recruited to the site to resolve inflammation, however continued monocyte attraction followed by inflammation causes monocyte/macrophage dysfunction. This eventually will convert macrophage into foam cells and be visible as a fatty streak in the vasculature [43].

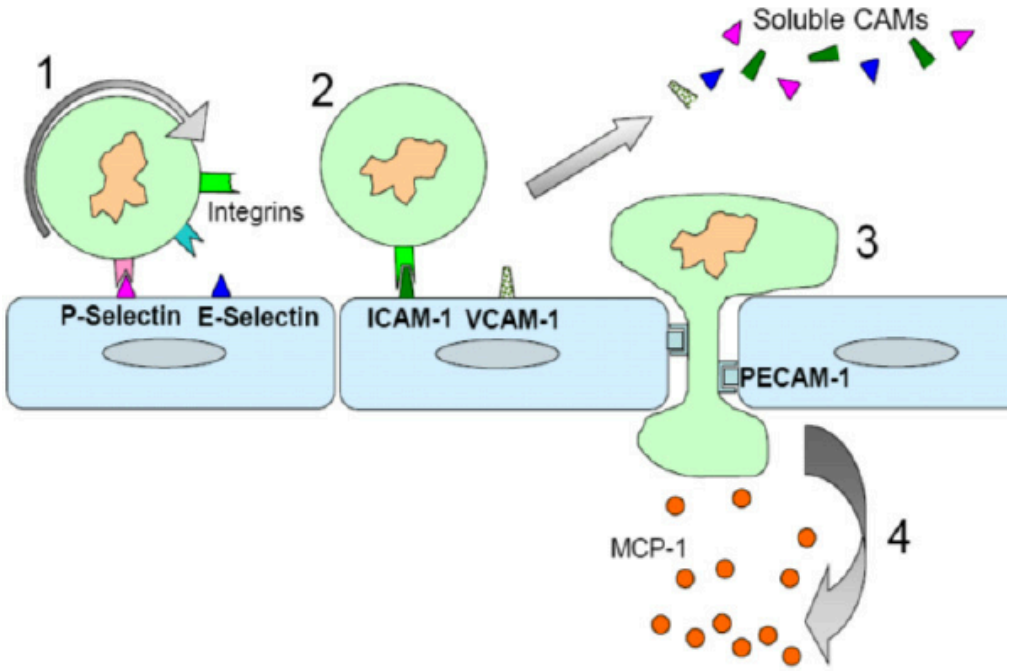

Figure 1.2 Leukocyte migration aided by cell adhesion molecules on the endothelium. (1) Leukocyte bind to selectins on the activated endothelium. (2) Leukocytes undergo structural changes and bind firmly to ICAM-1 and VCAM-1. (3) Leukocyte migrate to the sub-endothelial space by binding to PECAM-1. (4) Migration is aided by chemokines such as MCP-1. Figure adapted from Body et al. (2012).

1.2.2 **Anti-atherogenic endothelium**

A healthy endothelium actively regulates vascular tone and blood pressure through stimulation of NO and endothelin whilst suppressing inappropriate coagulation factors [44-46]. ECs are continuously exposed to the forces of blood flow. A constant laminar flow of blood helps in maintaining an anti-inflammatory surface and EC apoptosis is prevented by increasing antioxidant mechanisms such as superoxide dismutase and stimulating nitric oxide mechanisms all of which can reduce inflammatory stimulus such as TNF-α [47]. Production of NO by the endothelium helps the cells to maintain an anti-atherogenic state. NO maintains vascular tone, cell growth and protects the vasculature against injury. It is produced by converting L-arginine to L-citrulline with the aid of the enzyme endothelial nitric oxide synthase (eNOS), which is a calmodulin dependant enzyme, activated by elevated intracellular calcium levels [48,49]. eNOS is activated through a homo-dimeric G-protein coupled cell surface receptor and held together by its essential cofactor tetrahydrobiopterin (BH4). A healthy endothelium modulates the production of eNOS by increasing its expression to stimuli such as shear stress and varying levels of oxygenation.

During atherosclerosis, the growing plaque disturbs the flow of blood. Such disturbance is also observed in the aortic arch, vessel bifurcation and branch points. The disturbed blood flow induces pro-atherogenic characteristics and increases endothelial activation, followed by inflammation and apoptosis. The pro-atherogenic state of the endothelium reduces the bioactivity of eNOS. This subsequently leads to degradation of NO, followed by increased generation of ROS by the endothelium. In the atherogenic state, the NOS system can itself contribute to further endothelial damage. In the absence of co-factors involved in production of NO, eNOS can become uncoupled from its dimeric state and induce oxidative damage, generating peroxynitrite, which eventually promotes plaque progression [50]. Reduced levels of eNOS is linked to several pathological conditions such as type 2 diabetes, Alzheimer's

disease and cancer [51]. Strategies to increase eNOS production and maintain its dimeric form has gained pharmaceutical attention. Drugs such as trans-resveratrol [52] and statins [53] can increase eNOS production thereby maintaining a healthy vasculature. NO, the effector molecule and soluble gas in this system, has a multitude of beneficial effects including inhibition of leukocyte adhesion, control of VSMC proliferation and modulation of platelet aggregation [54-56]. Thus, regulated production of NO helps in maintaining a healthy endothelium and vasculature.

To maintain an anti-atherogenic state, the endothelium also has to maintain a selective permeable membrane. This selective-permeability, regulated intracellular tight junctions, enables the ECs to exchange fluids and solutes between blood and tissue, control leukocyte entry and modulate themselves during angiogenesis. ECs have two types of cell-to-cell interactions, adherents and tight junctions. While adherents help in intracellular signalling, cytoskeleton remodelling and transcriptional regulation, tight junctions help in maintaining the monolayer permeability [57]. Vascular endothelial-cadherin (VE-cadherin), is an exclusive endothelial specific adherent, present between cell junctions, which controls vascular permeability and leukocyte extravasation [58]. VE-cadherin are also strongly associated with growth factors such as VEGF and FGF and play an important role in angiogenesis. Regulation of VE-cadherin is important as its pleiotropic effects range from angiogenesis to atherosclerosis [58,59].

A study by Miyazaki *et al.* (2011) showed that in hypercholesterolaemic mice, a primary characteristic of atherosclerosis, there was dysregulation of VE-cadherin. The vasculature became leaky and promoted extravasation of immunocompetent cells and monocytes and VE-cadherin disruption can lead to endothelial damage and progression of atherosclerosis [60]. Thus, maintaining anti-atherogenic state of the endothelium involves regulated production of NO and maintaining a selective permeable endothelial membrane.

1.2.3 **Anti-thrombotic endothelium**

Thrombosis is defined as the local coagulation or clotting of blood in the circulatory system. As mentioned earlier, a healthy endothelium is anti-thrombotic. ECs play a pivotal role in the control of haemostasis and thrombosis, and are the main source of source of haemostatic regulatory molecule [61]. ECs secrete multifunctional adhesive glycoproteins such as von willebrand's factor (vWF), fibronectin and thrombospondin. These proteins help prevent blood loss in face of vascular injury. However, the endothelium also releases thrombomodulin which serves as cofactor of thrombin and prevents uncontrolled coagulation and aggregation of proteins to the site of injury. This enables the endothelium to have a check on its thrombotic and anti-thrombotic activity. At homeostasis, the endothelium is at constant state of anti-thrombosis, but reverts to a pro-thrombotic state in face of vascular injury [62]. Importantly, during advanced atherosclerosis, an unstable or vulnerable plaque can result in life altering consequences. With increasing number of ECs damaged during atherosclerosis, EC properties are perturbed towards a more pro-coagulant and pro-thrombotic phenotype. When the large necrotic plaque ruptures there is spillage of highly thrombotic content, triggering an atherothrombotic occlusion [63]. Clots when lodged into the coronary artery of the heart or blood vessels in the brain can lead to myocardial infarction or stroke respectively. These clots can also lodge themselves in the peripheral veins leading to deep vein thrombosis.

1.3 VASCULAR SMOOTH MUSCLE CELLS

The second layer of the vessel wall, the tunica media is made up of vascular smooth muscle cells (VSMC's). This layer contributes to most of the cells in the vasculature. The principal function of these highly specialised cells are to regulate vessel tone, blood flow distribution and blood pressure [64]. Since these cells make up most of the blood vessel, they also play an important role in vessel remodelling in response to exercise, vascular injury or pregnancy.

During this remodelling, VSMC's have the ability to change their phenotype and their extracellular matrix.

1.3.1 **Phenotypic switching of VSMCs**

VSMC's are usually classified as either being contractile or synthetic. These phenotypes are in either end of the spectrum where the phenotype is interchangeable and transient. Contractile or synthetic VSMCs s can be identified by their different morphological structures. Contractile cells are elongated, and more spindle like in nature, however synthetic cells have a cobblestone morphology. Internally, synthetic VSMCs have high number of organelles and contractile cells have long contractile filaments in the cells. Apart from morphology, these cells also have very different gene markers and functions. As the name suggests contractile cells are contractile in nature, with less proliferative and migratory functions [65]. These cells are recognised by their gene markers such as smooth muscle-myosin heavy chain (SM-MHC), alpha-smooth muscle cell actin (α-SMA) and alpha-tropomyosin (α-tropomyosin). On the other hand, the synthetic phenotype is less contractile and are more prone to proliferate and migrate. Several biochemical factors aid in the conversion of VSMCs to either of the phenotypes. They either help the cell maintain the phenotype or convert to another depending on the situation [65]. Transforming growth factor- β (TGF-β) is considered an important factor in inducing contractile phenotype in VSMCs. Studies have shown that cultured VSMCs become more elongated and spindle-like when treated with TGF-β, specifically its isoform TGF-β1 which was also shown to increase contractile gene markers such as α-SMA, α-tropomyosin and myosin heavy chain (MYH) [66]. Two of Krüppel-like factor (KLF) isoforms, KLF-4 and KLF-5 are transcription regulating factors which help in maintaining or inducing a synthetic VSMC phenotype [67]. These isoforms play a major role in early stages of embryogenesis, aiding in proliferation and migration to form the vascular network [68]. At

homeostasis majority of VSMCs exists in the contractile phenotype to aid the blood vessel in blood pressure control. The regulation of VSMC is depicted in **Figure 1.2.**

Both these phenotypes work in balance during homeostasis. However, during a pathological condition such as atherosclerosis, VSMCs are induced to a more synthetic phenotype. Damage to VSMCs quickly convert them from a resting contractile phenotype to a synthetic one [65,69]. In atherosclerosis, synthetic VSMCs cause neo-intimal hyperplasia or lumen narrowing, aid in lipid retention for macrophages to form foam cells and induce an inflammatory environment [70]. All these factors lead to the progression of atherosclerosis and eventual rupture of the plaque. Though the critical signal transduction involved in VSMC phenotypic switching remains unclear, it is known that under a pathological environment, aberrant eNOS production can result in VSMC phenotypic switching. Whether peroxynitrite is involved in VSMC phenotypic switching needs investigation [71].

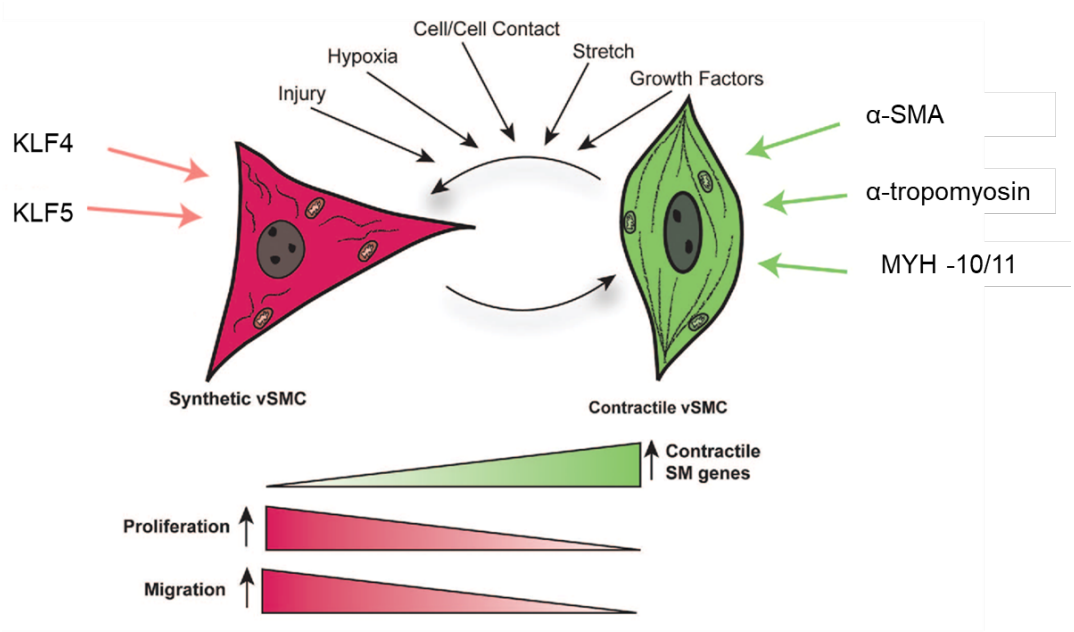

Figure 1.2 Regulation of VSMC phenotype. In response to variety of stimuli, including injury, hypoxia, cell-to-cell contact, stretch and growth factors, VSMCs can switch between contractile and synthetic phenotypes. Contractile VSMCs expresses genes such as α-SMA, α-tropomyosin and MYH-10/11. Synthetic VSMCs expresses, up-regulated transcription factors such as KLF-4 and KLF-5. These cells are more proliferative and migrative contributing to atherosclerosis. Figure adapted from Dusenbery *et al.* (2011) [2].

1.3.2 Extracellular matrix

In the tunica media, apart from VSMCs, ECM proteins help in maintaining the functions associated with this layer. The ECM is a collection of fibrous proteins and glycoproteins embedded in glycosaminoglycans and proteoglycans. This matrix provides elasticity, mechanical support and regulate the behaviour of other vascular cells [72]. Two major proteins of the ECM are collagens and elastin. Collagen proteins are composed of triple helix polypeptide chain, with several isoform existing in the human body. Collagen type I and III are the most predominant collagen in the vasculature. They provide tensile strength to the vessel

wall and play a role in atherosclerotic plaque development [73]. These isoforms of collagen were found to be synthesised by cultured VSMCs with the aid of growth factors such as TGF-β1 and epidermal growth factor (EGF) [74,75]. Though under homeostasis collagen production is limited and maintained to provide structural strength to the tunica media, several studies have indicated that collagen production is greatly accelerated in conditions such as atherosclerosis and neointimal hyperplasia. They have drawn corelative arguments with an increase in collagen production in the ECM to aid in VSMC proliferation and migration into the intima, which facilitates atherogenesis and plaque development [73]. The other important ECM protein is elastin, which confers elasticity and prevents tissue stretching in response to systolic and diastolic pressure change [76]. It is an autocrine regulator of VSMC activity through G-protein coupled pathway, inhibiting VSMC proliferation and regulating its migration. An early study conducted in 1970's found that primate arterial smooth muscle cells are capable of producing elastin in culture. Healthy contractile VSMCs are known to increase elastin deposition in their surrounding ECM to compensate the pulsating force of the blood [77]. Reduction in this deposition is a clear indication of phenotypic switch of VSMCs from contractile to synthetic phenotype. Both ECM and VSMCs regulate one another and control the tensile strength and elasticity of the vasculature and changes in ECM is an important indicator of pathological changes undergone by the vasculature.

1.4 OXIDATIVE STRESS

Oxidative stress is defined as the imbalance between anti-oxidants and free radicals, favouring the latter produced in the body. This imbalance creates the production of reactive oxygen species (ROS) which play a critical role in biological functions and cell processes. Several clinical studies have shown that ROS is upregulated in diabetes [78], hypertension [79]

and dyslipidaemia [80]. Reducing ROS may serve as a therapeutic target against the above-mentioned CVDs.

Vascular cells have been recognised in producing both ROS and reactive nitrogen species (RNS) which can produce by-products such as hydrogen peroxide (H_2O_2), hydroxyl radical and peroxynitrite ($OONO^-$). Though ROS can promote highly toxic redox reactions in the body, they also act to regulate homeostatic cell processes [81]. For example, ROS can regulate cell signalling by affecting MAP kinase (MAPK) and extra-cellular regulatory kinase 1/2 (ERK1/2) [82]. In EC's ROS and RNS can modulate cell proliferation, growth, permeability and cell death while in VSMC's they can promote growth by inducing auto/paracrine growth mechanisms [83], mediate agonist-induced hypertrophy, and induce apoptosis in a concentration dependant manner [84]. Having a clear idea of homeostatic mechanisms of ROS can enable us to identify changes which occurs during pathological conditions.

Any disturbances to this homeostatic balance of anti-oxidant and ROS may result in pathological conditions; specifically, up-regulation of ROS can result in systemic oxidative stress in the body. Large scale human studies examining markers such as malondialdehyde (MDA), involved in peroxidation of unsaturated fats, and F_2-isoprostane, a by-product of oxidation of lipids, revealed sex [85], race [86] and age [87] to be independent determinants of oxidative stress/damage in humans. Furthermore, dependant variables such as smoking, unhealthy lifestyle and environmental pollution can also induce oxidative stress [88]. Irrespective of dependant or independent variables, systemic oxidative stress can lead to diabetes, hypertension and other cardiovascular diseases, as mentioned earlier

There are various sources involved in producing ROS in EC, under basal and pathological settings. They include, xanthine oxidase, NADPH oxidase, mitochondrial electron transport chain, eNOS uncoupling and cytochrome P450. The mechanism of action of these endothelial ROS, a key component of endothelial dysfunction is largely unknown. Identification of these

mechanisms will drive the rationale for new intervention for the prevention of ROS and thereby vascular disease. In this thesis we focused on mitochondrial electron transport chain, NADPH oxidase and eNOS uncoupling systems.

1.4.1 **Mitochondria and oxidative stress**

Mitochondria are considered the power house of the cell and are one of the major producers of ROS, particularly within respiratory chain complexes [89]. The basic function of the respiratory chain is to oxidise glucose and other sugars to produce ATP or energy. This is achieved by creating a transmembrane electrochemical gradient by pumping protons between the mitochondrial membranes, involving a series of protein complexes (Complex I-V) in the inner mitochondrial membrane. The flow of protons back into the mitochondria produces ATP, the principal source of power in the cell [90,91]. The mitochondrial electron transport chain is depicted in **Figure 1.3.**

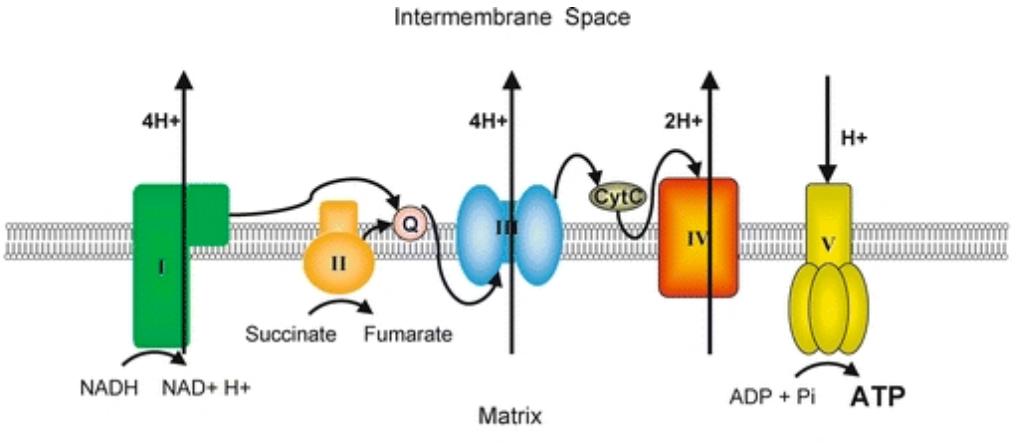

Figure 1.3 Schematic representation of mitochondrial electron transport chain. Transfer of electrons from complex 1 to complex 5 resulting in ATP production. Figure adapted from Agnihotri *et al*. (2014).

During the process of respiration, superoxides are produced by the electron transport chain due to incomplete reduction of oxygen. The superoxide formation in this chain occurs in the flavin mononucleotide (FMN) site in complex I, when there is a high NADH/NAD^+ ratio, and low ATP availability, enabling the electron received by complex 1 to be transferred to O_2 to produce superoxide. Complex III can also produce superoxide. The *in vivo* physiological importance of complex I verses complex III remains controversial as there are insufficient findings pertaining to the exact electron transport chain mechanisms [92,93]. Importantly however, the superoxide produced can be rapidly reduced to H_2O_2 with the help of copper-zinc superoxide dismutase or manganese superoxide dismutase (MnSOD) [94]. MnSOD was identified to be important in vascular homeostasis and knocking out MnSOD in an Apoe-null mice induced endothelial dysfunction [95].

Mitochondrial ROS (mtROS) have important signalling functions in the endothelium and is directly linked to health and disease processes. For example, NADPH oxidase 4 (NOX 4), a predominant source of ROS in the endothelium, can regulate mtROS and influence endothelial-dependant relaxation, and therefore the blood pressure. As mentioned previously NOX 4 preferentially produces H_2O_2. A recent study by Munoz et al. (2018) showed that under physiological conditions, mitochondrial ROS stimulates NOX 4 to produce H_2O_2 which acts as an endothelial dependant vasodilator [96]. Sub-cellular localisation of NOX 4 has been found to be predominant in the mitochondria. Here, mitochondria can form superoxide dismutase (SOD), a form of ROS, which can effectively stimulate NOX 4 to produce H_2O_2. Down-stream, H_2O_2 can stimulate nitric oxide synthase (NOS), an enzyme important in NO production, known to cause endothelial dependant vasorelaxation. Growth factor adaptor proteins such as p66Shc can oxidase cytochrome c, an important part of the electron transport chain to generate H_2O_2. This process occurs during a high glucose environment, where p66Shc can translocate to the intermembrane space of the mitochondria, initiating ROS mediated

signalling, and subsequently resulting in endothelial dysfunction [97-99]. In diabetes, endothelial mitochondria undergo fission releasing high levels of ROS, which blunt growth and alter expression of cell adhesion molecules [100-102].

In VSMC's oxidative stress causes the mitochondrial fission process to occur resulting in mitochondrial DNA (mtDNA) damage. This process involves an increase in PARP-1 enzyme, which is involved in chromatin remodelling, increasing VSMC proliferation and migration, and thereby facilitating the progression of atherosclerosis [103]. Furthermore, a reduction in mitochondrial MnSOD in an Apoe-null mice damaged mtDNA. A study has established a direct correlation between mtDNA damage and VSMC content in atherosclerotic lesion in mice and human aortic tissues [104].

1.4.2 **NADPH oxidase and oxidative stress**

Nicotinamide adenine dinucleotide phosphate (NADPH) oxidase is another major system involved in production of ROS in the cell. This system consists of seven isoforms including NOX 1-5, and dual oxidase (DUOX) 1 and 2. At homeostasis, NOX-generated ROS regulate defence mechanisms, signal transduction and hormone biosynthesis. In the vasculature, NOX 1, 2, 4 and 5 are present, with NOX 4 being predominantly expressed under basal conditions and NOX 2 under pathological conditions in ECs, and NOX 1 and 4 abundant in VSMCs [105]. NOX's main role is to produce ROS, whereby it transfers electrons from cytosolic NADPH to molecular oxygen, which catalyses and produces ROS, superoxide and H_2O_2 [106].

As mentioned previously, ECs express four isoforms of NOX, including NOX 1, NOX 2, NOX 4 and NOX 5. Each of these isoforms are characterised by specific cytosolic and membrane bound sub-units. NOX 1, 2, and 4 all have same membrane bound sub-unit $p22^{phox}$ and different cytosolic sub-units. With NOX 1 having cytosolic regulators such as NOXO1,

NOXA1 and Rac whilst NOX 2 assembling $p67^{phox}$, $p40^{phox}$, $p47^{phox}$ and Rac as their cytosolic sub-units and NOX 4 having POLDIP 2. On the other hand, NOX 5 is a calcium dependant isoform regulated by calmodulin [3]. All these isoforms are capable of reducing NADPH to NADP and H^+, whilst producing superoxide. Though NOX 4 produces superoxide, it primarily produces H_2O_2. H_2O_2 can go on to react with products such as iron, chlorine or nitric oxide to generate products such as hydroxyl radicals, hypochlorous acid and $OONO^-$ all which can majorly upregulate oxidative stress and cause cellular damage [107]. H_2O_2 acts via kinase driven pathways to instigate proliferation, migration and autophagy. It often modules cell function by affecting DNA folding and lipid production inside the cell. Isoforms of endothelial NOX are depicted in **Figure 1.4.**

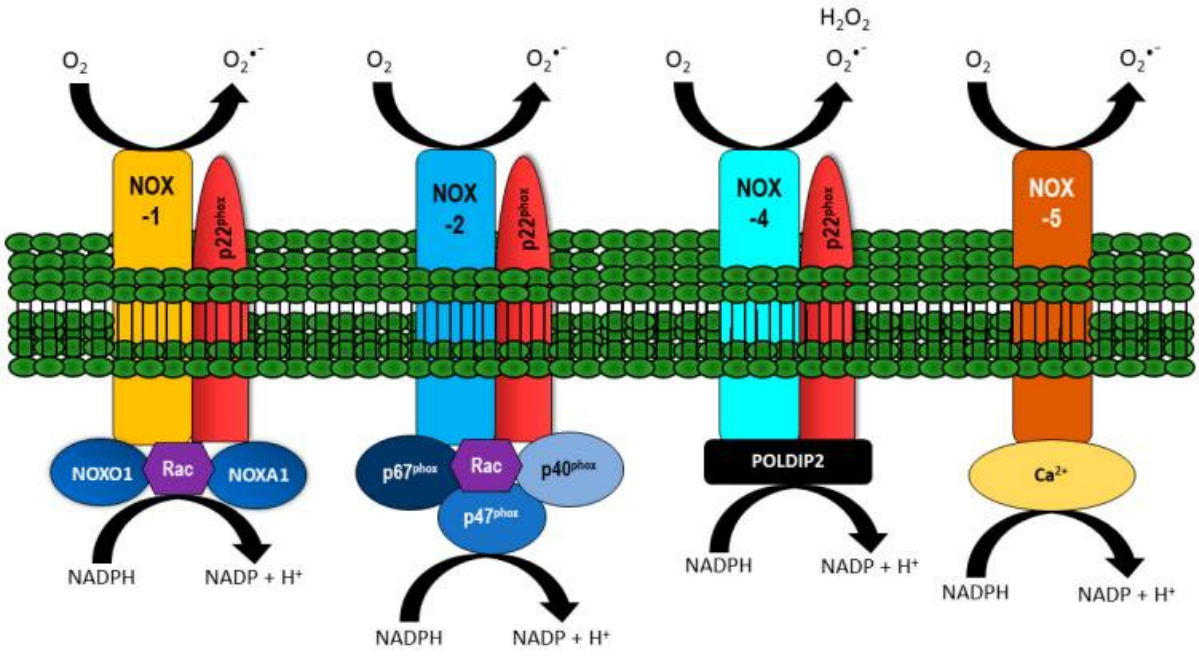

Figure 1.4 Vascular NADPH oxidase and their regulatory subunits. NOX 1, 2, 4 and 5 are present in the vascular cells. All NOX isoforms generate superoxides, with NOX 4 preferentially producing H_2O_2. Figure adapted from Manuneedhi Cholan *et al.* (2017) [3]

In ECs, NOX's role in cell growth was identified by Suh *et al.* (1999), with NOX 1 over-expression stimulating proliferation of both EC and VSMC's [108]. NOX 2, which was the first isoform identified in ECs, appears to be important in basal ROS production which is known to aid in proliferation, migration and tubule formation. However, like other systems generating ROS, aberrant ROS production by NOX can lead to EC dysfunction and cell death. *In-vitro* studies conducted in human umbilical vein endothelial cells (HUVEC) showed that knocking down NOX 1 significantly reduced production of ox-LDL and subsequent ROS production, indicating NOX 1 in both oxidative stress and atherogenesis [109]. Similarly, several studies showed that NOX 2 expression is inducible by lipoprotein particles or oxLDL [110,111], however, these same stimuli failed to activate NOX 4; the most abundant isoform in ECs. In contrast, NOX 4 activation was up-regulated in response to biologically active compounds such as pro-atherogenic sphingolipids or minimally modified LDL [112,113]. This difference suggests the complex nature of NOX activation in these cells. *In vivo,* NOX 1 and NOX 2 knockout mice were hypertensive, with increased vascular oxidative stress, EC dysfunction and aortic dissection [114,115]. Furthermore, studies looking at NOX's role in a hyperglycaemic condition or diabetes were conflicting. Some studies suggested NOX 1, 2 and 4's involvement in diabetes and EC damage, however, studies by Youn *et al.* (2012) disproved NOX 2's role in STZ-induced diabetic model and showed selective knockdown of NOX 4 did not improve conditions in these mice [116]. These varying studies shows us that further studies are needed to understand how NOX isoforms work under different pathology ical conditions. In particular to ECs, over expression NOX 2 in the endothelium *in vivo* showed augmented AngII-induced stress, however NOX 4 over expression seemed to be beneficial [114,117]. Further studies are needed to understand the role of NOX isoforms in endothelium.

Studies have shown that NOX 1 plays a supporting role in neointimal formation, thus both migration and growth of VSMC's are dependent on NOX 1 expression. *In vivo* studies

have shown that mice lacking NOX 1 affected lesion formation and healing by affecting VSMC's proliferative capacity. NOX 1 knockout mice have shown to reduce apoptosis, which can aid in neointimal formation as studies have shown that, early apoptosis after injury can aid in the wound healing process [118,119]. Another important change which VMSC's go through in response to ROS is phenotypic switching. Studies have shown that *in-vitro* knockdown of NOX 4 using siRNA in VSMC's resulted in reduction in ROS levels as well a reduction in p38MAPK pathway which is important in producing factors necessary for differentiational maker genes in VSMC's [120]. On the other hand, inhibition of NOX's at a pharmacological level has to be done considering several other factors, since some studies have shown that NOX 4 activity reduction or inhibition lead to permanent growth arrest in VSMC's and eventually stress-induced premature senescence [121]. Also, NOX 4 can be activated by mechanical stretch of VSMC's and becomes important in cytoskeleton reorganisation in these cells with the help of the cofilin signalling pathway. Hence understanding the signalling pathways in response to a mechanical sensor becomes vital [122]. The functions of NOX isoforms in EC and VSM C are summarised in the table below.

Cell Type	Isoform	Function
EC	NOX 1	• Over-expression stimulates cell proliferation [108] • siRNA knockdown of NOX 1 reduces oxLDL and ROS production [109] • In vivo NOX 1 knockdown resulted in hypertensive mice causing aortic dissection [114,115].
VSMC	NOX 1	• Growth and migration of VSMC into the neointima [118,119]
EC	NOX 2	• Stimulated by lipoprotein [110,111]

		• In vivo NOX 2 knockdown resulted in hypertensive mice causing aortic dissection [114,115] • Over-expression of NOX 2 in EC aids in Ang II induced stress [114,117]
EC	NOX 4	• NOX 4 protect against Ang II induced stress [114,117]
VSMC	NOX 4	• NOX 4 knockdown increases ROS production via MAPK pathway in VSMC [120]

1.4.3 **Nitric oxide and oxidative stress**

NO is the smallest signalling molecule and the only gas found in the body. It is produced with the help of the enzyme NOS. Three isoforms of NOS exist and include neuronal NOS (nNOS), inducible NOS (iNOS) and endothelial NOS (eNOS) [123]. Each of these isoforms are present in different systems in the body, however this thesis will focus on eNOS.

eNOS is a calcium calmodulin enzyme that converts L-arginine to L-citrulline and NO. It plays an important role in maintaining a healthy endothelium by modulating vascular tone, regulating cell growth and protecting against circulating platelets. eNOS can exist in monomeric or dimeric form, however, only the dimeric form of eNOS is considered active. Each monomeric domain contains a reductase domain and an oxygenase domain. The reductase domain consists of NADPH, FAD and FMN binding domain, whereas the oxygenase domain contains tetrahydrobiopterin (BH4), heme, heat shock protein and a zinc binding domain [124,125]. The ability of eNOS to produce NO depends on a variety of factors including BH4 which is responsible for preventing the monomerization of eNOS. BH4 biosynthesis is catalysed by the rate limiting enzyme GTP cyclohydrolase I (GCH 1), and recent studies

showed that GCH1 expression is an important determinant for the synthesis of BH4 and subsequently eNOS activity.

Research over the past 20 years identified that loss of NO is the earliest and important sign of stress and subsequent pathological state in the body. This molecule gradually declines with age, directly correlating to the decline in endothelial function [126]. When endothelial BH4 availability is reduced, eNOS becomes uncoupled from L-arginine oxidation, resulting in superoxide formation rather than NO production. In this system, superoxides rapidly inactivate NO and convert it to $OONO^-$ which can damage tissue and induce platelet adhesion [127]. BH4 deficiency is linked to vascular oxidative stress and CVDs such as hypertension, atherosclerosis and diabetes [123,128,129]. Interestingly, BH4 supplementation improved endothelial function in humans [130]. The relationship between eNOS, BH4 and superoxides are depicted in **Figure 1.5**.

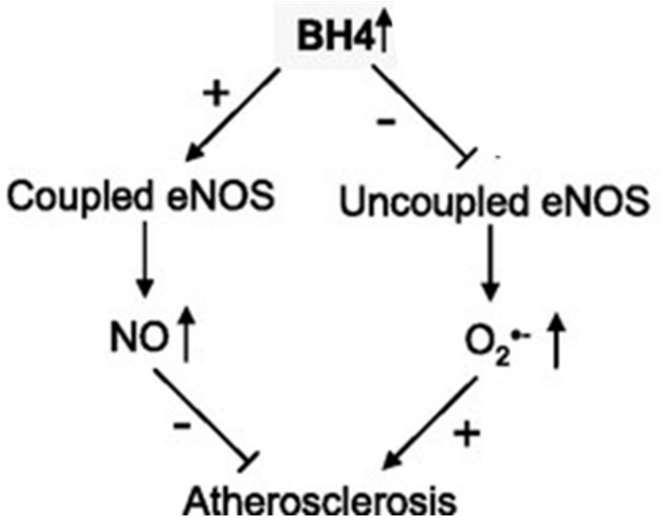

Figure 1.5 Relationship between eNOS, BH4 and superoxide production. The level of BH4 can induce coupling of eNOS leading to NO production and prevention of atherosclerosis. However, reduced BH4 production can lead to uncoupling of eNOS and superoxide production leading to accelerated atherosclerosis. Figure adapted from Fukai *et al.* (2007) [4]

As described earlier, reduced bioavailability of BH4 in ECs leads to endothelial dysfunction. In fact Apoe-null or diabetic mice have reduced BH4 levels which impair NO-mediated endothelial function [131,132]. The reduction in BH4 eventuates in eNOS uncoupling; eNOS in its monomeric form can lead to endothelial damage by increasing superoxide production instead of NO generation. Though eNOS is considered an important determinant of endothelial function, other studies have shown that in an *in vivo* model, eNOS dependant oxidative stress did not affect endothelial dependant vasodilation [133], highlighting the importance of other sources of vascular ROS affecting the endothelium.

eNOS derived NO plays an important role in maintaining vascular tone by stimulating VSMCs. The effector molecule NO produced by ECs, diffuse to the underlying VSMCs and control its rate of vaso-constriction and relaxation along with maintaining its contractile phenotype [134]. However, during oxidative stress, the uncoupled eNOS can combine with NO and become pro-atherogenic leading to phenotypic switching of VSMCs. The switching occurs via Akt/eNOS and MAPK signalling pathway creating a proliferative and migrative VSMC phenotype, leading to up-regulation of synthetic markers such as OPN [71]. These cells begin to proliferate and migrate thereby creating neointimal hyperplasia [134]. This suggest that eNOS derived from the endothelium can impact VSMCs during oxidative stress.

1.4.4 **Oxidative stress and atherosclerosis**

Several sources of ROS including NOX, uncoupled eNOS and mitochondrial electron transport chain were discussed along with their effect on vascular cells. There is growing evidence to indicate ROS producers to be involved in the development of atherosclerosis [135,136].

Research has shown that accelerated atherosclerosis and mitochondrial ROS production is seen in mice with Apoe and anti-oxidant deletion suggesting a role for mtROS in

atherosclerosis [137]. Similarly, in human aortic tissue with increased atherosclerosis, there has been increased mitochondrial DNA damage [104] which can accelerate ROS production and atherogenesis [138]. Mitochondrial dysfunction also increases lipid peroxidation, important for atherosclerosis progression. One product of lipid peroxidation is 4-hydroxyneal, which was significantly increased in atherosclerotic patient plasma [139,140].

In addition to the mitochondria, several lines of evidence implicate NOX in ROS production in atherogenesis. For example, NOX 1 or NOX 2 knockout mice had reduced lesion size, reduced blood pressure and reduced neo-intimal formation due to injury, all of which are factors aiding in atherosclerosis initiation and progression [119,141,142]. Age, which itself an important risk factor of atherosclerosis, was shown to have a positive correlation with NOX enzymes, and NOX 2 deletion in mice negated age related atherosclerosis development [143].

Majority of risk factors associated with atherosclerosis are due to impaired endothelial dependant relaxation, indicating a dysfunctional eNOS/NO system [144,145]. Absence of eNOS increased blood pressure and leukocyte adhesion to the vasculature, resulting in accelerated atherosclerosis [146,147]. Though eNOS production was suspected to be reduced in atherosclerotic models, most models showed either no change or upregulation of eNOS [148,149]. In fact, transgenic modulation of eNOS over-expression in the endothelium promoted atherosclerosis [150]. These studies show that in the absence of substrate and co-factors, eNOS produces superoxide rather than NO [150]. Furthermore, increased inflammation during atherosclerosis can decrease sensitivity or degrade NO, thereby causing it to react with superoxides.

1.5 TNF-RELATED APOPTOSIS INDUCING LIGAND

In this thesis, I have focused on a protein called TNF-related apoptosis-inducing ligand (TRAIL), which is also referred to as Apo2L, TNFSF10 or CD252. TRAIL is a cytokine that exists as a membrane-bound and soluble protein. This protein is a type 2 trans-membrane protein belonging to the TNF superfamily and ubiquitously expressed in humans and in mice [151]. Murine TRAIL and human TRAIL have 65% sequence homology [152]. Like other TNF family ligands, TRAIL causes homo-trimerization when it binds to its receptor and activates it. TRAIL can exist as a membrane bound protein and also can be cleaved to exists as a soluble form and can be produced by all normal cells in the body. Further research is needed to identify the predominant source of TRAIL [153]. There are five identified receptors in humans which include 2 functional receptors death receptor 4 (DR4), death receptor 5 (DR5) and 3 decoy receptors which include decoy receptor 1 (DcR1), decoy receptor 2 (DcR2) and osteoprotegerin (OPG).

Initially, TRAIL was thought to only promote apoptosis of cells, and was extensively studies in regard to cancer therapy. Several studies have used recombinant soluble TRAIL, which are currently at phase 1 and phase 2 clinical trials [154-157]. However, in recent times, TRAIL's non-apoptotic role on non-cancer cells have been of interest.

1.5.1 TRAIL receptor interaction

As mentioned above, TRAIL when binding to either DR4 or DR5 causes trimerization and activation of the receptor thereby initiating the intracellular mechanisms. This can cause the formation of the death inducing signalling complex (DISC) which consists of FAS associated death domain (FADD) and pro-caspase 8/10. DISC formation can eventually initiate activation of the caspase cascade. TRAIL signalling can also activate caspase 9 through the intrinsic mitochondrial pathway, by cleaving to the activate form of BH3 interacting-domain

(Bid) or directly activate caspase 3, 6, or 7 from their pro-caspase form to cause programmed cell death or apoptosis.

On the other hand, in recent times it has been found that TRAIL receptor trimerization can also activate a secondary complex. This is achieved when death inducing signalling complex (DISC) recruits several other adapter proteins such as TNF-receptor-associated DD (TRADD), TNF-receptor-associated factor-2 (TRAF2) and receptor interacting protein-1 (RIP1). This secondary complex can stimulate NF-κB translocation into the nucleus leading to pro-survival gene activation. This non-apoptotic pathway of TRAIL initiates cell proliferation and survival. TRAIL signalling through the secondary complex can also stimulate Akt phosphorylation and activate MAPKs such as ERK, c- Jun N-terminal kinase (JNK) and p38 [158]. There is significant cross-talk between these pathways, which can activate NF-κB, leading to proliferation or cell death. Thus, activation of secondary complex does not guarantee cell survival [1,159]. The direction in which the cell goes in response to TRAIL receptor trimerization is not fully understood. Thus, up-regulation or down-regulation of genes and mRNA/protein expression have importance in TRAIL's net outcome in a cell. The mechanism of action of TRAIL and its receptors are depicted in **Figure 1.6.**

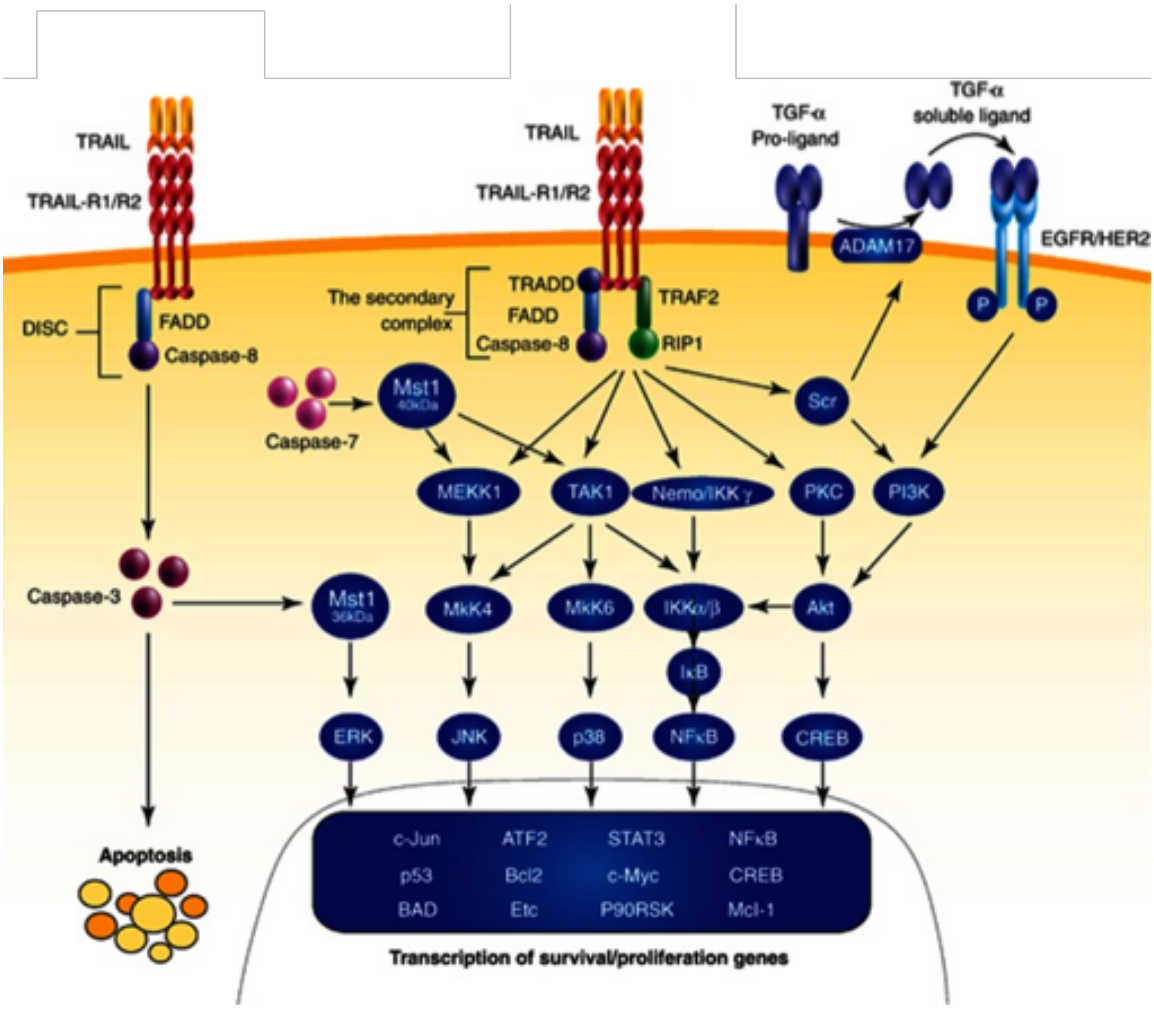

Figure 1.6 Mechanism of action of TRAIL. TRAIL upon binding to its receptors, activates DISC leading to caspase cascade activation and eventual apoptosis. On the other hand, TRAIL binding to its receptors can also activate its secondary complex. This can phosphorylate IκB kinase and activate NF-κB, which can translocate in to the nucleus to activate pro-survival gene activation. This figure was adapted from Azijli *et al.* [1]

1.5.2 **Clinical relevance of TRAIL**

TRAIL was initially identified because of its ability to kill cancer cells; however, we now know that it has multiple pleiotropic functions other than killing. In CVD, a protective association has been identified. For example, low serum TRAIL measured in older patients with significant CVD revealed that low TRAIL was a strong indicator of death in these patients over a period of 6 years [160]. In subsequent studies, TRAIL had a strong negative correlation with acuate coronary artery syndrome (ACS) patients, suggesting it can be used as a strong indicator of this disease in a clinical setting [161,162]. Heart failure which is the next step after ACS, has also shown a strong negative correlation with low plasma TRAIL levels [163]. Furthermore, a genome-wide meta-analysis study identified 11 loss of function single-nucleotide polymorphisms of TRAIL to be associated with carotid artery atherosclerosis [164].

Another major disease associated with CVD is type 2 diabetes. Though there has been research which disprove any relationship between TRAIL and type 2 diabetes in patients, there are two studies which state otherwise [165,166]. These studies have shown that circulating TRAIL levels were low in newly diagnosed diabetics as a part of longitudinal study measuring before and after the on-set of diabetes [167,168]. These confounding studies maybe due to the fact that low TRAIL levels may pre-dispose people to type 2, whilst TRAIL levels maybe high in a chronic type 2 diabetes. Clinical relevance of TRAIL in other organs such as liver was also studied in diseases such as non-alcoholic steatohepatitis (NASH) patients. In this model of disease, it was found that DR5 expression in human livers are desensitised to TRAIL, thereby making this protein unable to confer its protective nature in the liver of NASH patients [169]. Concurrent to this study, our lab has also shown that, patients with NASH, identified by increased circulating alanine transaminase (ALT), had significantly reduced plasma TRAIL and a negative correlation was established between TRAIL and circulating ALT [170]. Furthermore, a clinical study was conducted in examining TRAIL's diverging relationship

between heart and kidney. In this study, patients undergoing heart transplant, serum TRAIL levels fell along with glomerular filtration rate which is a strong indicator of kidney function. This suggests that TRAIL has a systemic effect ranging from CAD to diabetes and kidney diseases [171]. Comprehending from the above-mentioned clinical findings, we can conclude that TRAIL plays an important role in metabolic and inflammatory diseases in human. Rather than it being just used as a diagnostic marker, TRAIL's intervention in these diseases would be the next logical step. However, to proceed to this step, understanding the mechanistic properties of TRAIL through various *in vivo* and *in-vitro* studies are essential.

1.5.3 **TRAIL role in *in vivo* studies**

To address changes observed in clinical studies several *in vivo* analyses was conducted to discover TRAIL's role and mechanisms in CVDs. As mentioned earlier atherosclerosis is the main root cause of many CVDs. Our lab was the first to show the importance of TRAIL against atherosclerosis. *Trail*$^{-/-}$*Apoe*$^{-/-}$ mice fed a 12-week HFD had significantly elevated plaque size in the brachiocephalic artery and the aorta which are main sites where plaque formation. These changes were observed in concurrence with increased plasma cholesterol, triglycerides and increased inflammatory markers such as IL-6 compared to the *Apoe*$^{-/-}$ control. This suggest that knockdown of TRAIL from an Apoe null mice exacerbates conditions favouring development of atherosclerosis [172]. Since atherosclerosis is chronic progressive condition spaning decades, where composition of the plaque changes, the role of TRAIL becomes important in how this protein tackles the changes occurring in the plaque. The 12-week HFD model showed that, the *Trail*$^{-/-}$*Apoe*$^{-/-}$ mice had characteristics of unstable plaque including macrophage accumulation at the shoulders of the plaque and increased caspase 3 activity, meaning these plaques had a more apoptotic environment. The plaque was also deemed unstable due to reduced collagen, thin fibrous cap and reduced smooth muscle cell content [172]. As the plaque progresses and witnesses the increased migration of VSMCs,

calcification/hardening of these cells accelerates the rupture of the plaque. The 20-week HFD model showed that *Trail*$^{-/-}$*Apoe*$^{-/-}$ mice had increased calcification in their plaques and up-regulation of RANK ligand which is responsible for vascular calcification [173]. These cross-sectional studies observing atherosclerosis at different stages showed that TRAIL gene deletion in the Apoe-null mice had a detrimental effect.

This study paved pay to look at TRAIL's role in type 2 diabetes *in vivo* as many markers observed in a diabetic model was seen in *Trail*$^{-/-}$*Apoe*$^{-/-}$ mice. Both *Trail*$^{-/-}$ and *Trail*$^{-/-}$*Apoe*$^{-/-}$ mice had hallmark sign of diabetes. Our lab has shown that, TRAIL deletion results in reduced glucose clearance and increased plasma cholesterol, glucose, insulin and triglycerides, which indicate features of type 2 diabetes. Global TRAIL deletion was resulted in insulin resistance due to impaired insulin signalling and glucose homeostasis [170,174]. Insulin resistance, a main characteristic of type 2 diabetes, can contribute to CVD, hypertension and metabolic diseases [175]

Furthermore, similar changes were observed with TRAIL's effect on type I diabetes or autoimmune diabetes. One study had used non-obese diabetic (NOD) mice and induced type I diabetes with cyclophosphamide (CY) injection. To block the action of TRAIL, soluble DR5 (sDR5) was injected. Mice injected with sDR5 showed accelerated development of diabetes and as a result had increased lesion in pancreas due to macrophage infiltrations. This study also saw when *Trail*$^{-/-}$ mice were injected with streptozotocin (STZ), there was again an accelerated development of diabetes along with inflammatory damage to the pancreas. These diabetic studies reveal the importance of TRAIL in managing the inflammatory environment which was seen as the major cause of accelerated type 1and type 2 diabetes [176]. The initial study on atherosclerosis as well as studies on type 1 and type 2 diabetes, saw an increase in plaque sizes when TRAIL was deleted.

A major physiological outcome of atherosclerosis and diabetes is ischaemia or the lack of oxygen supply to any part of the body. According to Diabetes Australia, 4,400 diabetes related amputations occur every year (http://www.diabetesaustralia.com.au). These amputations not only severely decrease the patient's lifestyle, it is also a major burden to the economy. A way to overcome ischaemia is to stimulate the development of collateral vessels, bypass the occlusion and improve blood flow to the lower extremities. My laboratory demonstrated that TRAIL plays an important role in this process. For example, *Trail*$^{-/-}$ mice had reduced capillary density 28 days after hindlimb ischaemic surgery. This was reflected by the blackened toes due to necrosis observed the *Trail*$^{-/-}$ mice. More importantly this study found that giving intra-muscular adenoviral TRAIL injections to wild type and *Trail*$^{-/-}$ mice after hindlimb ischaemia, improved blood flow to the leg. Further analysis revealed that blood flow was increased due to the presence of more capillaries (predominantly ECs) and VSMC remodelling in the ischaemic leg after TRAIL injection [177]. This finding established evidence that TRAIL can be used as a therapy to increase angiogenesis and prevent limb amputations. Table below summarises clinical and pre-clinical studies on TRAIL.

Clinical/ Pre-clinical	Disease	TRAIL's effect
Clinical studies	Coronary artery disease (CAD)	Low TRAIL levels (659.2±176.6 pg/mL) were seen in CAD patients [161] and GWAS study identified 11 loss of function single-nucleotide polymorphism of TRAIL in CAD patients [164].
	Acute coronary syndrome (ACS)	ACS patients have low serum TRAIL levels (57.1 pg/mL), establishing a negative correlation between ACS and sTRAIL [161,162].
	Heart Failure	Patients with TRAIL concentration below 44.6 ng/mL were considered at risk of heart failure and likely to die within the next 6-months after experiencing myocardial infraction [162].
Pre-clinical studies	Atherosclerosis	*Trail*$^{-/-}$ *Apoe*$^{-/-}$ mice on HFD had significantly elevated plaque size compared to the control *Trail*$^{-/-}$ *Apoe*$^{-/-}$ mice had unstable plaque phenotype. These mice had impaired glucose and cholesterol metabolism [172].
	Atherosclerosis	Research by Secchiero *et al.* (2006) showed that IP injection on 3µg of rTRAIL in Apoe$^{-/-}$ mice reduced atherosclerotic plaque and improved plaque stability by VSMC proliferation [178].
	Hind limb ischaemia (HLI)	*Trail*$^{-/-}$ mice had reduced blood supply following 28 days of hind limb ischaemia and adeno-viral TRAIL injection (10^9 plaque-forming units) in the gastrocnemius, 2-days before performing HLI improved blood flow. This suggests TRAIL plays an important role in improving angiogenesis which is severely impaired in CVD patients [177].

1.5.4 **TRAIL and *in-vitro* studies**

Clinical and pre-clinical studies have shown TRAIL to have a profound impact on the vasculature. Generally, TRAIL was considered a pro-apoptotic protein, capable of killing cells including ECs. *Li et al. (2003)* showed that when HUVEC were subjected to TRAIL treatment at 20 ng/mL, there was ~ 30% increase in cell death. With higher concentration of TRAIL, there was an increase in inflammatory and cell adhesion markers which was shown to be up-regulated due to NF-κB activation [179]. However, in the same year, *Secchiero et al.* (2003) published that TRAIL and its receptors promote endothelial proliferation and survival without the activation of NF-κB. Instead the authors suggested that the proliferative effect was due to p-Akt and p-ERK activation in these cells [158]. These confounding results were harder to explain as both studies had used same cell type, however with different sources and concentration of TRAIL.

The non-apoptotic function of TRAIL has been the focus in recent times with various research groups discovering and acknowledging the importance of TRAIL in the vascular tissue. Our lab has shown that TRAIL promotes angiogenic properties such proliferation and migration and increased tubule formation in human microvascular endothelial cell (HMEC-1) at physiologically relevant concentrations [180]. Our lab has also shown that these angiogenic properties on ECs are downstream to fibroblast growth factor (FGF) and involves NOX 4 and NO signalling [177]. A finding supported in other EC such as HUVEC where, proliferation and migration was seen at lower physiologically relevant concentration and apoptosis at a higher dose [181]; the higher concentrations were found to activate caspase-8. TRAIL was also observed to promote features required for angiogenesis such as tubule formation in a matrigel *in-vitro* model. TRAIL increased tubule formation compared to control and was similar to potent angiogenic factors such as VEGF and FGF. These results well support the findings

observed in the *in vivo* matrigel plug model where TRAIL supplementation in the plug along with growth factors such as VEGF and FGF increased angiogenesis [180].

The mechanism behind the positive role of TRAIL against CVDs and its associated co-morbidities is not well understood. An important marker instigating many of the above-mentioned diseases including diabetes and kidney disease is oxidative stress. Though not much is investigated into the role of TRAIL in oxidative stress, a study by Zauli *et al.* (2003) showed that TRAIL treatment increased eNOS activity and thereby NO production by the p-Akt pathway, which is essential to reduce oxidative stress and maintain a healthy endothelium [182]. Our lab has shown that TRAIL has the potential to increase NOX 4, which is usually involved in oxidative stress, however recent studies have shown that it can exert protective effect against CVDs [177]. Although isoforms of NOX are involved in ROS production, EC dysfunction and initiation of CVD, NOX 4 has been shown to exert a protective effect. For example, NOX 4 deletion in mice attenuated ischaemia-induced angiogenesis and increased pro-inflammatory cytokine production and signalling in endothelial and kidney cells [117,183]. In vitro, NOX 4, via its ability to produce H_2O_2 in low doses can also stimulate cell proliferation [177]. However, it is to be noted that, the amount of NOX 4 produced, and the surrounding environment will determine whether its' effect will be protective or deleterious to the vasculature. This dual role of NOX 4 needs further investigation. Further research is needed to analyse TRAIL's protective mechanisms against CVDs.

In regard to VSMCs, our lab pioneered in identifying non-apoptotic function of TRAIL in vascular cells. We have shown that at physiologically relevant concentrations, TRAIL can stimulate proliferation of VSMCs by regulating anti-apoptotic factor such as insulin-like growth factor-1 receptor (IGF1R), which requires activation of NF-κB *in-vitro* [184]. Other growth factors such as platelet derived growth factor-betta (PDGF-β) also stimulated VSMC proliferation and migration in a TRAIL dependant manner [185]. These research indicate that

TRAIL may play an important role in regulating VSMCs in atherosclerosis in an NF-κB dependant manner.

These findings indicate TRAIL's importance in vascular cells and their ability to tackle CVDs and its associated co-morbidities. Identification of TRAIL's mechanism of action and in the vasculature can pave way for TRAIL to be used as a therapeutic target in the fight against CVDs.

1.6 RESEARCH HYPOTHESIS

Several clinical models have shown that low circulating TRAIL levels are an indication of CVDs and other metabolic diseases [154-157]. Pre-clinical models have also shown TRAIL deletion to result in accelerated atherosclerosis, type 2 diabetes, NASH and other metabolic disorders. However, the protective mechanism of action on TRAIL against CVDs is unknown. In this thesis, we hypothesis that, TRAIL's key action is its ability to protect vascular function in CVD setting.

1.7 RESESARCH AIMS

To investigate the hypothesis, the following aims were identified:

i. Assess relationship between TRAIL and oxidative stress in healthy vs CAD patients

ii. Identify whether TRAIL deletion in mice affects features of endothelial dysfunction which includes oxidative stress, inflammation and vessel permeability.

iii. Identify whether TRAIL protects against AngII-induced oxidative stress and negates AngII-induced cell processes such as increased monocyte adhesion and permeability *in-vitro* in ECs.

iv. Identify the effect of EC-specific TRAIL deletion in vivo at baseline and following 12 -week HFD.

v. Identify the effect of VSMC-specific TRAIL deletion in vivo at baseline and following 12-week HFD.

Chapter 2: **Methods**

2.1 MATERIALS

All general reagents were analytical grade and purchased either from BDH or Sigma. Solutions were made with nano-pure water (nH2O) or Baxter water.

2.1.1 **Buffers**

Radio-Immunoprecipitation Assay (RIPA) buffer (x1)

RIPA buffer contained 50 mM of Tris-base, 150 mM of NaCl, 1% (w/v) of sodium deoxycholate, 100 mM of EDTA (Sigma-Aldrich, #E5134) and 0.1% of 10% (w/v) of SDS. The buffer was adjusted to pH 8.0. RIPA buffer also contained protease inhibitor cocktail (Sigma-Aldrich, #P2714) and phenulmethanesulfonyl fluoride (PMSF, Sigma-Aldrich, #P7626) in 1:1000 dilution.

PBST

Tween-20 (Sigma-Aldrich, #P1379) was added to 1x PBS to give a final concentration of 0.05% (v/v).

Antigen retrieval buffer

Antigen retrieval buffer consisted of 10 mM of sodium citrate tribasic dehydrate (Sigma-Aldrich, #C8532), 0.05% Tween 20, and the solution was adjusted to pH 6.0.

4x SDS protein loading sample buffer

1 mL of 0.5 M Tris-hydrochloric acid, pH 6.8 (Sigma-Aldrich, #T5941), 800 µL of 20% (v/v) SDS, 800 µL of (v/v) 100% glycerol (Sigma-Aldrich, #G5516) and 400 µL of 0.05% (v/v) bromophenol blue (Sigma-Aldrich, #B0126) were mixed.

Transfer buffer

100 mL of Tris- Glycine (10X) and 200 mL of methanol made up to 1 L with RO (Reverse osmosis) water.

Eicosanoid affinity column buffer

Eicosanoid affinity column buffer contained 13.3 g of potassium phosphate (dibasic) (Sigma-Aldrich, #P3786) 3.22 g potassium phosphate (monobasic) (Sigma-Aldrich, #P0662), 0.5 g sodium azide (Sigma-Aldrich, #S8032) and 29.2 g of sodium chloride (Sigma-Aldrich, #S5886) in 1 L of ultra-pure water. The buffer was adjusted to pH 7.4.

EIA buffer

EIA buffer contained 13.3 g of potassium phosphate (dibasic), 3.2 g of potassium phosphate (monobasic), 23.4 g of sodium chloride and 370 mg of EDTA, 100 mg of sodium azide and 1 g of bovine serum albumin in 1 L of ultra-pure water.

TBS

10x TBS solution was made by using 24 g Tris-hydrochloric acid, 5.6 g of Tris base, 88 g of sodium chloride in 1 L of distilled water. TBST solution was using 0.1% Tween 20 in 1x TBS solution.

Krebs-Henseleit Buffer

Krebs solution consists of 115 mM sodium chloride, 4.7 mM potassium chloride, 1.2 mM magnesium sulphate, 2.5 mM calcium chloride, 1.2 mM potassium phosphate

(monobasic), 25 mM sodium bicarbonate and 10 mM glucose. The solution is adjusted to pH 7.4.

2.2 HUMAN STUDIES

2.2.1 **Blood collection and ethics**

To understand the implications of circulating TRAIL, peripheral blood was collected from 9 patients presented at The Royal Alfred Hospital, Sydney Australia for a stable coronary artery disease (CAD). Blood was collected from 8 healthy individuals as controls. Blood collection and plasma extraction was performed by our collaborator in Cell Therapeutics group, Heart Research Institute. All procedure was conducted in accordance with the Sydney Local Health District Human Ethics Committee (Approval number X12-0241; Sydney, Australia).

2.2.2 **Human TRAIL ELISA**

Plasma samples collected was assessed for TRAIL concentration using the kit Human TRAIL/TNFSF10 Imunnoassay (Quantikine ® ELISA; DTRL00); based on a quantitative sandwich enzyme immunoassay using supplied plates pre-coated with a human monoclonal antibody specific for TRAIL. 50 μL of sample and standards were loaded onto pre-coated plates and incubated using an orbital shaker for 2 h at room temperature. All the wells were aspirated and washed three times, before the addition of human TRAIL conjugate (supplied in kit), followed by incubation for a further 2 h on the shaker. The plate was again emptied and washed 3 times, before addition of substrate solution for 30 min. Plates were protected from light, by covering with alfoil. Finally, stop solution was added. Colour change from yellow to green was ensured, and optical density measured at 450 nm with wavelength corrections made at 540 nm using a plate reader (CLARIO star, BMG Labtech).

2.2.3 **8-isoprostane purification**

Purification of 8-isoprostane in human plasma was essential before assessing the concentration. 8-isoprotense Affinity Columns (Cayman Chemicals; 401111) were obtained for purification. After the passage of the storage solution present in the column containing the affinity sorbent, the column was washed twice with eicosanoid affinity column buffer (2.1.1) followed by a wash with UltraPure water. Plasma samples were then applied to the column, followed by elution with 95% ethanol. The elution solution was evaporated until dry using a vacuum centrifuge (CT04-50-SR; CHIRST®) and dry nitrogen. The samples were then dissolved in EIA buffer (2.1.1) ready to be assessed for 8-isoprostane concentration.

2.2.4 **8-isoprostane ELISA**

8-isoprostane concentration was analysed using 8-isoprostane EIA kit (Cayman Chemicals; 516351). This assay is based on competition between 8-isoprostane and an 8-isoprostane-acetylcholinesterase (AChe) conjugate (8-isoprostane Tracer) for a limited number of binding sites. 50 µL of standards and 8-isoprostane eluted in EIA buffer, containing 8-isoprostane AChe tracer and 8-isoprostane EIA antiserum were incubated in the pre-coated plate over night at 4^0C. The plate was then emptied and washed five times. Following the wash, Ellman's reagent (supplied in kit) was added to all wells and colour developed in 90 min. The plate was read at 405 nm using a plate reader (CLARIO star, BMG Labtech). Sample values were calculated according to kit instruction, by performing a logistic four-parameter fit.

2.3 CELL CULTURE

2.3.1 **Propagation**

For this study an immortalized strain of human microvascular endothelial cells-1 (HMEC-1) was used. These cells were transfected with PBR-322-based plasmid containing coding region

for simian virus 40 A, and a large T antigen thereby making it immortalized. They were sourced from the Centre for Disease Control and Prevention (MTA M1224I). Cells were plated in T75 flask (Gibco) for propagation. Cells were incubated at 37^{o}C and at a 5% CO_2 humidified environment. HMEC-1 were propagated with 1:4 split after reaching 100% confluency. 1 mL trypsin was used to coat the flask and lift cells, whilst serum media was added to deactivate trypsin after the cells were lifted. No cells were used beyond passage 35.

2.3.2 **Cell culture media**

Human microvascular endothelial cells (HMEC-1), are a transformed cell line maintained until passage 95 without signs of senescence. Though this cell line behaves differently to ECs isolated from larger vessels, it retains most of the morphological, phenotypic and functional characteristics of a normal endothelium [186]

HMEC-1 cells were grown in MCDB 131 medium (Life technologies, 10372019), supplemented with epidermal growth factor (0.01 µg/mL; Life technologies, #PHG6045), 5 U/mL penicillin/streptomycin (Sigma Aldrich; P433), L-glutamine (2mmol/L) (Thermo Fisher; 25030081), hydrocortisone (500 µg/mL; Sigma-Aldrich, H0888) and 10% foetal bovine serum (Bovogen biologicals, SFBS-AU).

2.3.3 **RNA extraction of cells**

Cells grown in T75 flasks, were plated in a 6-well-plate (Corning). Total RNA from cells was extracted using Tri Reagent®. Media was removed, and cells washed twice with cold PBS. 1 mL of Tri Reagent® (Sigma-Aldrich; T9424) was added, to each well, and pipetted up and down to ensure collection of all cells. Lysates were frozen at -20^{0}C until ready for extraction, then, 200 µL of 1-bromo-3-chloro propane (Sigma Life Science; B9673) was added, vortexed for 15 s and rested for 5 min at room temperature. The solution was spun at 8500 rpm for 15 min at 4°C to separate into 2 different phases. The top phase (clear aqueous layer) was

transferred to a new tube and 500 µL (equal volume) of isopropanol (Sigma Aldrich; I9516) was added, vortexed for 15 s and incubated at room temperature for 1 h to allow RNA to precipitate. Samples were then spun at 8500 rpm for 20 min at 4°C. Supernatant was carefully removed without disturbing the pellet, and the pellet was washed with 70% (v/v) of ethanol. Ethanol was decanted, and the pellet was air dried. The pellet was then dissolved in 50 µL RNAase free water. Concentration of RNA was quantified using Nanodrop 2000c (Thermo Scientific) and the purity was measured by A260/280 ratio. After assessment of RNA concentration and purity, samples were either diluted to ensure equal concentrations with RNAase free water for cDNA synthesis or stored at -80°C for later use.

2.3.4 **cDNA synthesis from total RNA**

Following RNA extraction and quantification, cDNA was generated. For this conversion, the following substrates were added

Chemical	**Quantity (µL)**
5x iScript™ reaction mix (BioRad)	2
iScript™ Reverse Transcriptase (BioRad)	0.5
RNA	1
Nuclease free water	6

Samples were then placed into a T100™ Thermo Cycler (BioRad). The following temperatures were implemented:

Temperature	Duration
Lid was heated to 105ºC	
25ºC	5 min
42ºC	30 min
95ºC	5 min
4ºC	Until samples are retrieved

Samples were then diluted 1:5 with nuclease free water, before their usage in real time quantitative PCR.

2.3.5 **Quantitative real time PCR**

RNA expression was analysed using CFX96 Real-Time system (BioRad) and values were normalised to the house keeper genes. Reactions were performed in a final volume of 10 µL containing, 0.2 µL of forward and reverse primer at 10 µM, 3.6 µL of nuclease free water, 5 µL of IQ^{TM} SYBR Green Supermix (Bio-Rad, #1708880) and 1 µL of cDNA sample. Relative gene expression was calculated using ΔΔ Ct method. qPCR conditions were maintained as follows:

Hold: 95ºC, 3 min

Melt: 95ºC, 15 seconds

Anneal/Extension: 60ºC, 60 seconds

Melt and Anneal/Extension steps were repeated 40 times in total

2.3.6 **Primer sequences**

Human primers

Gene	Forward primer (5' to 3')	Reverse primer (5' to 3')
GAPDH	GAAGGCTGGGGCTCATTT	CAGGAGGCATTGCTGATGAT
ICAM-1	GTATGAACTGAGCAATGTGC AAG	GTTCCACCCGTTCTGGAGTC
VCAM-1	TTTGACAGGCTGGAGATAGA CT	TCAATGTGTAATTTAGCTCGGCA
VE-cadherin	CAGCCCAAAGTGTGTGAGAA	CGGTCAAACTGCCCATACTT
NOX-5	GCAGTCTTTCTGGGACCTGT	GGTGCCTCTACAGCCTTCAG
NOX-4	CTGGAGGAGCTGGCTCGCCA ACGAAG	GTGATCATGAGGAATAGCACCAC CACCATGCAG
eNOS	AGCACCGGAGCCTAGC	AGGGCCCATCCTGCTGAG

2.3.7 **BCA protein assay**

Bicinchoninic acid (BCA) assay was used to determine the protein concentration of samples prior to sample loading for Western blotting. Bovine serum albumin (BSA) (Thermo Scientific; #23209) was used to as a standard in a 96-WTP. RIPA buffer diluted with RO water in a 1:1 ratio was used as a diluent for standards and lysates. 200 µL of Pierce® BCA (Thermo Scientific; #23209) was added to each well containing copper II sulphate ($CuSO_4$) (Sigma Aldrich; C2284) at a 50:1 ratio. The plate was incubated at 37°C for 1 h. Colour changed was observed and the plate was read at 570 nm using a plate reader Clario Star (BMG Labtech). A

standard curve was used to determine protein concentration in the samples. To maintain equal loading, sample concentration was adjusted using RIPA buffer.

2.3.8 **Western blotting**

Prior to extraction, cells were washed with ice-cold PBS and scraped with a cell scraper. Aortic tissue, frozen upon extraction was lysed in ice-cold PBS using Fastprep-24 Instrument (MP Biomedicals). BCA protein assay was performed as described above to determine the concentration of proteins. Protein lysates were lysed by pushing through a 23-guage needle and were mixed with 4x SDS sample loading buffer and 2-mercaptoethanol (Sigma; M3148) followed by boiling at 95^{o}C for 5 min. Protein samples were loaded into pre-cast polyacrylamide gel Bolt^{TM} 4-12% Bis-Tris Plus (Invitrogen; NW04120). 5 µL of Precision Plus Protein Kaleidoscope^{TM} (Bio Rad; #161-0375) marker was loaded onto one well. Gels were placed in a mini gel tank (Life Technologies) with buffer MES-SDS running buffer (Life Technologies; B0002) until proteins were separated. Once protein separation was achieved, proteins were transferred to a nitrocellulose membrane using the iBlot Gel Transfer system (Invitrogen). Membranes were incubated for non-specific binding protein with either 5% BSA in TBST for 1 h. Membranes were then incubated with primary antibody overnight, followed by three 5 min wash with TBST and 1 h horseradish peroxidase-conjugated secondary anti-mouse (Dako) or anti-rabbit (Dako) and visualised using chemiluminescence (ChemiDoc^{TM} MP imaging system; BioRad). The primary antibody, its dilution and duration of incubation is given in the table below.

Antibody	Catalog/Supplier	Dilution	Duration
Anti-VE Cadherin antibody	ab33168/Abcam	1:1000	Over-night
Monoclonal Anti-β-actin antibody	A5316/ Sigma-Aldrich	1:10,000	25 min

2.3.9 **Monocyte adhesion assay**

Confluent layer of HMEC-1 were grown on glass cover slips, followed by serum-starvation. Cells were then subjected to Ang II (50 ng/mL) for 2 h, with and without over-night pre-treatment of TRAIL (1 ng/mL). Buffy coat (Red Cross Blood Bank) was used to isolate human monocytes as described previously [187]. Monocytes were stained with CellTrace™ CFSE (5μM) (Invitrogen; C34554) for 1 h were plated on the monolayer of cells at a concentration of 2 million cells/ml. Cells were then incubated with monocytes for 2 h and the cover slips were washed in HBSS 1387 (Sigma-Aldrich, #H1387) by gently dipping them, following fixing cells in 10% formalin. Images of monocytes attached to a monolayer of ECs were taken using Olympus microscope at 20x magnification. Minimum of three field of views were obtained per treatment, per experiment. Monocyte attached (fluorescent green) was counted in each field of view and averaged per condition.

2.3.10 **DHE staining of cells**

To analyse cytosolic oxidative stress produced *in vitro*, dihydroethidium (DHE) (Thermo Fisher; D11347) was used. I DHE was initially dissolved in dimethylsulfoxide (DMSO) to a concentration of 5 mM. This stock solution was stored at -20^{o}C. Before staining, cells were washed twice with warm PBS and adherent cells were lifted using trypsin EDTA. Cells were

then spun in glass tubes at 10,000g for 10 min to remove the trypsin. DHE stock solution was mixed with HBSS to a concentration of 10 µM and added to the cell pellet. The glass tube was gently shaken to ensure dissolution of the pellet in the solution. The solution was incubated for 25 min in a tissue culture incubator maintained at 37°C and a 5% CO_2 humidified environment. Florescence was analysed using the BD FACS Verse™ (BD Bioscience). BD FACSuite™ CS&T Research beads (BD Bioscience) was used to initialise and calibrate the flow cytometer before samples were run.

Gating strategy for DHE staining

10,000 events/ samples were collected. Live cell population was identified on an SSC-A (side scatter area signal) vs FSC-A (forward scatter area signal) and were selected with a round gate (Figure X). Gated cells were displayed on a histogram to monitor DHE fluorescence, which is at a 318 nm excitation and at an emission of 605 nm **(Figure 2.1)**.

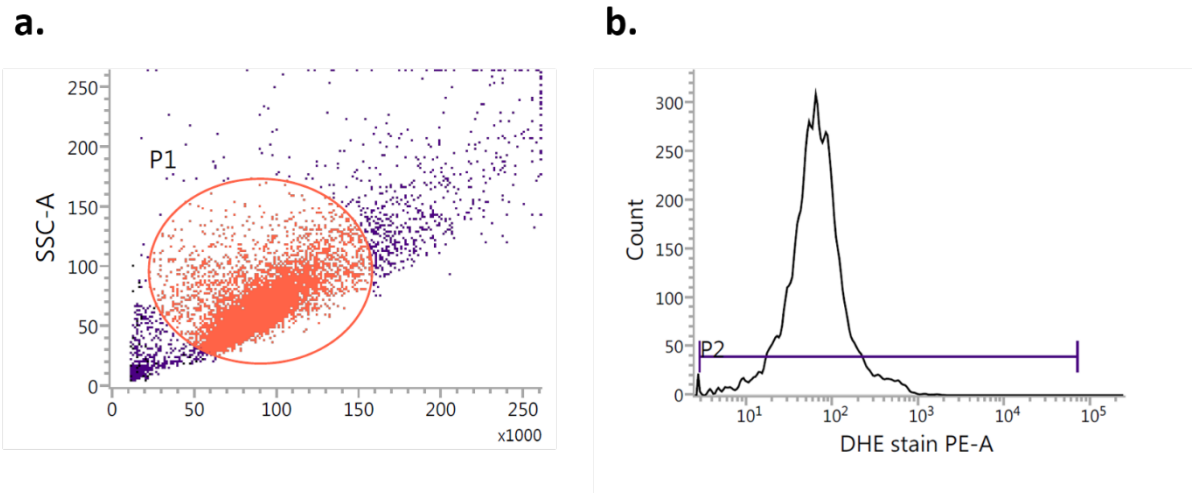

Figure 2.1 Gating strategy for DHE fluorescence staining. (a) Live cell population was gated on an SSC-A vs FSC-A graph. **(b)** DHE fluorescence of the gated population at 318 nm excitation and an emission of 605 nm on the histogram.

2.3.11 **Mitosox staining of cells**

To analyse mitochondrial superoxide production, MitoSOX™ (Thermo Fisher; M36008) was used. The stock solution was prepared by dissolving MitoSOX™ with DMSO to a concentration of 5 mM which was stored at -20°C. Similar to DHE staining, cells were prepared and dissolved with MitoSOX™ stain at a working concentration of 5 μM. Florescence was analysed using the BD FACS Verse™ (BD Bioscience) with absorption at 510 nm and emission at 580 nm. Gating strategy is same as described in section 2.3.10.

2.4 ANIMAL STUDIES

2.4.1 **Animal housing**

All animals were bred at Australian BioResource (Moss Vale, NSW Australia). At 5 -8 weeks of age, animals were transported to the Heart Research Institute (HRI) by in-house Australian BioResource van. Animals at HRI were grouped to a maximum of 5 mice, in OptiMice Hepa filter system. The animals were conditioned for a fixed 12-hour light/dark cycle and temperature was maintained at 21^{o}C. Animals had ad libitum access to food and water.

2.4.2 **Genotypes of mice**

This thesis made use of number of different genotypes of mice. They were:

Genotype	Use
Trail$^{+/+}$*Apoe*$^{-/-}$, *Trail*$^{-/-}$*Apoe*$^{-/-}$ (Males) (n = 6)	Myography
Trail$^{+/+}$*Apoe*$^{-/-}$, *Trail*$^{-/-}$*Apoe*$^{-/-}$ (Males) (n = 3)	Aortic DHE staining
Trail$^{+/+}$; *Trail*$^{-/-}$ (Females) (n = 6-7/group)	Vessel permeability
Trail$^{+/+}$; *Trail*$^{-/-}$ (Males) (n = 4)	Aortic mRNA extraction
Trail$^{EC+/+}$, *Trail*$^{EC-/-}$ (Males) (n = 4-5/group)	Baseline study
Trail$^{EC+/+}$, *Trail*$^{EC-/-}$ (Males) (n = 6-12/group)	12 w HFD study
Trail$^{VSMC+/+}$, *Trail*$^{VSMC-/-}$ (Males) (n = 4-5/group)	Baseline study
Trail$^{VSMC+/+}$, *Trail*$^{VSMC-/-}$ (Males) (n = 4-11/group)	12 w HFD study

EC: *Endothelial cells;* ***VSMC****: Vascular smooth muscle cells;* ***HFD****: High Fat Diet*

2.4.3 **Animal ethics**

All methods involving mice were carried out in accordance with the National Health and Medical Research Council of Australia guidelines. Experimental protocols were approved under the following ethics:

	Ethics number
University of New South Wales	11-71B
Sydney Local Health District Animal Welfare Committee	2013-020
Sydney Local Health District Animal Welfare Committee	2014-027
Sydney Local Health District Animal Welfare Committee	2017-020

2.4.4 Cell-specific TRAIL gene deletion mice

Endothelial cell-specific TRAIL gene deletion

To identify the role of TRAIL in the vascular endothelium *in vivo* endothelial-specific TRAIL gene deleted mice were created using Cre/Lox breeding system in a C57bl/6 background. TRAIL gene consists of 5 exons. Exon 5 was flanked with insertion of LoxP site on either of its ends. This genotype mouse was crossed with VE-cadherin promoter - Cre transgenic mice. Since VE-cadherin is expressed exclusively in the vascular endothelium, these cross enables TRAIL gene to be deleted in cell expression VE-cadherin, i.e ECs. The cross resulting in EC-specific TRAIL gene deleted mice is shown in **Figure 2.2**.

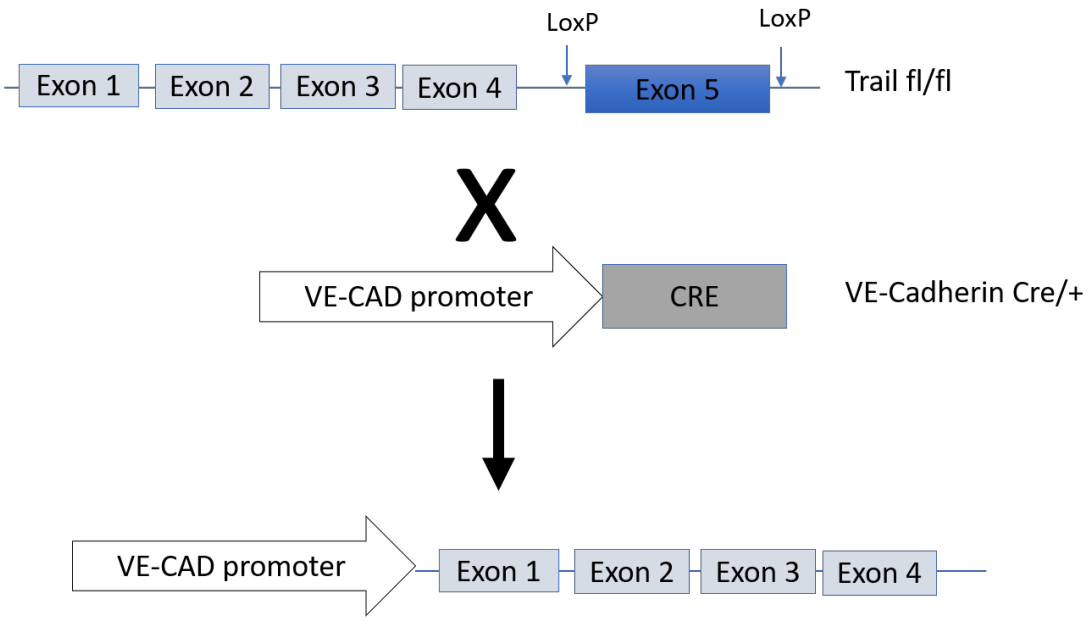

Figure 2.2 Gene cross of EC-specific TRAIL deleted mouse. Cre-Lox system used to cross TRAIL exon 5 deleted mouse with Cre-VE-cadherin mouse to yield EC-specific TRAIL deleted mouse.

An example of the breeding strategy for *Trail*$^{EC-/-}$ mice is below. An identical strategy was used to generate *Trail*$^{VSMC-/-}$

F1 *Trail*$^{flox/flox}$ x *Trail*$^{+/+}$ VEC Cre/+

Offspring possibilities include:

- Trail$^{flox/+}$ VEC Cre/+
- Trail$^{flox/+}$ VEC +/+

F2 Trail$^{flox/+}$ VEC Cre/+ x Trail$^{flox/+}$ VEC Cre/+

Offspring possibilities include:

- *Trail*$^{flox/flox}$ VEC Cre/+*Trail*$^{flox/+}$ VEC Cre/+
- *Trail*$^{+/+}$ VEC Cre/+
- *Trail*$^{flox/flox}$ VEC+/+
- *Trail*$^{flox/+}$ VEC+/+
- *Trail*$^{+/+}$ VEC+/+

Our control mice were littermate control *Trail*$^{+/+}$ VEC Cre/+ mice. All on a C57Bl6 background.

Vascular smooth muscle cell-specific TRAIL gene deletion

To identify the role of TRAIL in the vascular smooth muscle cells (VSMCs) *in vivo*, vascular smooth muscle cell-specific TRAIL gene deleted mice were created using Cre/Lox breeding system in a C57bl/6 background. TRAIL gene consists of 5 exons. Exon 5 was flanked with insertion of LoxP site on either of its ends. This genotype mouse was crossed with transgelin promoter- Cre transgenic mice. Since transgelin is expressed exclusively in the VSMCs, these cross enables TRAIL gene to be deleted in cell expression transgelin, i.e VSMCs. The cross resulting in VSMC-specific TRAIL gene deleted mice is shown in **Figure 2.3**.

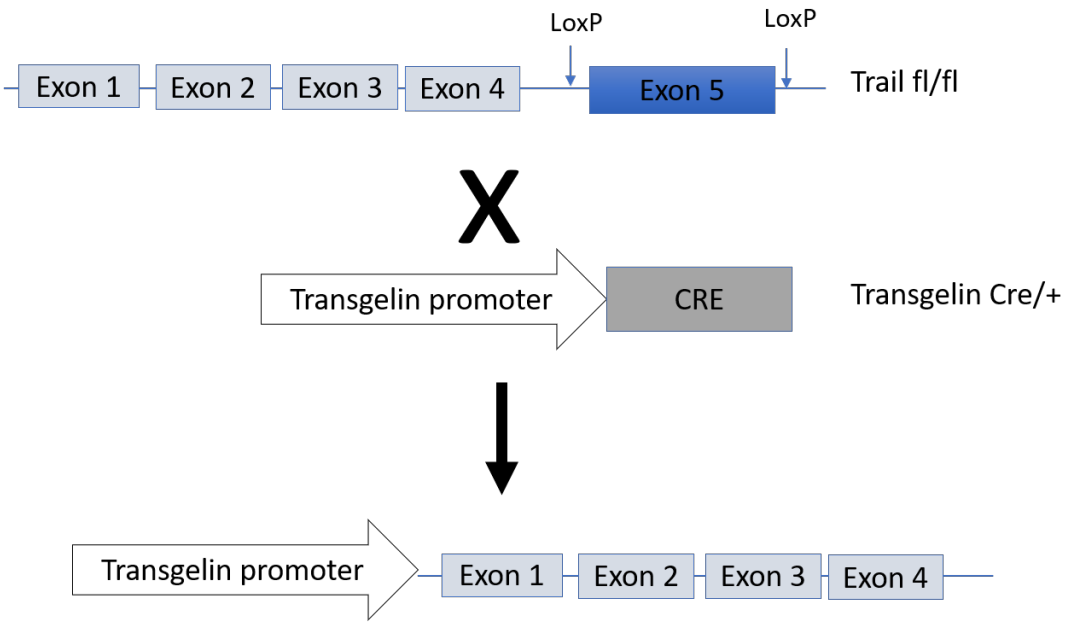

Figure 2.3 Gene cross of VSMC-specific TRAIL deleted mouse. Cre-Lox system used to cross TRAIL exon 5 deleted mouse with Cre-Transgelin mouse to yield VSMC-specific TRAIL deleted mouse.

2.4.5 **High fat feeding study**

Animals were brought to HRI at 5 weeks of age and acclimatised for a week. At 6 weeks, body weights were recorded, and mice placed on 12-week high fat diet (HFD, SF00219; Specialty Feeds). For the next 12 weeks animals were weighed and monitored on a weekly basis. Before euthanasia, animals were fasted overnight. Blood glucose and weights were recorded just before euthanasia. Animals were anaesthetized using isoflurane (3-4%), and euthanised via cardiac exsanguination. Blood collected were stored in EDTA tubes, spun and plasma collected, snap frozen using liquid nitrogen and stored at -80^{0}C. Sections of liver and heart were fixed in OCT, formalin and snap frozen in liquid N_2 whilst other organs including spleen, fat, pancreas, intestine, colon, retro fat, kidney, lung, aorta, muscle and eye were processed in 10% formalin and snap frozen in liquid nitrogen (N_2). This experiment was performed in accordance with ethics protocol 2017-020.

2.4.6 **Blood pressure measurement**

Blood pressure was measured via a tail cuff in mice fed an HFD between week 10 and 12 w. Mouse and Rat Tail cuff Blood Pressure (MRBP) system (IITC Life Science) was used. Chambers were kept warm at a temperature of 32^{0}C. Animals were placed in the chamber, and lights were turned off to ensure a dark, stress-free environment prior to blood pressure measurements. Mice were restrained with the cuff attached to their tail and given a chance to settle down in their new environment for 5 min. The start pressure was set at 150 mm of Hg and the termination pressure was set at 30 mm of Hg. The trigger level was set at 100 mv; the experiment was typically run 3 times with a gap of 10 s between experiments. Systolic pressure, diastolic pressure, mean arteriole pressure (MAP) and heart rate were recorded by the machine. Multiple measurements were obtained to identify and exclude stress and movement related pressure spikes. It was crucial to identify a good blood pressure reading and determining the

systolic and diastolic points in the wave graph generated by the system. The consistently appearing lower amplitude wave just before a series of higher amplitude wave was assigned the systolic pressure. The higher amplitude waves were assigned diastolic pressure. The correct identification of wave graph is depicted below in **Figure 2.4**.

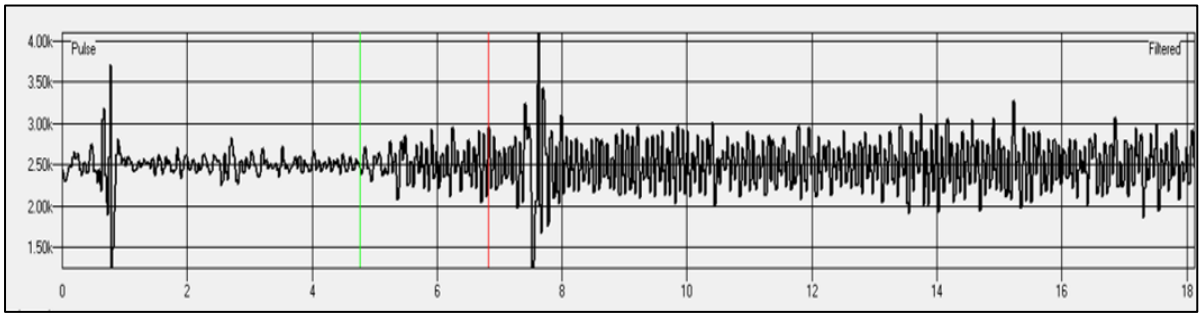

Figure 2.4. Identification of systolic and diastolic wave points. Systolic wave point is defined as the lowest amplitude wave right before the increase in frequency of waves. This is indicated by the green line in the figure above. The diastolic wave point is defined as the highest consistent amplitude wave immediately after the systolic wave point. This is indicated by the red line in the above figure.

2.4.7 **Glucose and insulin tolerance**

Prior to the end of the 12 w HFD, at 10 and 11 weeks, glucose tolerance test (GTT) and insulin tolerance tests (ITT) were carried out respectively [170]. For GTT, mice were fasted overnight, transferred to a new cage with only ad libitum water. Overnight fasting was not required for ITT. Mice were injected intraperitoneally with 1 g/kg body weight of D-glucose (Sigma Aldrich) for GTT, or 1 U/kg of human insulin for ITT. Blood glucose was measured at baseline, 15, 30, 60 and 120 min after administration of glucose/insulin via tail nick using a glucometer (Accu-check Performa; Roche). Water was not supplied for the duration of the experiment.

2.4.8 **RNA extraction of mouse aorta**

RNeasy® Fibrous Tissue Mini Kit (Qiagen, 74704) was used to extract RNA from snap frozen aortic tissue. Buffers (including RLT, RW1 and RPE) and reagents were supplied with the kit. Snap-frozen tissue was homogenized in 300 µL RLT buffer containing 1% (v/v) 2-Mercaptoethnaol (Sigma Life Science; M3148) in a 1.5 mL tube containing ceramic beads (MP Biomedicals; 6913-500) using Fastprep-24 Instrument (MP Biomedicals). Tissue lysate were transferred to an autoclaved 1.5 mL eppendorf tube. Lysate were then mixed with RNase free water containing proteinase K (1:60 dilution) and incubated at 55^0C for 10 min. Samples were spun at 10,000 g for 3 min, supernatant collected and mixed with 0.5 volume of absolute ethanol. The lysate was then transferred through the RNeasy column (supplied in kit) and washed multiple times with RW1 and RPE buffer according to the supplied protocol. Finally, RNA was eluted from the column with 50 µL of RNase-free water. RNA was assessed for concentration and converted to cDNA as described in section 2.3.3.

2.4.9 **Primer sequence**

Mouse primers

Gene	Forward primer (5' to 3')	Reverse primer (5' to 3')
β-actin	AACCGTGAAAAGATGACCCAGAT	CACAGCCTGGATGGCTACGTA
α-SMA	GTCCCAGACATCAGGGAGTAA	TCGGATACTTCAGCGTCAGGA
α-tropomyosin	AGCTCGACAAAGAGAACGCC	ATCTTCCAGCTGCTTGCTCC
eNOS	AGCACCGGAGCCTAGC	AGGGCCCATCCTGCTGAG

iNOS	CGAAACGCTTCACTTCCAA	TGAGCCTATATTGCTGTGGCT
MYH-10	GAAGAGCGGAACCAGATCCTAC	TAGCCTCTGCTGTCACCTTCTC
MYH-11	AAGCTGCGGCTAGAGGTCA	CCCTCCCTTTGATGGCTGAG
KLF-4	CTATGCAGGCTGTGGCAAAACC	TTGCGGTAGTGCCTGGTCAGTT
KLF-5	AGCTCACCTGAGGACTCATACG	AGAAGCTGCGTTGGCACACCAT
ICAM-1	GTGATGCTCAGGTATCCATCCA	CACAGTTCTCAAAGCACAGCG
VCAM-1	TTGGGAGCCTCAACGGTACT	GCAATCGTTTTGTATTCAGGGGA
IL-1β	GTTTCTGCTTTCACCACTCCA	GAGTCCAATTTACTCCAGGTCAG
VE-cadherin	TCCTCTGCATCCTCACTATCACA	GTAAGTGACCAACTGCTCGTGAAT
NOX 1	AATGCCCAGGATCGAGGT	GATGGAAGCAAAGGGAGTGA
NOX 2	CCCTTTGGTACAGCCAGTGAAGAT	CAATCCCGGCTCCCACTAACATCA

2.4.10 **Myography**

Myography was performed on *Apoe*$^{-/-}$ and *TRAIL*$^{-/-}$*Apoe*$^{-/-}$ mice on a 12 w HFD to measure the percentage of relaxation in response to acetylcholine (ACh) and sodium

nitroprusside (SNP). This part of the study was performed by our collaborators from the Redox Cell Signalling group, Centre for Vascular Research, UNSW.

Thoracic aortas of mice were placed in Krebs-Henseleit buffer solution. Adherent connective tissue and fat surrounding the aorta was removed. Following this, aortas were cut into ~2 mm aortic rings and mounted into individual organ chambers of a MultiMyograph 610M Myobath (Danish Myo Technology). PowerLab data acquisition system (AD instruments) was used to record changes in isometric tensions. Aortic rings were equilibrated for 60 min and then maintained at a baseline tension of 9.8 mN for a further 30 min. Following this, aortic rings were exposed to high potassium salt solution (KPSS; equimolar substitution of potassium chloride and sodium chloride) 3 times, to achieve consistent maximal contraction. Aortic rings were washed with KHB solution between each KPSS wash for the rings to return to baseline tension. Isometric tension was applied to the aortic rings and monitored by a force transducer. The tension was slowly increased until it reached a resting or baseline tension of 9.8mN which was maintained for the rest of the experiment. Finally, ACh and SNP were supplied in increasing doses after a KPSS wash to measure percentage of relaxation by PowerLab.

2.4.11 **Vessel Permeability**

Evans blue experiment, a test for blood vessel permeability was carried out in accordance with Radu et al [188]. 8-12-week-old *Trail*$^{-/-}$ and littermate controls were injected with 200 µL of 0.5% sterile solution of Evans blue (Sigma Life Science; E2129) in PBS. After 30 min, mice were anaesthetized with isoflurane (3-4%) and euthanised via cervical dislocation. Organs collected were either fixed in 10% formalin (Sigma-Aldrich, #HT501128) or incubated at 55^{0}C for 48 hours in formamide (deionized) (Ambion®; #AM9342) to measure the intensity of dye leakage at 610 nm using a plate reader (CLARIO star, BMG Labtech). Organs collected include

brain, heart, lung, liver, spleen, intestine, colon, kidney and skin. This experiment was performed in accordance with ethics protocol 2017-020.

2.4.12 **Cholesterol assay**

Collected plasma samples from the animals were used to detect cholesterol concentration in serum using LabAssay^{TM} Cholesterol (Wako) kit. The samples were processed in accordance with the kit and colorimetric analysis was done at 600nm using a plate reader (CLARIO star, BMG Labtech).

2.4.13 **Insulin assay**

Collected plasma samples from the animals were used to detect insulin concentration in serum using Mouse Inulin ELISA (Mercodia, 10-1247-10), a solid phase two-site enzyme immunoassay. Calibrators in the kit was used as standards whist peroxidase conjugated mouse monoclonal anti-insulin was used as the enzyme conjugate. The bound conjugate was detected by reaction with 3,3',5,5'-tetramethylbenidine, while an acid was added to give a colorimetric endpoint. The samples were then analysed at 450 nm using a plate reader (CLARIO star, BMG Labtech).

2.4.14 **Nitrate/nitrite assay**

Collected plasma samples from mice were used to detect nitrate/nitrite concentration in serum using the Nitrate/Nitrite colorimetric assay kit (Cayman chemicals, 780001). The assay works on the principle of converting nitrate in the plasma to nitrite by nitrate reductase. This was followed by adding Griess reagents which converts the nitrite in the plasma into deep purple azo compound. A nitrate standard curve was set up ranging from 0 to 35 µM in concentration. Plasma samples were diluted 1:2 with the assay buffer before plating. 10 µl of enzyme cofactor mixture and 10 µL of nitrate reductase was added to each well (standards and unknown) and

incubated for 3 h at room temperature. After incubation, 50 µL of Griess reagent R1 and R2 was added. Colour developed in 10 min and the samples were analysed at 550 nm using a plate reader (CLARIO star, BMG Labtech).

2.4.15 **DHE staining of aortas**

Isolated frozen aortas were cut into 5 µm sections and incubated with Krebs solution for 15 min at 37ºC, followed by DHE (5 µM; Life Technology, ThermoFisher Scientific) for a further 30 min at 37ºC. Tissue sections were washed 3X in phosphate buffed saline (PBS), and once with water. Fluorescent images were captured using a DP72 Camera (Olympus) on an Olympus BX 53 fluorescence microscope using a filter with an emission range of 570–640 nm. NIH Image J was used to quantify DHE red fluorescence staining per field of view.

2.4.16 **Histology**

Tissue processing, embedding and cutting

Organs in formalin overnight were transferred to 70% ethanol closed in cassettes, for immediate or future use. The tissue processing system (Leica biosystems; TP1020) was used for processing prior to embedding in paraffin. The following program was used to process the tissue:

Reagent	**Duration**
70% Ethanol	1 h
80% Ethanol	1 h
95% Ethanol	1 h 15 min
Absolute ethanol	3 x 1 h
Xylene	2 x 1 h 30 min

Paraffin	2 x 2 h

After processing, the embedder (Leica biosystems; EG1150C) was used to embed organs in paraffin, which were cooled to form blocks. Aortas were embedded to achieve cross-section when cut.

Paraffin embedded samples were placed on wet ice 1 h prior to cutting. HM 200 Microm microtome (Ergostar) was used to cut blocks in 5 µm sections and floated on warm water (42^{o}C). Starfrost® slides (ProSciTech) were used to mount the section. Slides were checked immediately under Olympus microscope (CKX41), to ensure there was no folded tissues. Slides were left to dry over night at 42^{o}C and stored at room temperature for future use.

Deparaffinization and hydration

All slides prior to any stain were deparaffinized and hydrated. The protocol for the procedure is listed below:

Protocol	**Duration**
Xylene	2 x 10 min
Absolute ethanol	2 x 2 min
90% ethanol	2 x 2 min
70% ethanol	1 x 2 min

Dehydration and mounting

Following staining protocol, slides were dehydrated with increasing concentration of alcohol as listed below:

Reagent	Duration
1. Slides were dehydrated through increasing concentrations of alcohol a. 70% ethanol b. 90% ethanol c. Absolute ethanol	 2 x 2 min 2 x 2 min 2 x 2 min
2. Slides were placed in xylene	2 x 10 min

Following this procedure, slides were mounted with coverslips (Automat-Star) using mounting media DPX (Sigma; 06522). Slides were left to dry over-night at room temperature before imaging was performed. Imaging was performed using Axio scanner (Zeiss Axio Scan Z1) at x20 magnification (objective magnification). The experimenter was non-blinded.

Hematoxylin and eosin (H&E) stain

H&E analysis was performed to analyse the aortic architecture. Slides were deparaffinized and hydrated and the stain was performed according to the table below.

Reagent	Duration
Haematoxylin	3 min
Water	2 x 2 min
Acid alcohol	3 quick dips
Water	1 dip

Scott's blue	30 s
70% ethanol	1 x 2 min
Eosin	2 x 40 s
95% ethanol	4 dips
Absolute ethanol	4 dips
Xylene	2 x 10 min

Slides were then dehydrated and mounted. For H&E stained slides, aortic cell wall thickness was measured using Image Pro® (Premier version 9.2).

Elastin staining

Elastin staining was performed on baseline and 12 w HFD mice to assess the presence or absence of breaks in elastin fibres, which is an indication of vascular disease. Slides were first deparaffinized and hydrated before starting the procedure. Elastin staining procedure was done according to the kit (Sigma; HT25A)

Protocol	**Duration**
1. Slides were placed in Working elastin stain solution, which contains 20 mL hematoxylin solution (alcoholic), 3 mL ferric chloride solution, 8 mL Weigert's iodine solution and 5 mL deionized water	10 min
2. Slides were rinsed in deionized water	

3. Slides were dipped in working ferric chloride solution (3 mL of ferric chloride with 37 mL of deionized water) for differentiation of sections. Slides were microscopically checked to ensure differentiation	
4. Slides were rinsed in 95% ethanol	
5. Slides were rinsed in deionized water	
6. Slides were placed in Van Gieson solution	3 min
7. Slides were rinsed in 95% ethanol	

Slides were then dehydrated and mounted. For Elastin staining, after selecting the area of the aorta, threshold colour (i.e. purple) was chosen using dropper function using Image Pro® (Premier version 9.2). Data was expressed as percentage area stained. Breaks in elastin layer in the aortic wall was also quantified.

Picrosirius Red Stain

Picrosirus red stain was used to stain for collagen type 1 and 3 in aortas of 12 w HFD and baseline mice [189]. Slides were first deparaffinized and hydrated before starting the procedure. The protocol was followed based on Picrosirius red stain kit (Polysceince, Inc.; 24901)

Protocol	Duration
1. Slides were stained using Weigerts Hematoxylin stain	8 min
2. Slides were rinsed in distilled water	

3. Slides were placed in solution A (Phosphomolybdic acid).	2 min
4. Slides were rinsed in distilled water	
5. Slides were placed in solution B (Picrosirius Red F3BA stain)	1 h
6. Slides were then placed in solution C (0.1N of hydrochloric acid)	2 min
7. Slides were then placed in 70% ethanol	45 s

Slides were then dehydrated and mounted. For collagen staining, after selecting the area of the aorta, threshold colour (i.e. dark red) was chosen using dropper function using Image Pro® (Premier version 9.2). Data was expressed as percentage area stained.

2.5 STATISTICAL ANALYSIS

All analysis was performed on GraphPad Prism Version 7.0 (GraphPad Software). All data was tested for normality using Shapiro-Wilk normality test. Statistical comparisons were made either using Students *t*-test, Mann-Whitney *U*-test, one or two-way ANOVA. All results were expressed as mean ± SEM, unless otherwise stated. Statistical outliers in data set was excluded by Grubb's test. A value of $p<0.05$ was considered as significant result.

Symbol	**p-value**
*	$p<0.05$
**	$p<0.01$

***	$p<0.001$
****	$p<0.0001$

Chapter 3: **TRAIL's role against oxidative stress in clinical and pre-clinical models**

3.1 INTRODUCTION

The results from this chapter are part of a publication in "Free Radical Biology and Medicine", under the title **"TRAIL inhibits Angiotensin-II-induced oxidative stress and inflammation in vascular endothelial cells."** [190].

Endothelial cells (ECs) are critical for cardiovascular homeostasis by maintaining an anti-thrombotic, anti-inflammatory and anti-atherogenic state within the vessel wall [191], and endothelial dysfunction is a clinically relevant early indicator of atherosclerosis [192]. Oxidative stress mediates reactive oxygen species (ROS), which are chemically active compounds containing oxygen and are implicated in endothelial dysfunction [191]. Identifying novel stimuli that protect the vascular endothelium against ROS-induced dysfunction is an attractive strategy for development of new therapeutics against cardiovascular disease.

TRAIL is a protein discovered and named for its ability to promote cell death by binding to its specific death receptors [193]. However, work from our laboratory and others have shown that TRAIL stimulates EC proliferation and migration *in vitro* and *in vivo* [194-196], and importantly plays an overall protective role in CVD. Patients with CVD and its complications have reduced circulating TRAIL concentrations [163,168,197], and mice lacking TRAIL exhibit accelerated atherogenesis [172]. The mechanisms by which TRAIL regulates EC function and protects against atherosclerosis are unclear. In this chapter, multiple approaches were used to identify the protective role of TRAIL on the vasculature, particularly the endothelium. We aim to establish a relationship between TRAIL and oxidative stress in human

samples and to investigate if TRAIL deletion in mice promotes oxidative stress and endothelial dysfunction in an *in vivo* model.

3.2 BRIEF METHODS

3.2.1 **Human TRAIL and 8-iso prostaglandin F2α ELISA**

Human plasma was collected from healthy and CAD individuals under ethics X12-0241; Sydney, Australia. Plasma was purified and assessed for TRAIL and 8-*iso* prostaglandin $F_{2\alpha}$ circulating concentration as described in the method sections 2.2.2, 2.2.3 and 2.2.4.

3.2.2 **Myography**

To detect endothelial function in *Apoe*$^{-/-}$ and *Trail*$^{-/-}$*Apoe*$^{-/-}$ mice myography was performed as described in method section 2.4.10.

3.2.3 **DHE aortic staining**

5 μm frozen aortic section was incubated with Krebs solution for 15 minutes at 37^{o}C. Sections were then stained with 5 μM of DHE for a further 30 min and at 37^{o}C and then washed with PBS followed by water. Sections were imaged using DP73 Camera (Olympus) on an Olympus BX 53 fluorescent microscope using a filer with an emission range of 570-640 nm. NIH Image J was used to quantify the fluorescence.

3.2.4 **4-Hydroxyneal ELISA**

Mouse aortas (males) were lysed with RIPA buffer containing PMSF (1:100) and protease inhibitor cocktail (1:100). Lysates were then used to detect 4-hydroxyneal (HNE) concentration using OxiSelect^{TM} HNE adduct competitive ELISA kit (Cell Biolabs, Inc.) Absorbance was read at 450 nm using a plate reader (Clario Star, BMG Labtech).

3.2.5 **Vessel permeability**

Vessel permeability was detected in *Trail*$^{+/+}$ and *Trail*$^{-/-}$ female mice as described in method section 2.4.11.

3.2.6 **Mouse aorta RNA extraction**

RNA extraction was performed in males 12 w HFD *Apoe*$^{-/-}$, *Trail*$^{-/-}$*Apoe*$^{-/-}$ and baseline *Trail*$^{+/+}$ and *Trail*$^{-/-}$ mice as described in method section 2.4.8. VE-cadherin and β-actin primer sequences described in 2.4.9 were used.

3.2.7 **Western blotting**

Western blotting was performed on mouse aortic lysates as described in method section 2.3.8.

3.3 RESULTS

3.3.1 CAD patients have reduced circulating TRAIL levels that negatively correlate with 8-iso prostaglandin F2α

Oxidative stress can increase ROS production and thereby promote endothelial dysfunction [191]. To investigate the relationship between circulating TRAIL levels and oxidative stress, human plasma was assessed (Ethics X12-0241; Sydney, Australia). We first examined levels of circulating TRAIL and the widely used *in vivo* marker of oxidative stress, 8-*iso* prostaglandin $F_{2\alpha}$ using ELISAs, in healthy verses coronary artery disease (CAD) patients [198]. Plasma TRAIL levels were significantly reduced by ~40% in CAD patients when compared to healthy controls (healthy vs CAD; 128.0 ± 6.8 pg/mL vs 81.7 ± 9.3 pg/mL; p = 0.0021) **(Figure 3.1a)**, whereas plasma 8-*iso* prostaglandin $F_{2\alpha}$ was significantly increased in CAD patients by ~25% (healthy vs CAD; 30.3 ± 1.8 pg/mL vs 38.2 ± 2.1 pg/mL; p = 0.0164) **(Figure 3.1b)**. Furthermore, a strong inverse correlation was established between TRAIL and 8-*iso* prostaglandin $F_{2\alpha}$ **(Figure 3.1c)**. These findings indicate that circulating TRAIL may be a predictor of oxidative stress in CAD patients.

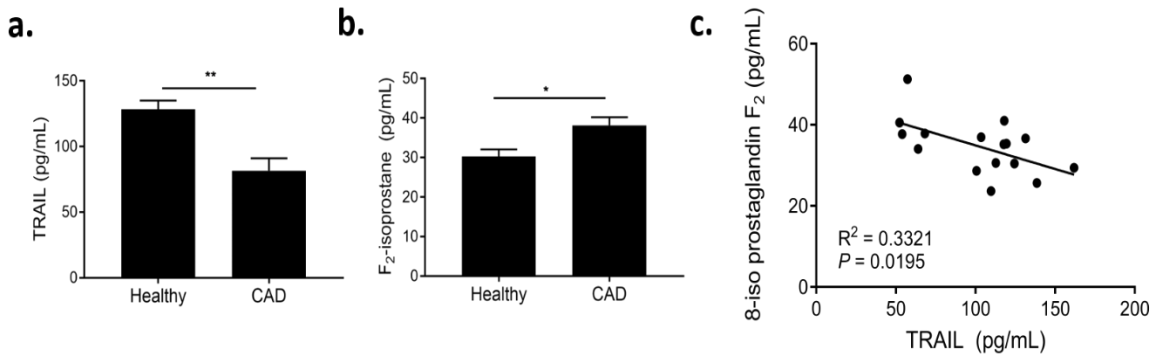

Figure 3.1 Patients with CAD have reduced circulating TRAIL and increased 8-*iso* prostaglandin $F_{2\alpha}$. Plasma from peripheral blood of healthy and CAD patients were analysed for **(a)** TRAIL and **(b)** 8-*iso* prostaglandin $F_{2\alpha}$ (n = 7-9/group) **(c)** Correlation between TRAIL and 8-*iso* prostaglandin $F_{2\alpha}$ in CAD. Normality was assessed using D'Agostino-Pearson omnibus normality test and Mann-Whitney U-test was performed; results expressed as mean ± SEM, * $p < 0.05$, **$p < 0.01$.

3.3.2 **TRAIL deletion in mice promotes EC dysfunction**

We have previously shown that TRAIL gene deletion in an *Apoe*$^{-/-}$ mice placed on a 12-week HFD resulted in accelerated atherosclerosis [172]. We used the same model to examine endothelial dysfunction. After 12 w of HFD, following euthanasia, thoracic aortas were collected and mounted into an individual organ chambers and assessed for concentration dependant vaso-relaxation. *Trail*$^{-/-}$*Apoe*$^{-/-}$ aortas had impaired relaxation in response to increasing doses of the endothelial-dependent vasodilator acetylcholine, but not to sodium nitroprusside, which dilates vessels in an endothelium-independent manner (**Figure 3.2a-b**). The pEC_{50} (half maximal effective concentration) value of *Apoe*$^{-/-}$ and *Trail*$^{-/-}$ *Apoe*$^{-/-}$ mice are -7.6 and -7.4 respectively. These findings confirm that *Trail*$^{-/-}$*Apoe*$^{-/-}$ vessels have impaired endothelial function.

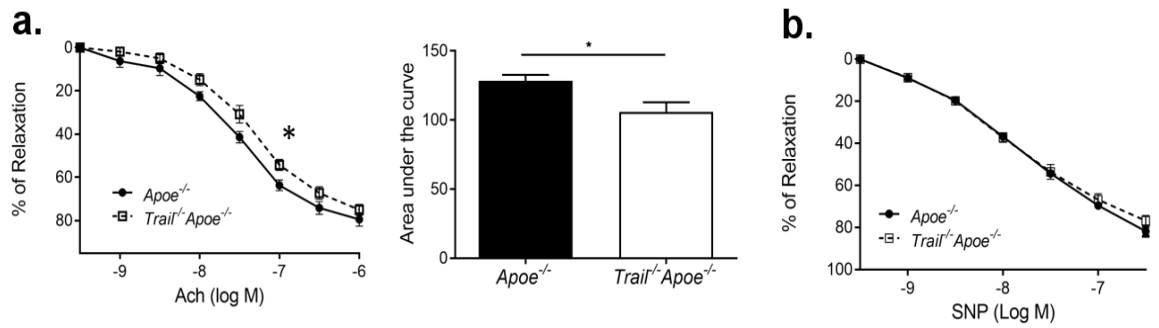

Figure 3.2 TRAIL deletion in mice promotes EC dysfunction. (a) Left, myography of aortae from 12 w HFD *Apoe*$^{-/-}$ and *Trail*$^{-/-}$*Apoe*$^{-/-}$ mice in response to acetylcholine (Ach). Right, area under the curve (n = 6/genotype). **(b)** Sodium nitroprusside (SNP) has no effect (n = 3/genotype). Results expressed as mean ± SEM; * $p < 0.05$, Student's *t-test*.

3.3.3 TRAIL deletion in mice promoted vascular ROS generation

We next examined vascular tissues of 12 w HFD-fed *Trail*$^{-/-}$*Apoe*$^{-/-}$ and *Apoe*$^{-/-}$ mice for oxidative stress. Frozen aortae were stained for DHE, a marker of cytosolic oxidative stress. *Trail*$^{-/-}$*Apoe*$^{-/-}$ mice had ~2-fold increase in DHE fluorescence staining when compared with *Apoe*$^{-/-}$ vessels **(Figure 3.3a)**. Furthermore, analysis of 4-hydroxyneal concentrations, a marker of lipid peroxidation which is known to be increased due to ROS production, was also increased in vascular tissues of *Trail*$^{-/-}$*Apoe*$^{-/-}$ mice compared to the control **(Figure 3.3b)**. These findings indicate that TRAIL deletion promotes vascular oxidative stress.

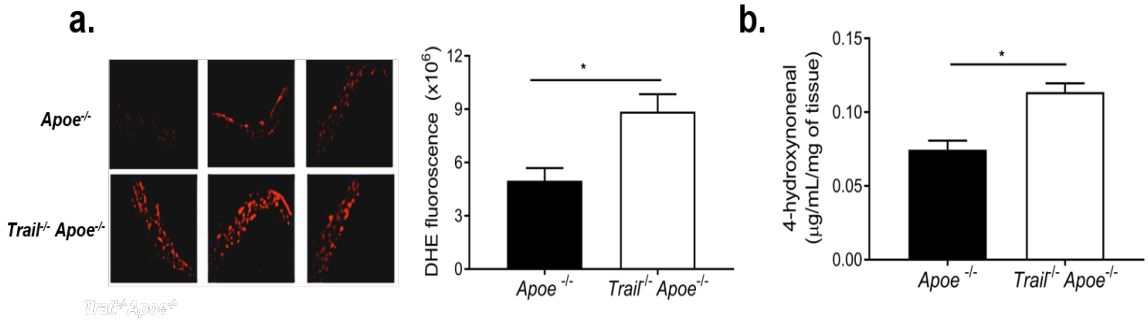

Figure 3.3 TRAIL deletion in mice promotes vascular ROS generation. (a) DHE fluorescence staining (n = 3/group) and **(b)** 4-hydroxynonenal concentrations of aortic tissue from 12 w HFD *Apoe*$^{-/-}$ vs *Trail*$^{-/-}$*Apoe*$^{-/-}$ mice (n = 4/genotype). Results expressed as mean ± SEM; *p < 0.05, Student's t-test.

3.3.4 **TRAIL deletion increases vascular permeability and reduces VE-cadherin expression in mice**

Permeability is strictly maintained in a healthy endothelium [199], and another measure of endothelial dysfunction is increased vascular permeability. To analyse the effect of TRAIL deletion on vascular permeability, Evan's blue, a dye that has high affinity to serum albumin in the blood, was injected intravenously (i.v.) and vascular leak was determined by measuring the amount of dye leaked into organs. Highly vascularised organs such has liver, intestine and colon were assessed and had increased Evan's blue dye in *Trail*$^{-/-}$ mice compared to the controls, indicating increased vascular leak with TRAIL deletion (**Figure 3.4a**). VE-cadherin is considered an important molecule in regulating permeability, controlling expression levels and signalling activity of adherents and tight junction proteins [200]. VE-Cadherin was analysed to assess whether TRAIL-dependent vascular permeability involved changes to VE-Cadherin expression. Importantly, *Trail*$^{+/+}$ and *Trail*$^{-/-}$ (normal chow diet) mice had a significantly reduced aortic VE-cadherin mRNA expression (**Figure 3.4b**). Similarly, 12 w *Trail*$^{-/-}$*Apoe*$^{-/-}$ aortae also had reduced VE-cadherin mRNA ~50% (**Figure 3.4c**) and VE-Cadherin protein expression compared to aortae of *Apoe*$^{-/-}$ mice **(Figure 3.4d).** Collectively, these results suggest that TRAIL regulates VE-cadherin expression, and this may represent a mechanism as to why mice with TRAIL deletion have increased vascular permeability.

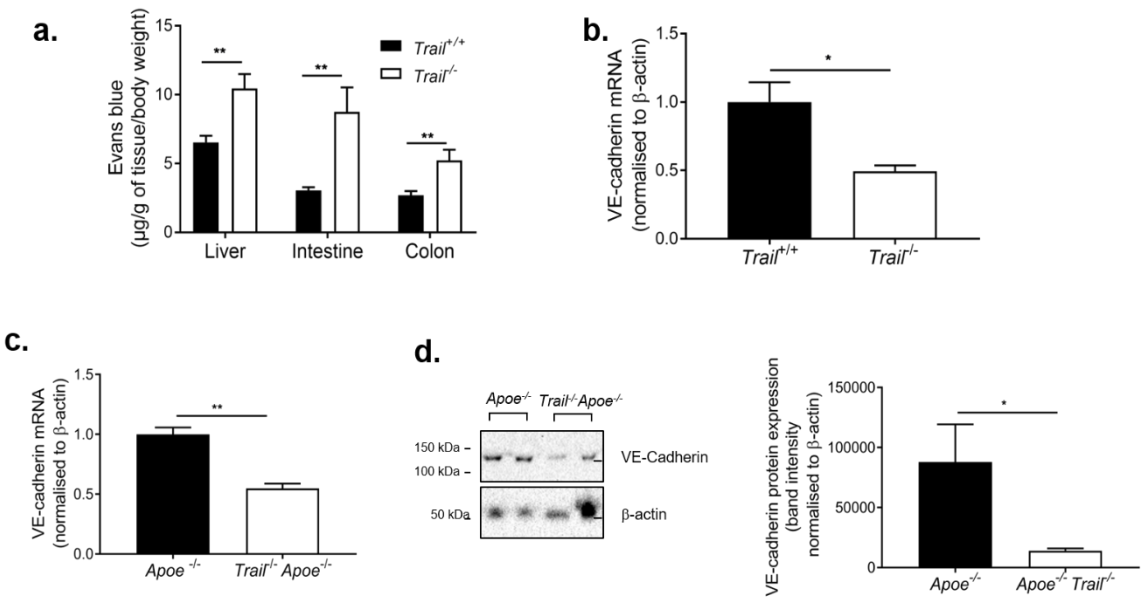

Figure 3.4 TRAIL deletion increases vascular permeability and reduced VE-cadherin expression. (a) Evans blue detection in liver, intestine and colon of *Trail*$^{+/+}$ and *Trail*$^{-/-}$ mice 30 minutes after injection (n = 6-7/group). Aortic mRNA expression of VE-cadherin in **(b)** *Trail*$^{+/+}$ and *Trail*$^{-/-}$ (n= 4/group) and **(c)** 12 w HFD *Apoe*$^{-/-}$ and *Trail*$^{-/-}$*Apoe*$^{-/-}$ (n = 5-6/group); normalised to β-actin mRNA. **(d)** Aortic VE-cadherin protein expression measured by Western blotting; 12 w HFD Apoe$^{-/-}$ vs *Trail*$^{-/-}$*Apoe*$^{-/-}$ mice. Quantification on the right, normalised to β-actin protein expression (n = 7/group). Results expressed as mean ± SEM, *p < 0.05, **p < 0.01, Student's *t-test*.

3.4 DISCUSSION

In the endothelium, the regulated endogenous production of ROS plays important roles as mediator of redox cell signalling and maintaining vascular homeostasis [191] However, in response to an elevation in cardiovascular risk factors, EC ROS production becomes excessive or aberrant from various enzyme sources, with the resulting oxidative stress capable of promoting endothelial dysfunction and atherogenesis [191,201]. This study investigated the impact of TRAIL deletion on oxidative stress and endothelial dysfunction. Three key finding were identified. First, an inverse correlation between circulating plasma TRAIL and a marker of oxidative stress, 8-*iso* prostaglandin $F_{2\alpha}$, was identified. Second, vascular tissues of HFD-fed *Trail*$^{-/-}$*Apoe*$^{-/-}$ mice displayed impaired endothelial dependant vasorelaxation in response to acetylcholine, associating with increased ROS. Third, TRAIL deletion in mice resulted in greater vascular leak, in part via TRAIL's ability to regulate VE-Cadherin mRNA and protein expression. Impact of TRAIL in clinical and pre-clinical studies have been depicted in a graphical form in Figure 3.5

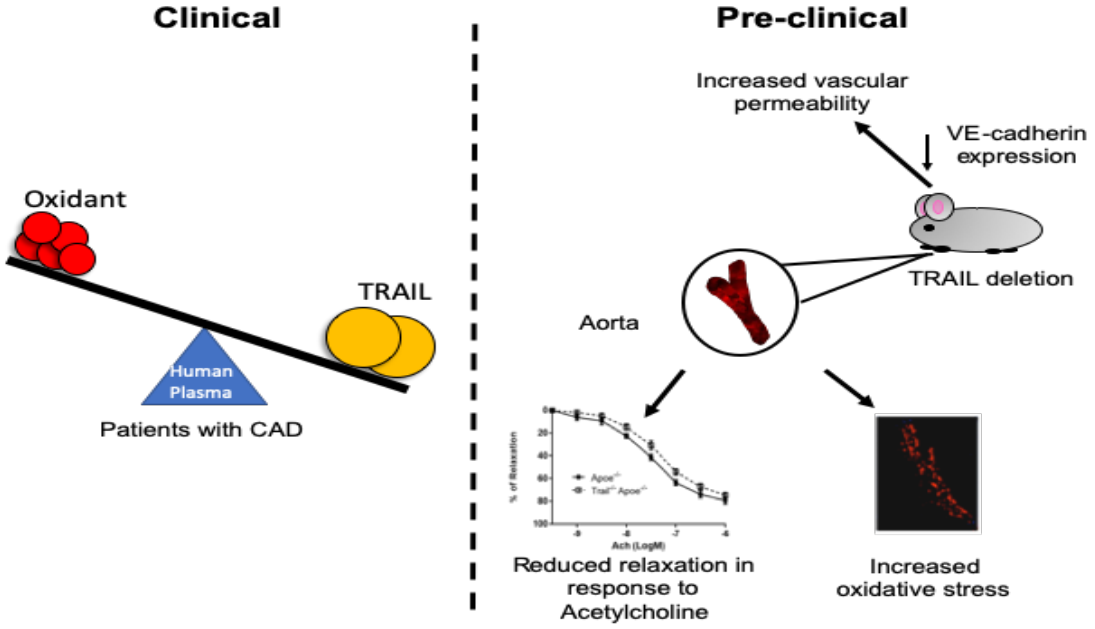

Figure 3.5. Graphical representation of finds from Chapter 3. In a clinical setting, an inverse correlation was established with circulating plasma TRAIL and oxidative stress marker 8-*iso* prostaglandin $F_{2\alpha}$. In an *in vivo*/ pre-clinical setting TRAIL deletion in mice lead to EC dysfunction, increased vascular oxidative stress and increased vascular permeability. This figure is adapted from Manuneedhi Cholan et al. (2018) (PMID 3016510).

TRAIL is a TNF cytokine that can stimulate apoptosis of cancer cells, but leave normal cells unaffected [156]. Several associations implicate a protective role for TRAIL in CVD. For instance, low circulating TRAIL levels associate with unstable CAD [162], heart failure and myocardial infarction [163]. It was also shown that elderly patients that had a myocardial infarction, and low levels of circulating TRAIL, were more likely to die within 6 years. In agreement with these studies, we showed significantly reduced plasma TRAIL levels in CAD patients [162]. Studies have shown that these metabolic and inflammatory diseases have systemically up-regulated oxidative stress markers. We have shown the oxidative marker 8-*iso* prostaglandin $F_{2\alpha}$ was augmented in the CAD patients. This finding was in corroboration with several studies indicating increased oxidative stress in CVD patients [202,203]. More importantly, we established a significant negative correlation between TRAIL and 8-*iso* prostaglandin $F_{2\alpha}$ in CAD patients suggesting that circulating TRAIL might play a protective role against oxidative stress.

Systemic increase in oxidative stress leads to free radical production. These free-radicals combine with molecular oxygen producing ROS. The initial effect of ROS is to cause EC dysfunction, which is defined as a shift in properties characterised by impaired vasodilation and a pro-inflammatory and pro-thrombotic status [204]. Our lab has previously shown that TRAIL deletion from an *Apoe*$^{-/-}$ mouse resulted in accelerated atherosclerosis. EC dysfunction and vascular oxidative stress play an important role in atherosclerosis progression [63,205]. Here, we show that HFD-fed *Trail*$^{-/-}$*Apoe*$^{-/-}$ mice have impaired endothelial function compared to *Apoe*$^{-/-}$. Disruption in EC-dependant vasodilation is a clear indicator of EC dysfunction and an early marker of atherosclerosis [206]. Furthermore, these *Trail*$^{-/-}$*Apoe*$^{-/-}$ mice on the HFD, had increased vascular oxidative stress. This effect is a pro-atherogenic factor, involved in endothelial damage and initiation of atherosclerosis [205].

Endothelial dysfunction and vascular oxidative stress can have a damaging impact on the integrity of the vessel wall [207]. The blood vessel maintains a selective-permeable membrane by controlling cell-to-cell adherent proteins such as VE-cadherin. TRAIL deletion in mice resulted in increased vascular leakiness and reduced VE-cadherin expression [208]. This is suggestive that TRAIL deletion impairs vessel integrity by disrupting the cell-to-cell contact protein. These leaky vessel walls play an important role in atherosclerosis progression by allowing easy transmigration of adhered monocytes into the sub-endothelial space [209]. Interestingly, control of vessel wall integrity may not be specific to TRAIL alone, but also involve other TNF ligands. For example, TNF-α reduced mRNA and protein expression of VE-cadherin in ECs [210], whereas transgenic mice stably expressing EC-specific Fas ligand protected against neutrophil extravasation following myocardial-ischaemia reperfusion injury [211]. Nevertheless, we show that increased ROS generation and endothelial dysfunction *in vivo*, may be one potential mechanism by which TRAIL deletion in mice, or TRAIL suppression in people, accelerates vascular diseases. Though *Trail*$^{-/-}$*Apoe*$^{-/-}$ vasculature have been shown to have increased ROS damage, this project in future will warrant an interventional study to identify whether antioxidant treatment will normalise EC function in the vasculature of these mice. In this Chapter, the involvement of TRAIL on ROS producing sources such as eNOS, NOX and mitochondrial systems have been described. The potential modulatory pathways via which TRAIL limits oxidative stress and maintains vascular permeability is described in Chapter 4.

Chapter 4: **Protective role of TRAIL against AngII-induced oxidative stress**

4.1 INTRODUCTION

The results from this chapter have been published in "**Free Radical Biology and Medicine**"; manuscript titled **"TRAIL protects against endothelial dysfunction *in vivo* and inhibits angiotensin-II-induced oxidative stress in vascular endothelial cells *in vitro*"** [190].

Oxidative stress is defined as the imbalance between free radicals and anti-oxidants produced in the body. These free radicals with extra electrons combine with molecular oxygen and form reactive oxygen species (ROS), which are highly reactive compounds [212]. Several clinical studies have established elevated ROS production to be the hallmark of cardiovascular diseases (CVDs) [202,213,214]. Excessive circulating angiotensin II (AngII) is a strong indicator of CVD and oxidative stress in humans [215,216]. At homeostasis, AngII regulates blood pressure, however during CVD, excessive circulating AngII can induce EC dysfunction and ROS production [217,218]. In the endothelium, various molecular pathways are involved in ROS production, including NADPH oxidase (NOX), the mitochondrial electron transport chain and eNOS uncoupling. In ECs, multiple isoforms of NOX are expressed including NOX-1, NOX-2, NOX-4 and NOX-5, with NOX-4 being the abundant source in the endothelium [3]. In the mitochondria, the electron transport chain produces superoxides which can increase ROS production in the cell [219]. Finally, NO, an important molecule in maintaining a healthy endothelium is produced with the help of eNOS enzyme. The process of uncoupling of eNOS

in response to other cellular sources of ROS such as NOX and mitochondria can lead to eNOS monomerization from its dimeric state and lead to further ROS production in the endothelium.

Elevated AngII is also linked to inflammation in the vessel wall, specifically by reducing NO production and upregulating ROS. Inflammation and vessel permeability are exacerbated by ROS in CVD. Expression of adhesion molecules, including vascular cell adhesion protein-1 (VCAM-1) and intercellular adhesion molecule-1 (ICAM-1) are upregulated by ROS, and this promotes leukocyte adhesion to the endothelium and increases inflammation in the vessel wall.

Identifying novel stimuli that protect the vascular endothelium against ROS-induced dysfunction during atherosclerosis is important in the development of new therapies for patients. In this chapter, AngII was used as a model of oxidative stress in ECs in vitro. Since TRAIL was protective of oxidative stress and EC dysfunction *in vivo* (chapter 3), it was hypothesised that TRAIL would protect against AngII-induced ROS production and inflammation in ECs *in-vitro*.

4.2 BREIF METHODS

4.2.1 **DHE and MitoSOX cell staining**

DHE and MitoSOX staining on HMEC-1 cells were performed according to the methods described in sections 2.3.10 and 2.3.11.

4.2.2 **Drug treatments**

All inhibitors including losartan (20 μM), PD123177 (20 μM), apocynin (100 μM), L-NAME (1 mM) and rotenone (5 μM) were added 30 mins prior to AngII (50 ng/mL) stimulation.

Previous studies have shown TRAIL concentrations ranging from 1-400 ng/mL to induce proliferation and migration of vascular cells without the induction of apoptosis [170,173,177,180,194].In HMEC-1 the optimum concentration was 1-10 ng/mL [180] . Hence, in this chapter, cells were treated with 1 ng/mL of TRAIL over-night prior to AngII stimulation'

4.2.3 **siRNA treatment**

Serum starved HMEC-1 were transiently transfected with 200 nmol/L of NOX 1, NOX 2, NOX 4 and NOX 5 siRNA (Santa Cruz Biotechnology Inc.) over-night using FuGENE6 (Promega). AllStar control siRNA (Qiagen) was used as a siRNA control. Transfected cells were subjected to 2 h of AngII treatment and assessed by DHE staining or mRNA using PCR.

4.2.4 **Hydrogen peroxide assay**

HEMC-1 were seeded into 96 WTP at 8000 cells/well density and serum-starved overnight. After treating the cells accordingly, the media containing the cells were treated with red peroxidase substrate and horseradish peroxidase as described in Fluorometric Hydrogen Peroxide Assay Kit (Sigma-Aldrich). Fluorescence was detected at an excitation of 540 nm and emission of 590 nm using a plate reader (Clario Star, BMG Labtech).

4.2.5 **VE-cadherin localisation**

HMEC-1 were grown as monolayers on glass coverslips in a 12-WTP and serum starved and treated accordingly. Cells were then fixed using 2% formalin for 25 min, followed by blocking with 5% BSA in PBST. Cells were incubated over-night with rabbit polyclonal VE-cadherin (1:1000, Abcam), followed by 1 h incubation with Alexa Fluor 594 (1:400, Abcam). The coverslips were mounted using fluorescent mounting media containing DAPI (SouthernBiotech). Images were taken using 60X magnification on a Nikon A1R confocal microscope.

4.3 RESULTS

4.3.1 AngII stimulates ROS production in ECs *in-vitro*

At homeostasis, the renin-angiotensin system's (RAS) effector protein angiotensin II (AngII) is involved in maintaining blood pressure. However, during vascular disease, circulating AngII has nearly a 3-fold increase [220]. Studies have shown that this increase in AngII leads to EC dysfunction via increased ROS [217,221,222]. Here, the endothelial cell line, HMEC-1, was treated with AngII (50 ng/mL) and ROS levels were then measured by staining with dihydroethidium (DHE); DHE reacts with superoxides ($O_2^{\bullet -}$) and in turn produces a red fluorescent product, 2-OHE^+. HMEC-1 cells exposed to AngII, showed a time dependant increase in ROS production that peaked between 2-4 h, returning to baseline by 24 h (**Figure 4.1a**). AngII signalling occurs via two receptors, angiotensin type I receptor (AT_1R) and angiotensin type 2 receptor (AT_2R). To identify the involvement of the AngII receptors, losartan (20 μM) and PD123177 (20 μM), which inhibit AT1R and AT2R, respectively were used. Inhibition of the AT_1R reduced DHE fluorescence after 2 h AngII, with no change observed when AT_2R was blocked by PD123177 (**Figure 4.1b**). This suggests that AngII-induced oxidative stress occurs via the AngII-type 1 receptor.

To investigate the involvement of NOX in AngII-induced oxidative stress, HMEC-1 cells were treated with the pan NOX inhibitor, Apocynin (100 μM). A significant reduction in DHE fluorescence was observed in cells pre-treated with Apocynin followed by 2 h of AngII (**Figure 4.1c**), indicating the involvement of NOX in AngII-induced ROS production in these cells. To assess the contribution of eNOS in AngII-induced ROS production, cells were pre-treated with the competitive NOS inhibitor, L-NAME (1 mM). A reduction in DHE fluorescence was observed after 2 h AngII treatment (**Figure 4.1d**), confirming the involvement of eNOS in AngII-induced ROS production. Finally, to assess the involvement of mitochondria, HMEC-1

were pre-treated with Rotenone (5 μM), a mitochondrial complex I inhibitor. Similarly, rotenone pre-treatment reduced AngII-induced ROS production (**Figure 4.1e**); a finding that was supported by MitoSox™ staining. Of note, MitoSox™ is a dye that specifically targets mitochondria in live cells, producing red fluorescence when oxidised. Importantly, HMEC-1 cells exposed to AngII, showed a time-dependant increase in mitochondrial ROS production, that peaked at 6 h, returning to baseline by 24 h, indicating AngII can also specifically increase mitochondrial ROS production in ECs (**Figure 4.1f**). Combined, these findings establish that AngII-induced ROS production in HMEC-1 cells involves NOX, eNOS and mitochondrial pathways.

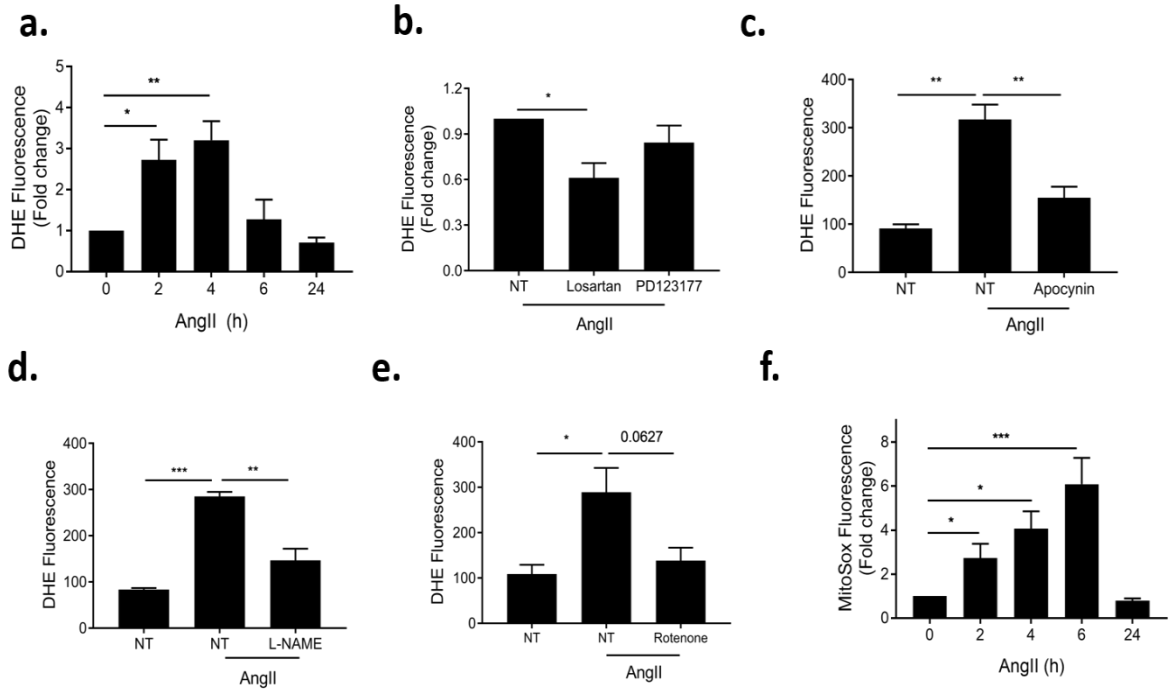

Figure 4.1 AngII-induces ROS production in HMEC-1. (a) Serum-starved HMEC-1 were treated with AngII (50 ng/mL) for 0, 2, 4, 6 and 24 h, followed with DHE assessment by flow cytometry. **(b)** AngII-induced ROS involves the AngII type-1 receptor. Serum-starved cells were treated with Losartan (20 μM) for 30 minutes prior to AngII stimulation for 2 h. DHE staining was quantified by flow cytometry. **(c)** AngII-induced ROS is inhibited with Apocynin (100 μM), (d) L-NAME (1 mM) and **(e)** Rotenone (5 μM) pre-treatment as described in the methods. **(f)** MitoSox^{TM} Red staining by flow cytometry. NT, no treatment, n = 3 - 4/group and results expressed as mean ± SEM; NT – no treatment *p < 0.05, **p < 0.01, ***p < 0.0001; ANOVA (Sidak's multiple comparison test) or Students *t-test*.

4.3.2 **AngII- induced ROS production involves NOX-4**

Given NOX is involved in AngII-induced ROS production, the next step was to identify which isoform(s) was involved in this process. Human endothelium expresses 4 isoforms, NOX-1, NOX-2, NOX-4 and NOX-5. In response to siRNA treatment, NOX-4 and NOX-5 were reduced (**Figure 4.2a**), whereas NOX-1 and NOX-2 were not detectable by qPCR (data not shown). Importantly, only siRNA knockdown of NOX-4 resulted in reduced DHE fluorescence after AngII treatment, shown in Figure 4.2b. This reduction was not observed when NOX5 was knocked down. These results indicate that the NOX isoform implicated in AngII-induced oxidative stress in HMEC-1 cells is NOX-4.

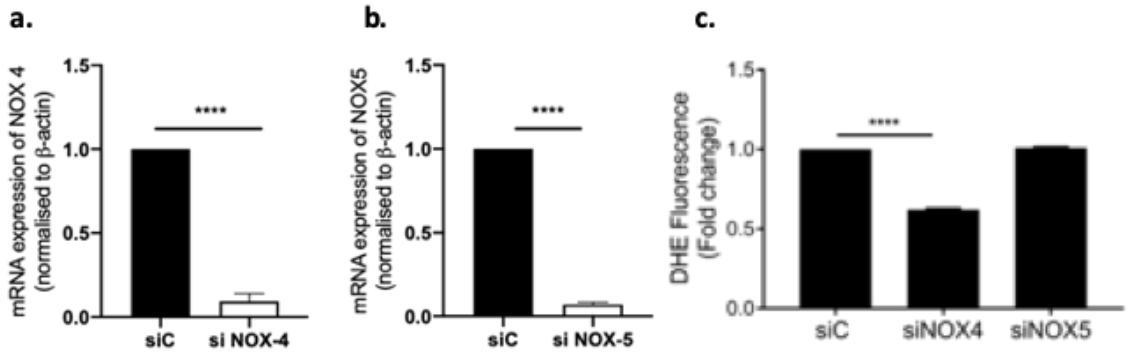

Figure 4.2 AngII-induced ROS production involves NOX-4. (a,b) Overnight transient transfection of siRNA targeting NOX-4, -5 or control siC. mRNA normalisation to GAPDH and β-actin. **(c)** AngII-induced DHE fluorescence was reduced with NOX-4 siRNA, but not NOX-5 siRNA, or siC. n = 3 – 4/group and results expressed as mean ± SEM; ****p < 0.0001; ANOVA, Sidak's multiple comparison test.

4.3.3 **AngII-induced oxidative stress is inhibited by TRAIL**

Chapter 3 investigated both clinical and *in vivo* models showing the protective potential of TRAIL in reducing oxidative stress and endothelial dysfunction. To investigate the effect and mechanism of TRAIL in an environment with increased ROS, cells were pre-treated with a clinically relevant dosage of TRAIL (1 ng/mL) followed by AngII treatment and assessment of ROS. Pre-treatment with TRAIL over-night prior to 2h AngII treatment, reduced AngII induced oxidative stress, measured by both DHE fluorescence and MitoSox^{TM} fluorescence (**Figure 4.3a-b**). Figure 4.1c implicated NOX-4 in AngII induced ROS production. NOX-4 is a unique isoform, due to its ability to produce hydrogen peroxide (H_2O_2) as a source of ROS [223]. Hence, H_2O_2 production was measured using a hydrogen peroxide detection kit. Importantly, H_2O_2 production was significantly elevated in response to 2 h AngII, and this was abrogated with TRAIL pre-treatment (**Figure 4.3c**).

AngII can increase NOX-4 and eNOS production within 1- 3 h [224,225]. Therefore, we investigated if AngII regulates NOX-4 and eNOS mRNA expression and observed that AngII increased mRNA expression of NOX-4 and e-NOS in response to 2 h of AngII (**Figure 4.3d**). Importantly, the augmented effect of eNOS due to AngII was brought back to baseline by TRAIL pre-treatment, however NOX-4 mRNA expression was not significantly reduced (**Figure 4.3d**). Collectively these findings suggest that, TRAIL effectively inhibits ROS production in a well-characterised model of oxidative stress induced by AngII by possibly reducing the production of H_2O_2 produced by NOX-4 and eNOS.

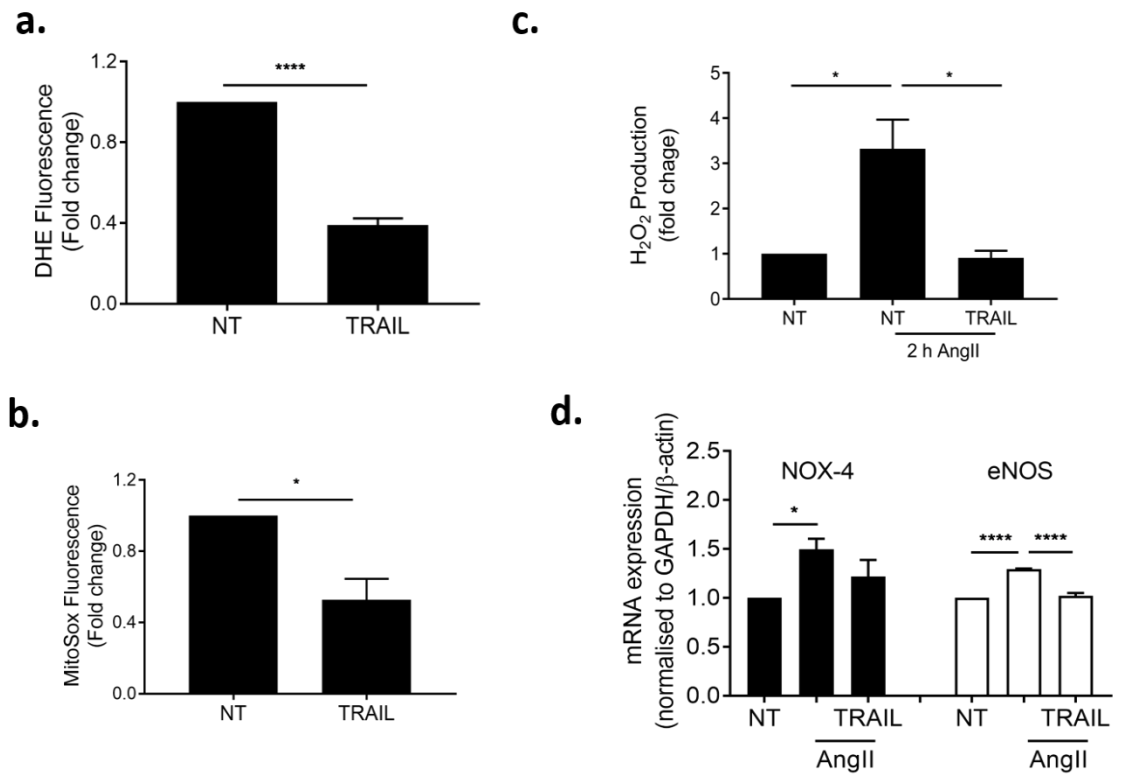

Figure 4.3 AngII-induced ROS is inhibited by TRAIL pre-treatment. (a) DHE fluorescence and **(b)** MitoSOX^{TM} Red reactivity in the presence of AngII (50 ng/mL) for 2 h, with or without TRAIL pre-treatment at 1 ng/mL overnight (n = 3/group); **(c)** AngII-induced H_2O_2 production is reduced with TRAIL pre-treatment at 1 ng/mL in HMEC-1 (n = 3/group). **(d)** HMEC-1 cells exposed to 2 h of AngII with/without TRAIL pre-treatment were detected for NOX-4 and eNOS mRNA expression, normalised to GAPDH and β-actin (n = 4/group). Results expressed as mean ± SEM, NT – no treatment; *p < 0.05, ****p < 0.0001 ANOVA (Sidak's multiple comparison test) or Student's *t-test*.

4.3.4 **TRAIL inhibits AngII-induced monocyte adhesion and alters the expression of VCAM-1 *in-vitro***

Two important factors affecting the endothelium in response to the production of ROS are inflammation and vessel permeability. ROS production can up-regulate expression of adhesion molecules such as ICAM-1 and VCAM-1 on the endothelial cell surface, enabling an increased number of leukocytes such as monocytes to adhere to the endothelium. In a monocyte adhesion assay, AngII treatment of HMEC-1 increased adhesion of fluorescently labelled monocytes to the monolayer of ECs. Crucially, pre-treatment of HMEC-1 with TRAIL (1 ng/mL) resulted in ~50% reduction in monocytes adhered to the endothelium (**Figure 4.4a**). Investigation of the mRNA expression of the adhesion molecule VCAM-1 showed 2 h AngII treatment increased expression, while pre-treatment with TRAIL inhibited this increase (**Figure 4.4b**), suggesting TRAIL protects against monocyte adhesion by preventing upregulation of adhesion molecules in a high oxidative stress environment.

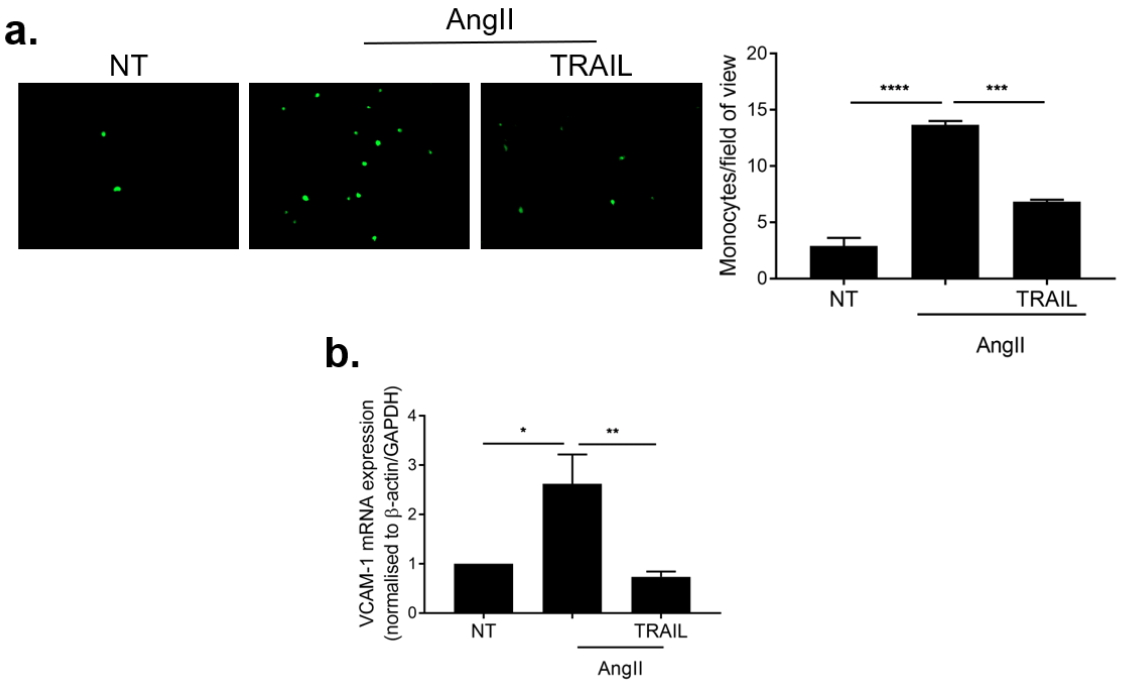

Figure 4.4 TRAIL inhibits AngII-induced monocyte adhesion by reducing expression of VCAM-1. (a) *Left*, representative 20 x magnification images of fluorescent monocytes adhering to a monolayer of HMEC-1 cells exposed to 2 h of AngII with/without TRAIL pre-treatment. *Right*, quantification of adhered monocytes (n = 3/group). mRNA analysis of **(b)** VCAM-1. Serum-starved HMEC-1 were exposed to AngII (50 ng/mL) for 2 h with/without 1 ng/mL of TRAIL pre-treatment overnight. mRNA expression was normalised to GAPDH and β-actin. NT, no treatment. Results are expressed as mean ± 4SEM, NT – no treatment; *$p < 0.05$, **$p < 0.01$, ***$p < 0.001$, ****$p < 0.0001$ ANOVA (Sidak's multiple comparison test) or Student's *t-test*.

4.3.5 **TRAIL inhibits AngII-induced VE-cadherin disruption *in-vitro***

VE-cadherin is important in endothelial permeability by maintaining intercellular junctions in the endothelium. *In vivo*, TRAIL deletion increased vascular permeability and resulted in reduced expression of VE-cadherin in the aorta, discussed in section 3.2.4 To further examine the role of TRAIL on endothelial permeability induced by ROS, and regulation of VE-cadherin, HMEC-1 cells were treated with AngII (50 ng/mL). 2 h AngII treatment showed no changes in mRNA expression by qPCR or protein expression by western blotting and pre-treatment with TRAIL (1 ng/mL) also had no effect on expression (**Figure 4.5a-b**). However, when HMEC-1 cells were stained for VE-cadherin, localisation in the cell membrane was disrupted with AngII treatment. Importantly, pre-treatment of cells with TRAIL prior to exposure to AngII for 2 h, stopped the disruption of VE-cadherin in the cell membrane (**Figure 4.5c**). Finally, a longer exposure of HMEC-1 to AngII (for 6 h), significantly reduced VE-cadherin expression, while pre-treatment with TRAIL VE-cadherin mRNA stopped this reduction (**Figure 4.5d**). Collectively, these results suggest that TRAIL targets VCAM-1 and VE-cadherin to protect the endothelium against inflammation and increased permeability induced by ROS.

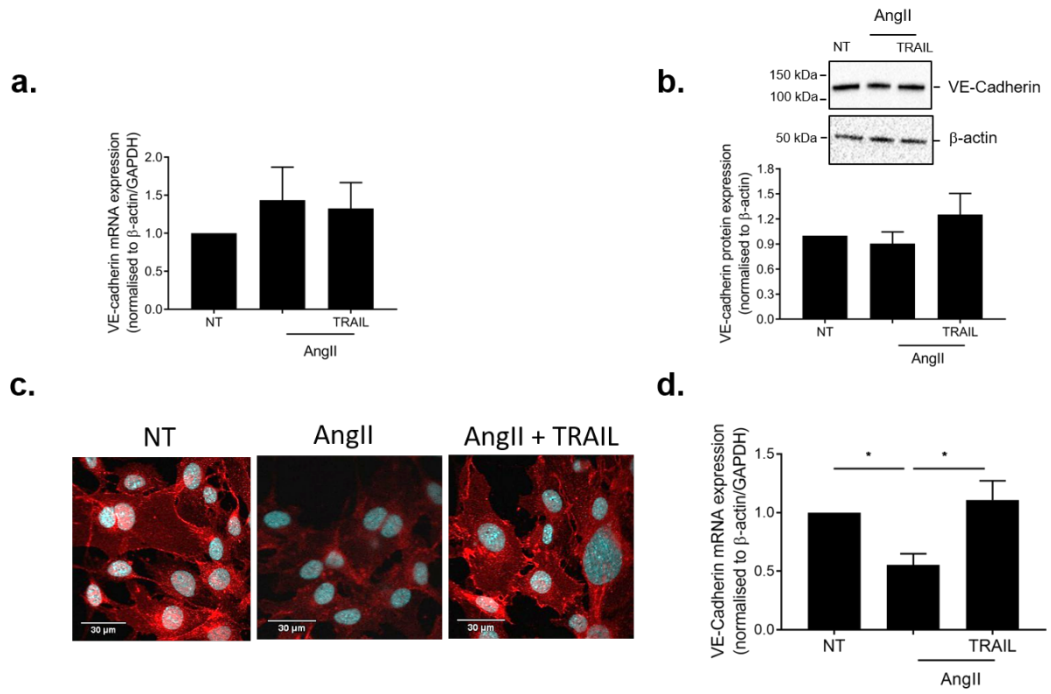

Figure 4.4 TRAIL inhibits AngII-induced VE-cadherin disruption *in-vitro*. Endothelial cell permeability marker VE-cadherin's level **(a)** mRNA and **(b)** protein expression. Quantification of protein (lower panel) was normalised to β-actin. **(c)** VE-cadherin localisation in HMEC-1 cells exposed to AngII (50 ng/mL) for 2 h, with/without 1 ng/mL of TRAIL pre-treatment overnight. **(d)** VE-cadherin mRNA expression is reduced by AngII after 6 h and rescued by TRAIL. mRNA expression was normalised to GAPDH and β-actin. NT, no treatment. Results are expressed as mean ± SEM, NT – no treatment; *$p < 0.05$, ANOVA (Sidak's multiple comparison test)or Student's *t-test*.

4.4 DISCUSSION

AngII plays an important role in pathogenesis of CVD, promoting atherosclerosis, hypertension and cardiovascular hypertrophy [226] with AngII increasing ROS production in both *in vivo* and *in-vitro* models [222,227]. Here AngII exposure was used as an *in-vitro* model of oxidative stress to investigate the mechanisms involved in AngII-induced oxidative stress in the endothelium. Importantly TRAIL inhibited AngII-induced EC ROS production, reduced EC VCAM-1 expression and monocyte adhesion to AngII-stimulated ECs, and prevented AngII-induced disruption of VE-cadherin localisation at the plasma membrane in part by downregulation of VE-cadherin expression; events important for the control of endothelial cell-cell adhesions and integrity

Under high levels of AngII, there is activation of NOX, eNOS and mitochondrial systems to produce ROS in the endothelium. We found that over-night TRAIL pre-treatment at low physiologically relevant concentration of 1 ng/mL was able to reduce AngII-induced ROS production in HMEC-1 cells, thereby establishing a direct link between TRAIL and its ability to reduce ROS production in the endothelium. In support of our findings Liu *et al.* demonstrated in an *in vivo* model that TRAIL treatment improved endothelial function in diabetic rats and in an *in-vitro* model TRAIL protected human umbilical vein ECs against high glucose induced ROS production. Consistent with the above findings, our lab has shown that TRAIL stimulates EC proliferation, migration and differentiation by activation of Akt, NOX-4 and eNOS pathways [177]. Conversely Li *et al.* (2013) have shown a higher dosage of TRAIL (100 ng/mL) can cause NOX-induced ROS production and lead to endothelial dysfunction in small mesenteric arteries in mice [228]. However, this is most likely due to the concentration of TRAIL used.

This study has established the protective effect of TRAIL in AngII-induced oxidative stress yet understanding the precise mechanism(s) requires more extensive studies. Our data indicated that production of ROS due to AngII involved NOX-4, mitochondria and eNOS uncoupling, with the latter involving L-Arg availability, BH4 oxidation/reduction and eNOS monomerization. Though various sources of ROS were investigated individually, cross-talk between these sources occurs, effecting ROS production, with some studies concluding that AngII induced oxidative stress is initiated by the NOX system which then activates other sources of ROS [229,230]. Interestingly our data shows that AngII increases NOX-4 production as well as its associated source of ROS, H_2O_2. Importantly, these augmentations associated with AngII exposure did not occur with TRAIL pre-treatment, suggesting TRAIL protects against AngII-induced oxidative stress by a reducing NOX-4 activation and its associated ROS production, preventing activation and production of ROS from other endothelial sources.

EC dysfunction initiates inflammation, attracts leukocytes which extravasate into the sub-endothelial space and initiate plaque progression [63]. Here AngII exposure lead to increased VCAM-1 mRNA expression and monocyte adhesion to ECs. These changes lead to an inflamed environment and can affect endothelial permeability. Prolonged exposure of EC to AngII reduced VE-cadherin, an important protein in endothelial permeability, which is present in the cell-membrane, was disrupted with AngII exposure. However, TRAIL pre-treatment, led to a reduction in VCAM-1 expression, reduced monocyte adhesion and prevention of VE-cadherin disruption. These findings demonstrate that the protective nature of TRAIL on the endothelium not only reduces ROS production but also prevents the associated negative effects due to oxidative stress. Therefore, we can conclude that TRAIL at physiological concentrations can protect and preserve endothelial structure and function against excessive ROS production. Though this study indicates TRAIL's protective role against

AngII-induced ROS production, it is to be acknowledged that this protective process is complicated with the involvement of eNOS uncoupling, mitochondria and NOX 4 ROS systems. Further research is warranted to tease out the exact mechanism(s) of TRAIL against AngII-induced ROS production.

Chapter 5: **Characterisation of EC-specific TRAIL knockout mice**

5.1 INTRODUCTION

At homeostasis, ECs are anti-thrombotic, anti-inflammatory and anti-atherogenic in nature [61,231,232]. The endothelium maintains a selective-permeable membrane by moderating the expression of adherents-junction protein such as VE-cadherin. ECs also regulate expression of cell adhesion molecules such as ICAM-1 and VCAM-1 which stimulate recruitment of circulating leukocytes to the endothelium and influence inflammatory status of the vessel wall. A healthy endothelium also produces NO, a soluble gas involved in reducing oxidative stress, and controlling the vessel diameter and blood pressure by influencing VSMC constriction and relaxation [233].

Endothelial damage is the initiating step in atherosclerosis progression. A damaged endothelium up-regulates its cell adhesion expression, along with inflammatory cytokine production. EC dysfunction also disrupts NO production, thereby increasing oxidative stress and dysregulating blood pressure [234,235]. Our lab reported that 12 w HFD-fed Trail-/- mice developed features of type 2 diabetes such as hyperglycaemia, hypercholesteremia, hyperinsulinemia and insulin resistance. In response to a HFD, *Trail*$^{-/-}$ vessels, showed increase expression of inflammatory markers, collectively implicating TRAIL to be protective, not only against metabolic dysfunction, but also vessel inflammation [170]. In this chapter we hypothesised that EC-specific TRAIL knockout mice may also develop features of metabolic disease in response to an HFD, as witnessed in global *Trail*$^{-/-}$ mice.

In this chapter, two models were used to characterise EC-specific TRAIL knockout mice and identify the importance of TRAIL in the endothelium in response to an HFD. This study will enable us to discover the mechanism through which TRAIL can initiate its protective effect on the vasculature.

5.2 BRIEF METHODS

5.2.1 Animals

In this chapter *Trail*$^{EC-/-}$ and *Trail*$^{EC+/+}$ male mice were generated as described in method section 2.4.4 and characterised at baseline and following 12 w HFD as described in method section 2.4.5. Animal ethics were obtained from Sydney Local Animal Welfare Committee (2017-020, 2014-027).

5.2.2 Mouse aortic RNA extraction

Aortas obtained from mice at baseline and 12 w HFD were extracted for RNA as described in method section 2.4.8 and PCR analysis was done with primers listed in method section 2.4.9.

5.2.3 Plasma biochemistry

Plasma extracted from mice at baseline and following 12 w HFD were measured for cholesterol, insulin and nitrate/nitrite as described in method section 2.4.12, 2.4.13 and 2.4.14.

5.2.4 Glucose and insulin tolerance test

GTT and ITT were carried out in 12 w HFD fed mice according to method section 2.4.7.

5.2.5 **Blood pressure**

Blood pressure was measured at week 10-12 in HFD fed mice according to method section 2.4.6.

5.3 RESULTS

5.3.1 Baseline characterisation of *Trail*$^{EC-/-}$ mice showed reducing trend in VCAM-1 expression

Adult mice aged between 6-14 weeks were euthanised and thoracic aortas were collected. RNA was extracted and analysed by qPCR. Though there were no difference in ICAM-1 mRNA expression (**Figure 5.1a**), VCAM-1 was reduced in *Trail*$^{EC-/-}$ mice compared to the control *Trail*$^{EC+/+}$, (**Figure 5.1b**). Analysis of nitric oxide synthase (NOS) gene expression, including eNOS and iNOS showed no difference between genotype (**Figure 5.1c-d**). VE-cadherin mRNA was undetectable (result not shown). Collectively, these finding suggest that TRAIL expression in ECs may influence VCAM-1 expression, but not ICAM-1 or NOS compared to *Trail*$^{EC+/+}$.

5.3.2 Baseline characterisation of *Trail*$^{EC-/-}$ mice showed reduced IL-18 and MCP-1 mRNA expression

Aortic RNA was extracted and analysed for various inflammatory gene expression. No difference was observed with mRNA expression of IL-1β (**Figure 5.2a**). However, both MCP-1 and IL-18 mRNA expression was significantly reduced in *Trail*$^{EC-/-}$ mice compared to the control *Trail*$^{EC+/+}$ (**Figure 5.2b-c**). These suggest that TRAIL expressed in ECs may influence expression of MCP-1 and IL-18 in the vasculature.

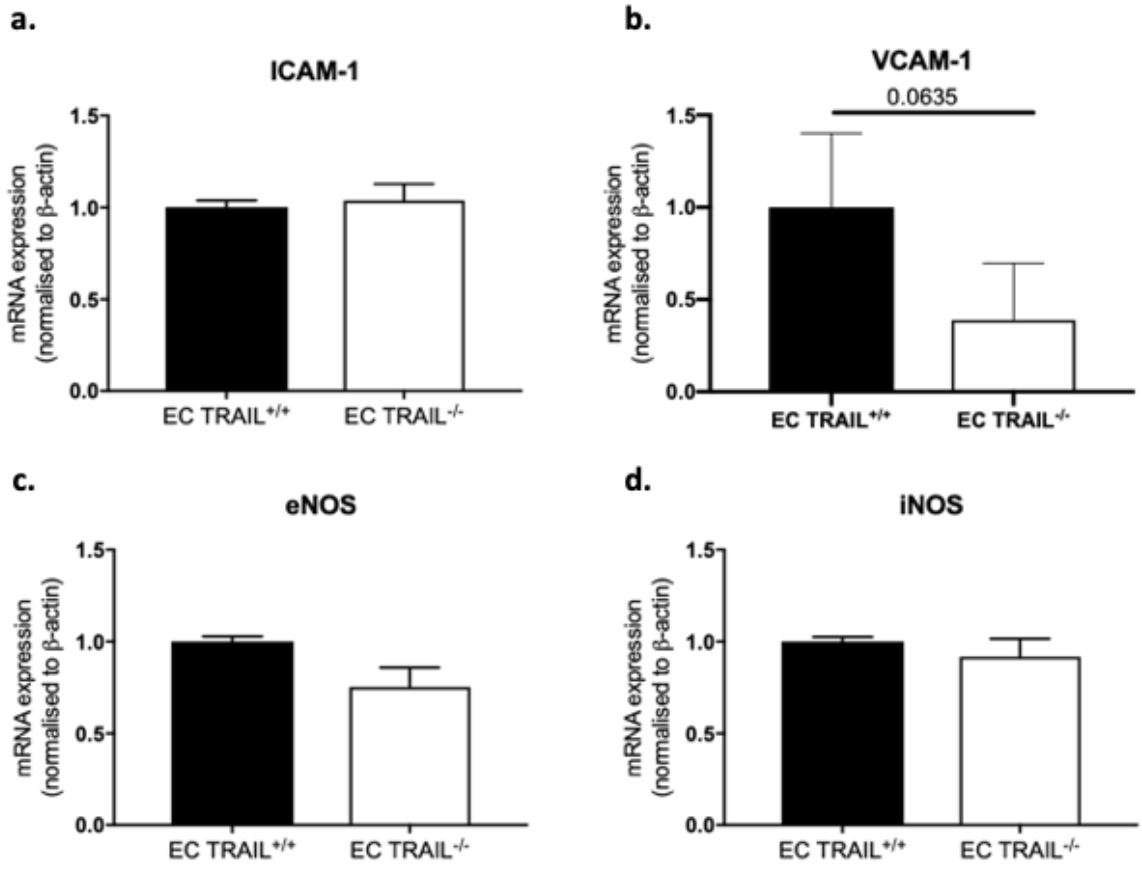

Figure 5.1 Baseline characterisation of *Trail*$^{EC-/-}$ mice showed reducing trend in VCAM-1 and no changes in NOS mRNA expression. 6 - 14-week-old *EC Trail*$^{+/+}$ and *Trail*$^{EC-/-}$ aorta were collected and RNA was extracted and quantified for gene expression using qPCR. Cell adhesion molecule mRNA expression such as **(a)** ICAM-1 showed no change between the two groups, but **(b)** VCAM-1 mRNA expression saw a reducing trend in *Trail*$^{EC-/-}$ mice compared to the control *Trail*$^{EC+/+}$. mRNA expression of NOS, such as **(c)** eNOS and **(d)** iNOS showed no significant changes. mRNA was normalised to β-actin. n = 4 – 5/group. Results expressed as mean ± SEM, Student *t-test*.

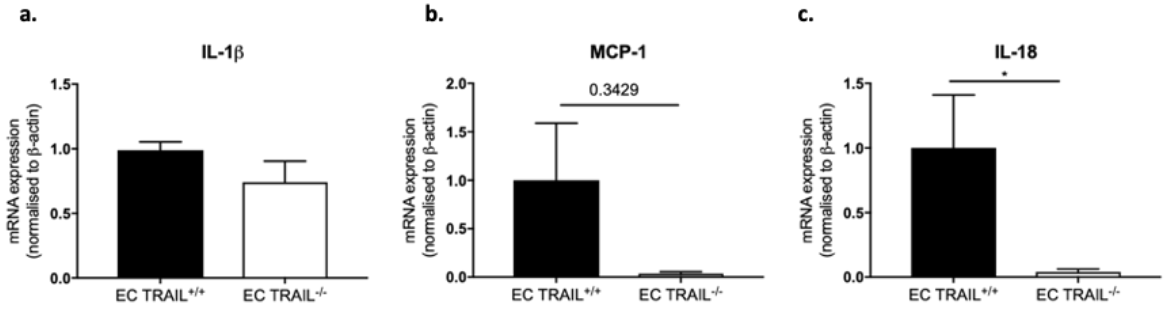

Figure 5.2 Baseline characterisation of *Trail*$^{EC-/-}$ mice showed reduced inflammatory gene expression. 6 - 14-week-old *Trail*$^{EC+/+}$vs *Trail*$^{EC-/-}$ mice's aortic mRNA expression of **(a)** IL-1β showed no significant difference, however, **(b)** MCP-1 showed a reducing trend and **(c)** IL-18 was significantly reduced. mRNA was normalised to β-actin. n = 4 – 5/group. Results expressed as mean ± SEM; *p < 0.05; Students *t-test*.

5.3.3 **Baseline biochemical plasma analysis showed no difference in *Trail*$^{EC-/-}$ mice**

Blood was collected from mice aged 6 to 14 weeks through cardiac puncture. Plasma was extracted from the blood and analysed. There were no difference ces in plasma cholesterol, insulin or nitrate/nitrite levels in *Trail*$^{EC-/-}$ mice compared to the control *Trail*$^{EC+/+}$ (**Figure 5.3a-c**).

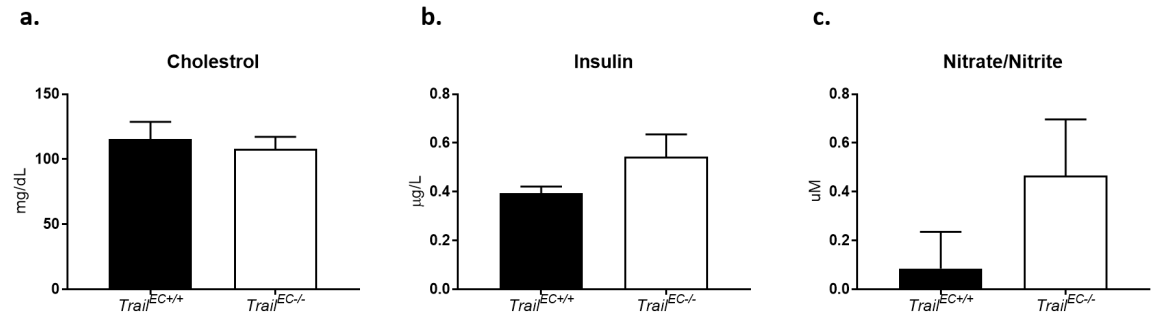

Figure 5.3 No significant difference was observed in plasma biochemistry in baseline *Trail*$^{EC-/-}$ mice. Blood was extracted from mice during euthanasia through cardiac puncture. Plasma was analyzed for **(a)** cholesterol, **(b)** insulin and **(c)** nitrate/nitrite level, which showed no significant difference between *Trail*$^{EC-/-}$ and the control *Trail*$^{EC+/+}$ at baseline. n = 6 – 8/group. Results were expressed as mean ± SEM, Student *t-test*.

5.3.4 **Baseline characterisation of *Trail*$^{EC-/-}$ mice showed no difference in the physical structure of the vasculature**

Thoracic aorta collected from 6 to 14-week old mice were fixed in paraffin for histology and cut into 5μm sections. H & E staining was performed to examine tissue architecture. There were no obvious visual differences, and no difference in the thickness of the media between genotype **(Figure 5.4a**). Because ECM proteins such as collagen and elastin, provides structural integrity to vessel wall, we wanted to examine if these were different in the aortae of mice lacking TRAIL from the endothelium. Consistent with no obvious changes, there were no difference in elastin or collagen content in aortae of *Trail*$^{EC-/-}$ vs. *Trail*$^{EC+/+}$ mice (**Figure 5.4b-c**).

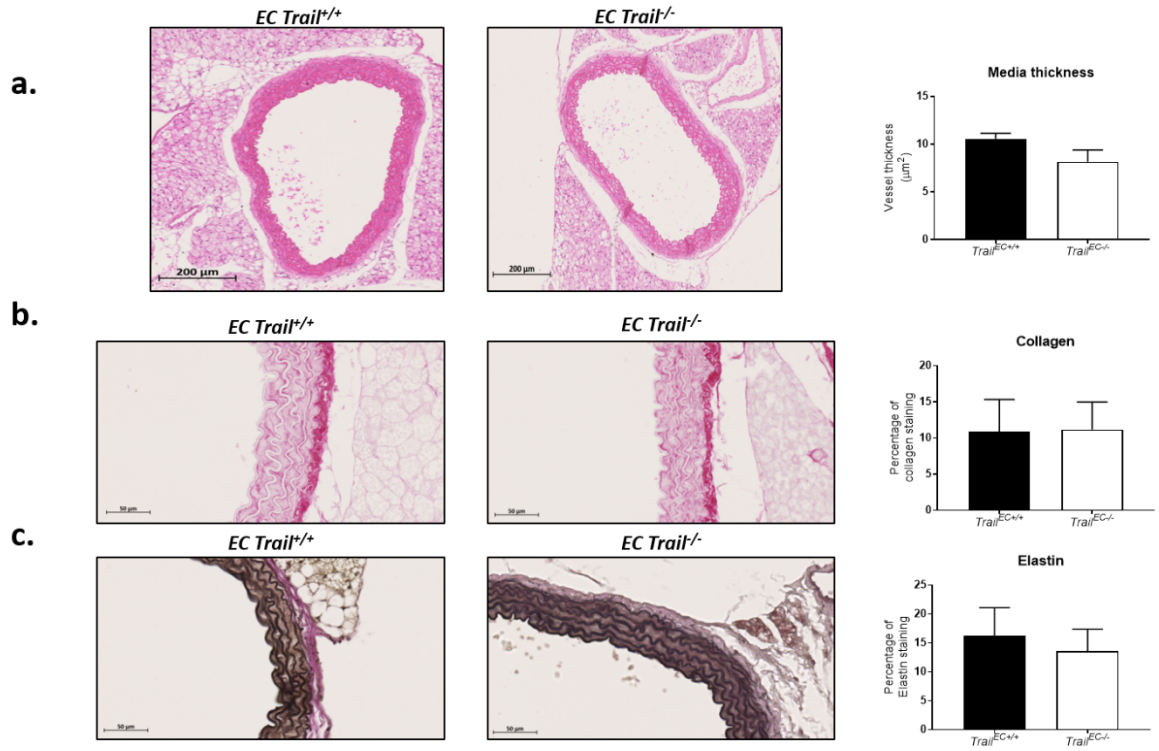

Figure 5.4 No significant difference at baseline in physical characteristic of vessel wall between *EC Trail*$^{-/-}$ and *EC Trail*$^{+/+}$ mice. 5µm histological sections of thoracis aorta stained for **(a)** *Left* – H & E staining of *Trail*$^{EC+/+}$ and *Trail*$^{EC-/-}$ and measured for media thickness; *Right* – Quantification of aortic medial thickens between the two groups showed no significant difference **(b)** *Left* – 20x magnification of *Trail*$^{EC+/+}$ and *Trail*$^{EC-/-}$ stained for collagen content; *Right* – quantification of collagen (dark red) staining between the two groups showed no significant difference. **(c)** *Left* – 20x magnification of *Trail*$^{EC+/+}$ and *Trail*$^{EC-/-}$ stained for elastin content; *Right* – quantification of elastin (dark purple) staining between the two groups showed no significant difference. n = 4 - 5/group. Results were expressed as mean ± SEM, Student *t-test*.

5.3.5 **12-week HFD mice showed no difference in body and organ weights between *Trail*$^{EC+/+}$ and *Trail*$^{EC-/-}$**

Because we observed little change in plasma, gene expression or vessel structure of 6-14-week-old *Trail*$^{EC+/+}$and *Trail*$^{EC-/-}$ mice, we next wanted to examine whether challenging these mice by feeding them an HFD for 12 w would affect any of these parameters. Mice were weighed weekly and the results were recorded. No difference change in body weight was observed between genotype throughout the 12-weeks of HFD (**Figure 5.5a**). Mice were fasted over-night before euthanasia. Following euthanasia, organs were collected and weighed. Consistent with no change in body weight, there was also no difference in weights of liver, spleen, epididymal fat, retroperitoneal fat or kidney between genotype (**Figure 5.5b-f**).

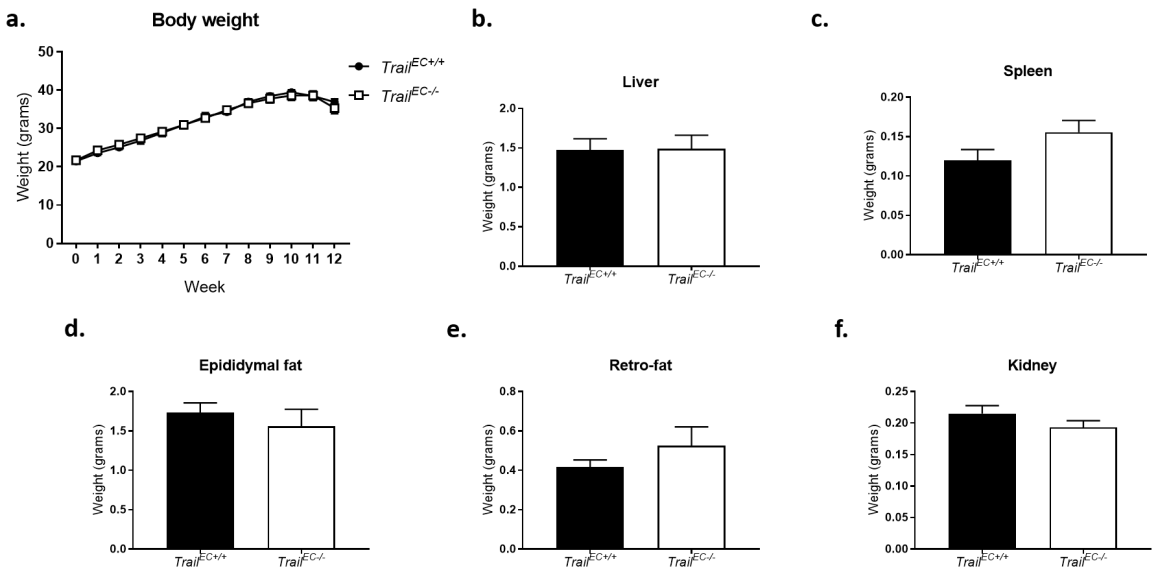

Figure 5.5 12-week HFD mice showed no significant difference in organ weights between *Trail*$^{EC+/+}$and *Trail*$^{EC-/-}$. 6-week old *Trail*$^{EC+/+}$and *Trail*$^{EC-/-}$ mice were placed on a 12-week HFD. **(a)** Body weight was measured weekly for 12 weeks with no significant difference. Following 12-weeks of HFD, over-night fasted mice were euthanised via cardiac puncture and organs were extracted and weighted. There was no significant difference between *Trail*$^{EC+/+}$and *Trail*$^{EC-/-}$ mice's organs such as **(b)** liver, **(c)** spleen, **(d)** epididymal fat, **(e)** retroperitoneal (retro) fat and **(f)** kidney. n = 6 – 12/group. Results were expressed as mean ± SEM, Student *t-test*.

5.3.6 **12-week HFD mice showed no difference in glucose and insulin tolerance test between *Trail*$^{EC+/+}$ and *Trail*$^{EC-/-}$**

Since HFD *Trail*$^{-/-}$ mice displayed glucose intolerance and insulin resistance compared to *Trail*$^{-/-}$ mice [170], we also examine glucose and insulin tolerance at week 10 and week 11 of HFD in *Trail*$^{EC+/+}$and *Trail*$^{EC-/-}$ mice respectively. In contrast to our findings in mice with global TRAIL deletion, glucose or insulin bolus had no effect on glucose and insulin clearance over time in *Trail*$^{EC-/-}$ and *Trail*$^{EC+/+}$mice (**Figure 5.6a-b**).

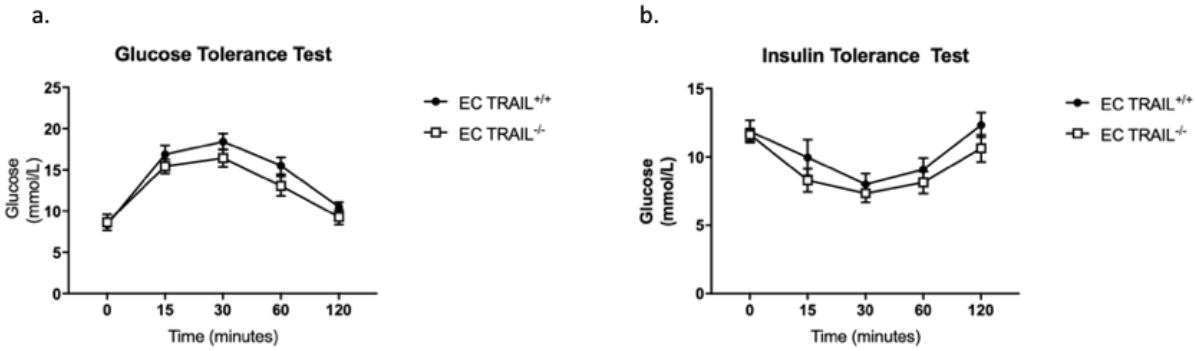

Figure 5.6 12-week HFD mice showed no significant difference in body weight, glucose and insulin tolerance test between *Trail*$^{EC+/+}$and *Trail*$^{EC-/-}$. (a) Over-night fasted mice were given a bolus of glucose and blood glucose level measured at baseline, 15, 30, 60 and 120 minutes after glucose administration and showed no significant difference. **(b)** Non-fasted mice were given a bolus of insulin and blood glucose level measured at baseline, 15, 30, 60 and 120 minutes after insulin administration and showed no significant difference. n = 6 – 12/group. Results were expressed as mean ± SEM, ANOVA (Sidak's multiple comparison test).

5.3.7 **Systolic and diastolic pressure was reduced in *Trail*$^{EC-/-}$ mice on a 12-week HFD**

Because TRAIL is protective of EC dysfunction (chapter 3), which can regulate blood pressure, tail-cuff blood pressure measurements were taken from *Trail*$^{EC-/-}$ and *Trail*$^{EC+/+}$mice between 10 to 12 weeks of HFD feeding. These animals were analysed for systolic and diastolic blood pressure, mean arterial pressure and heart rate. Interestingly, both systolic and diastolic blood pressure was significantly reduced in *Trail*$^{EC-/-}$ mice compared to the control (**Figure 5.7a-b**), indicating a significant reduction in mean arterial pressure in *Trail*$^{EC-/-}$ mice (**Figure 5.7c**). Furthermore, there was a significant increase in heart rate with *Trail*$^{EC-/-}$ mice compared to the control *Trail*$^{EC+/+}$ mice (**Figure 5.7d**). These experiments suggest that TRAIL expressed in ECs can influence blood pressure in mice.

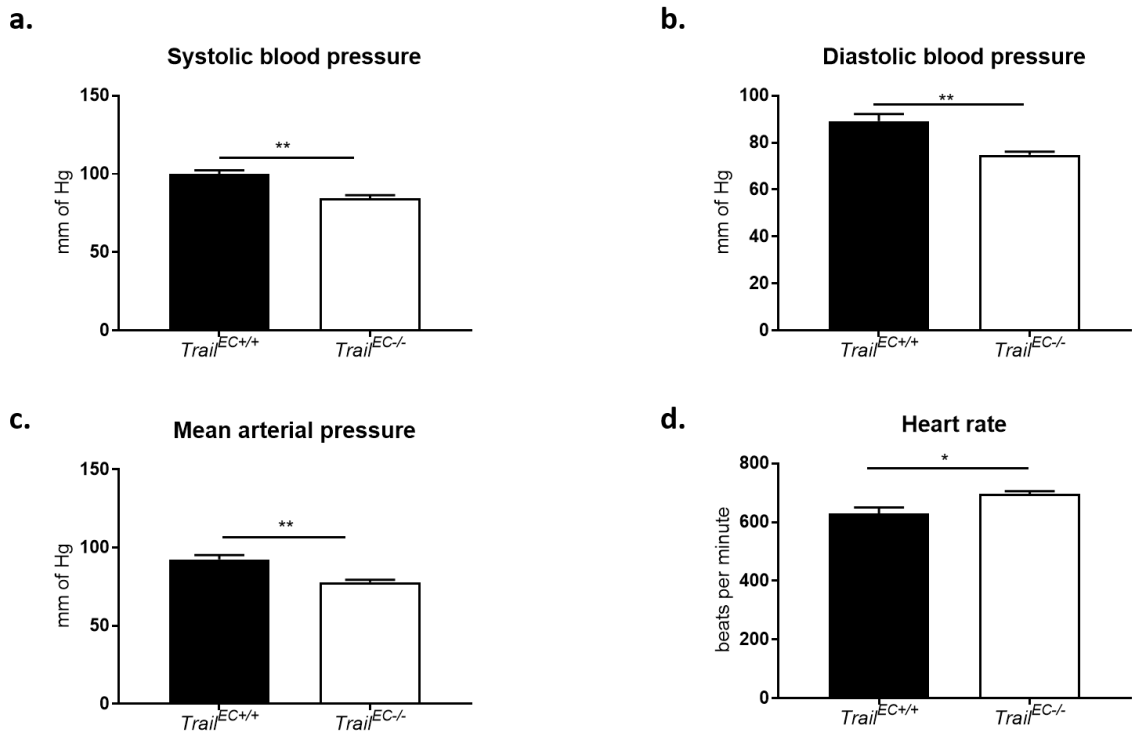

Figure 5.7 Systolic and diastolic pressure was reduced in *Trail*$^{EC-/-}$ mice on a 12-week HFD. Tail-cuff blood pressure was measured between the two groups between 10 – 12 weeks of HFD. **(a)** Systolic blood pressure was significantly reduced in *Trail*$^{EC-/-}$ mice compared to the control, similarly **(b)** diastolic blood pressure was also reduced in *Trail*$^{EC-/-}$ mice along with **(c)** mean arterial pressure. **(d)** Heart rate was significantly increased in *Trail*$^{EC-/-}$ compared to the control. n = 5 - 6/group. Results were expressed as mean ± SEM; *p < 0.05; **p < 0.01; Student *t-test*.

5.3.8 Increase in nitric oxide synthase mRNA expression in aortae of 12-week HFD *Trail*$^{EC-/-}$ mice

Thoracic aortas were obtained from 12-week HFD *Trail*$^{EC+/+}$and *Trail*$^{EC-/-}$ mice and RNA was extracted and analysed by qPCR. mRNA expression of NOS was analysed. It was observed that both eNOS **(Figure 5.8a**) and iNOS (**Figure 5.8b**) was up-regulated in *Trail*$^{EC-/-}$ mice compared to the control *Trail*$^{EC+/+}$mice. These findings are interesting because overexpression of eNOS and iNOS has been linked with hypotension [236,237], suggesting that the increase in NOS with EC TRAIL deletion may be one mechanism for the reduced blood pressure observed in *Trail*$^{EC-/-}$ mice (Figure 5.7). These results suggest that the endothelial nitric oxide production system is altered with TRAIL gene deletion from the endothelium.

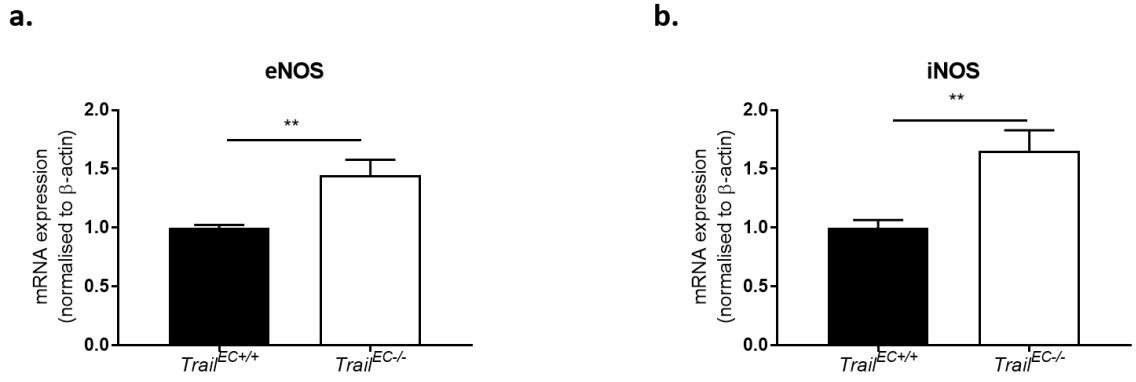

Figure 5.8 Changes in cell adhesion molecules and nitric oxide synthase mRNA expression in *Trail*$^{EC-/-}$ mice following a 12-week HFD. *Trail*$^{EC+/+}$ and *Trail*$^{EC-/-}$ mice fed a 12-week HFD, aorta was collected, and RNA was extracted and quantified for gene expression using qPCR. Both **(a)** eNOS and **(b)** iNOS mRNA expression was upregulated in *Trail*$^{EC-/-}$ mice compared to the control EC Trail$^{+/+}$ mice. mRNA was normalised to β-actin. n = 6 - 7/group. Results were expressed as mean ± SEM; **p < 0.01; Student *t-test*.

5.3.9 **No difference in vessel structure was observed in 12-week HFD *Trail*$^{EC-/-}$ mice**

Thoracic aortas were obtained from 12-week HFD fed *EC Trail*$^{+/+}$ and *Trail*$^{EC-/-}$ mice and fixed for histological analysis and cut into 5μm section for analysis. There were no obvious visual differences, and no difference in the thickness of the media between genotype **(Figure 5.9a**). Because ECM proteins such as collagen and elastin, provides structural integrity to vessel wall, we wanted to examine if these were different in the aortae of mice lacking TRAIL from the endothelium. Consistent with no obvious changes, there were no difference in elastin or collagen content in aortae of *Trail*$^{EC-/-}$ vs. *Trail*$^{EC+/+}$ mice (**Figure 5.9b-c**).

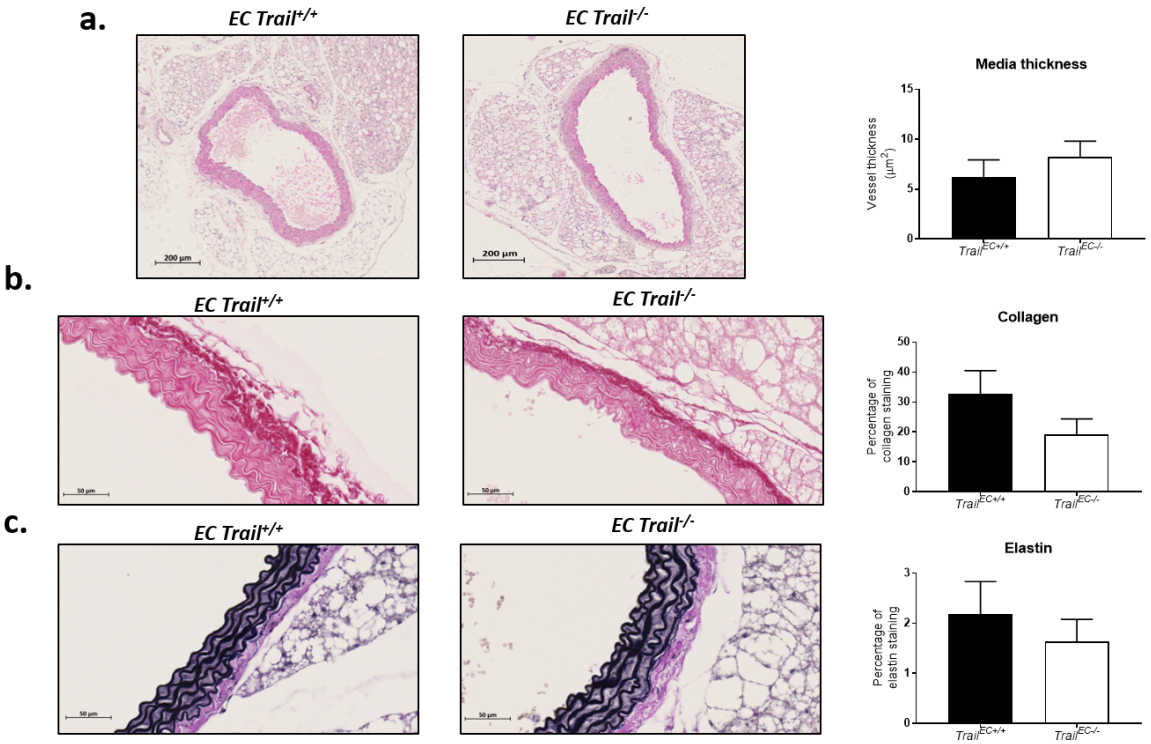

Figure 5.9 No significant difference in physical characteristic of vessel wall between *Trail*$^{EC-/-}$ and *EC Trail*$^{+/+}$ mice on a 12-week HFD. 5µm histological sections of thoracis aorta stained for **(a)** *Left* – H & E staining of *Trail*$^{EC+/+}$ and *Trail*$^{EC-/-}$ and measured for media thickness; *Right* – Quantification of aortic medial thickens between the two groups showed no significant difference **(b)** *Left* – 20x magnification of *Trail*$^{EC+/+}$ and *Trail*$^{EC-/-}$ stained for collagen content; *Right* – quantification of collagen (dark red) staining between the two groups showed no significant difference. **(c)** *Left* – 20x magnification of *Trail*$^{EC+/+}$ and *Trail*$^{EC-/-}$ stained for elastin content; *Right* – quantification of elastin (dark purple) staining between the two groups showed no significant difference. n =5- 8/group. Results were expressed as mean ± SEM, Student *t-test*.

5.3.10 **Plasma cholesterol levels are significantly increased in *Trail*$^{EC-/-}$ mice following 12-week HFD.**

As in baseline characterisation (section 5.2.4), plasma chemistries, specifically, blood glucose, insulin and cholesterol were assessed. No change in plasma glucose between the two groups were observed (**Figure 5.10a**). However, plasma cholesterol levels were significantly elevated in *Trail*$^{EC-/-}$ compared to the control *Trail*$^{EC+/+}$, by almost 7-fold (**Figure 5.10b**). In contrast, no changes were in plasma insulin or plasma nitrate/nitrite were observed between genotype (**Figure 5.10c-d**). These results suggest that in response to an HFD, TRAIL expressed specifically on the endothelium influences plasma cholesterol levels. Why this occurs is currently unknown.

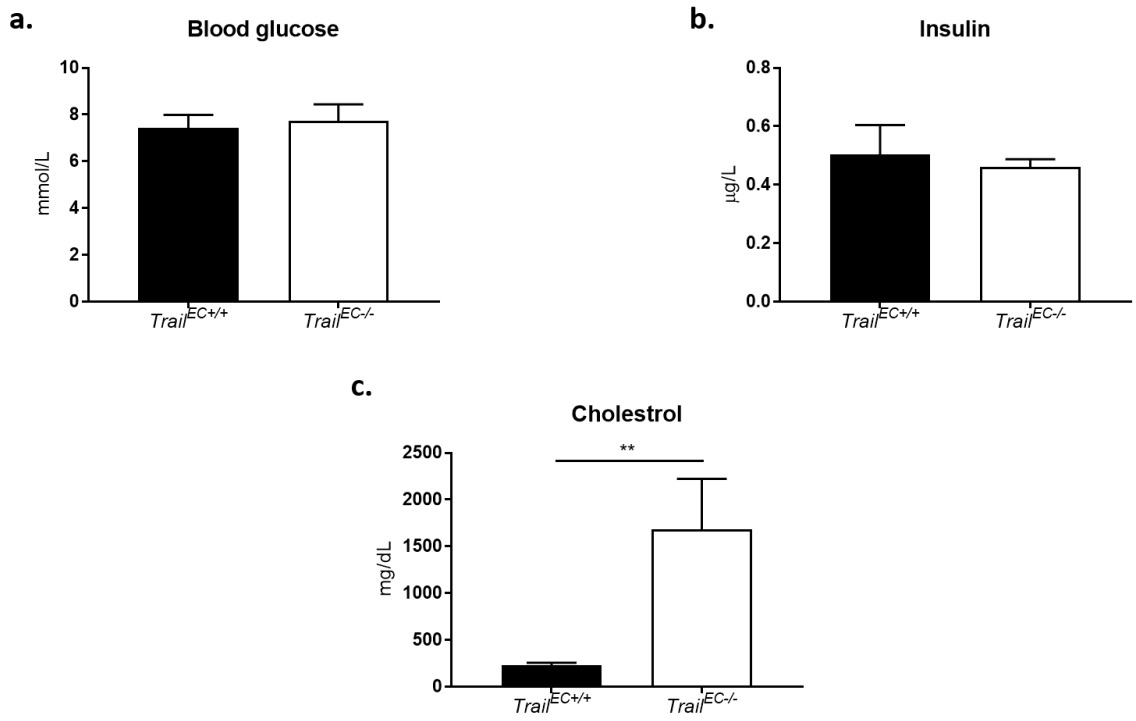

Figure 5.10 Plasma cholesterol levels are significantly increased in *Trail*$^{EC-/-}$ mice following 12-week HFD. Plasma was extracted from 12-week HFD mice during euthanasia through cardiac puncture. **(a)** Blood glucose and **(b)** insulin showed no significant difference between the two groups. **(c)** However, cholesterol level was significantly elevated in *Trail*$^{EC-/-}$ mice compared to the control *Trail*$^{EC+/+}$. n = 6 - 9/group. Results were expressed as mean ± SEM; **p < 0.01; Student *t-test*.

5.3.11 **Changes in cell adhesion and inflammatory genes in aortic mRNA expression in *Trail*$^{EC-/-}$ mice following 12-week HFD**

Thoracic aortas were isolated from 12-week HFD *Trail*$^{EC+/+}$and *Trail*$^{EC-/-}$ mice and RNA was extracted. Analysis of endothelial specific cell adhesions molecules revealed an up-regulation in ICAM-1 (**Figure 5.11a**), down-regulation in VCAM-1 (**Figure 5.11b**) and no change in VE-cadherin (**Figure 5.11c**) aortic mRNA expression between *Trail*$^{EC-/-}$ and control *Trail*$^{EC+/+}$ mice. Inflammatory gene expression revealed no difference in IL-18 and MCP-1 expression (**Figure 5.11d-e**), however, IL-1β expression was significantly reduced (**Figure 5.11f**) in *Trail*$^{EC-/-}$ mice compared to control *Trail*$^{EC+/+}$. These data suggest that, EC-specific TRAIL influences expression of some genes regulating cell adhesion and inflammation in the vasculature.

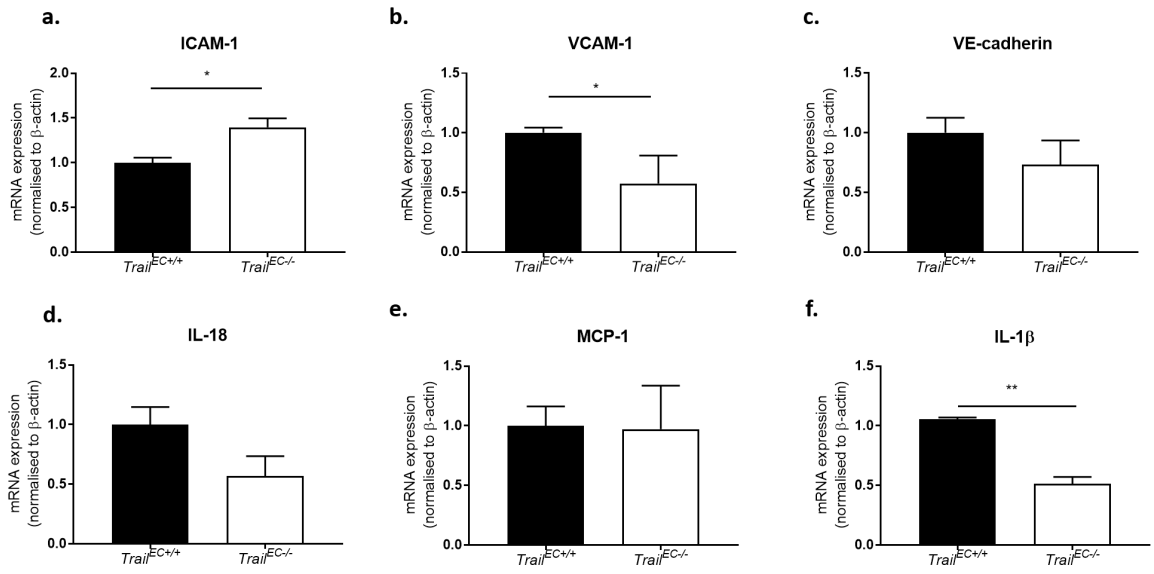

Figure 5.11 Changes in cell adhesion and inflammatory aortic gene expression in *Trail$^{EC-/-}$* mice on a 12-week HFD. Aortas were collected from *Trail$^{EC+/+}$* and *Trail$^{EC-/-}$* mice fed a 12-week HFD. RNA was extracted and quantified for gene expression using qPCR. Cell adhesion molecules gene expression such as **(a)** ICAM-1 was up-regulated, **(b)** VCAM-1 was down-regulated and **(c)** VE-cadherin showed no change between *Trail$^{EC-/-}$* mice and *Trail$^{EC+/+}$*. Inflammatory gene expression such as **(d)** IL-18 and **(e)** MCP-1 showed no significant difference, however **(f)** IL-1β mRNA expression was down-regulated in *Trail$^{EC-/-}$* mice compared to the control *Trail$^{EC+/+}$*. mRNA expression was normalised to β-actin. n = 6 - 7/group. Results were expressed as mean ± SEM; *p< 0.05; **p < 0.01; Student *t-test*.

5.4 DISCUSSION

This thesis demonstrates that TRAIL plays a critical role in EC homeostasis, such that global TRAIL deletion promotes oxidative stress, EC dysfunction and inflammation [170,190]. To examine the contribution of TRAIL specifically coming from EC on multiple vascular conditions, our laboratory recently generated world-first *Trail*$^{EC-/-}$ mice. Before any models could be employed, this thesis characterised features of these mice compared to littermate control mice. Specifically, this thesis identified that adult *Trail*$^{EC-/-}$ mice did not differ in plasma chemistries or mRNA expression of adhesion molecules, nor was there any change in vascular structure of the aortae compared to *Trail*$^{EC+/+}$ mice. However, it showed changes in inflammatory molecules such as IL-18 and MCP-1. The second part of this chapter examined these mice in response to a challenge, namely these mice were fed an HFD for 12 weeks. Interestingly, this chapter identified 3 major differences in mice with EC-TRAIL deletion. First, *Trail*$^{EC-/-}$ mice had 7-fold increased plasma cholesterol compared to *Trail*$^{EC+/+}$; second, these mice displayed reductions in blood pressure, both systolic and diastolic. Third, this reduced blood pressure was associated with overexpression of NOS, but reduced IL-1β mRNA in aortae. These findings are significant as they provide important information for the physiological function of TRAIL in endothelium at homeostasis and during a challenged situation.

Cholesterol metabolism plays an important role in the pathogenesis of atherosclerosis. Circulating cholesterol levels are dependent on factors such as diet, rate of synthesis of cholesterol in the liver and the rate of clearance of cholesterol from the body [238,239]. Firstly, in regard to the diet, our animals were placed on a 12-week HFD. Studies have consistently shown for mice to have high circulating plasma cholesterol under HFD compared to normal chow [240,241]. Interestingly, we observed that our *Trail*$^{EC-/-}$ mice placed on an HFD

experienced ~7-fold increase in plasma cholesterol compared to its control *Trail*$^{EC+/+}$mouse which was also on an HFD. This massive change due to endothelial specific TRAIL deletion signifies damages to cholesterol metabolism in these mice. High plasma cholesterol is usually associated with increased synthesis of cholesterol by the liver [242]. However, *Trail*$^{EC-/-}$ mice in this study showed no difference in liver weight or colour (data not shown). This might signify that the process of cholesterol synthesis is not affected as usually an increase in cholesterol synthesis is represented by a fatty liver and hypertrophic hepatocytes [243]. However, previous findings from our lab have indicated that global TRAIL deleted mice on an HFD had increased oil-red O staining indicative of increased lipid content with no change in liver weight [170]. Hence further histological analysis of *Trail*$^{EC-/-}$ mice's liver is required to identify any differences in cholesterol synthesis. Finally, another factor which can affect plasma cholesterol level is the rate of cholesterol clearance in the body. This process is referred to as reverse cholesterol transport (RCT), whereby cholesterol from peripheral tissue is transported to the liver for clearance/excretion. Genes such as ATP-binding cassette transporter A1 (ABCA1) and G1 (ABCG1) are involved in clearance of cholesterol from the periphery [244]. Downregulation of these factors aid in acceleration of atherosclerosis [245,246]. We suspect the sinusoidal capillaries present in the liver to be defective as they play an important role in cholesterol clearance between the liver and the capillaries [247,248]. Even with proper metabolism of cholesterol in the liver, damage to these sinusoidal ECs in *Trail*$^{EC-/-}$ mice can affect systemic cholesterol intake and efflux [249]. Furthermore, I have shown that TRAIL deletion from an Apoe-null mouse had increased EC dysfunction in Chapter 3. This can lead to disruption in endothelial permeability which can affect inter-cellular transport of cholesterol. Studies have shown that, disruption in endothelial barrier, affect transcytosis of LDL and HDL from the interstitial space to the lumen and thus deregulate RCT [250,251]. My previous published work has shown that global TRAIL deletion mice had increased permeability along

with disruption in cell-to-cell contact protein, VE-cadherin [190]. This offers the possibility that mice with EC-specific TRAIL deletion, can have increased permeability and dysfunctional RCT. Various factors as described above play a role in cholesterol metabolism and analysis of these pathways in *Trail*$^{EC-/-}$ mice can provide us the role of TRAIL in cholesterol metabolism in ECs.

I have shown that TRAIL modulates expression of adhesion and inflammatory makers (Chapter 4). The current study using Trail$^{EC-/-}$ mice support these findings with reduced expression of aortic IL-18 and MCP-1 mRNA. The mechanism(s) of action for this are not known and currently under investigation. Additional studies with increased animal numbers and multiple different techniques need to be employed to confirm this finding. Interestingly, this chapter also discovered that HFD *Trail*$^{EC-/-}$ mice had reduced blood pressure associating with increased expression of NOS including eNOS and iNOS. Importantly hypotension can be due to over-production of NO [252]. Though NOS induced NO production can confer a protective effect on the vasculature, over-production of NO combined with ROS can result in cytotoxic molecules such as peroxynitrite [253]. eNOS over-production can also result in its monomerization, which can potentiate ROS production, and iNOS over-expression can initiate inflammatory cascade [254]. In this chapter, I have shown eNOS and iNOS expression is upregulated in Trail$^{EC-/-}$ aortae, suggesting that TRAIL deletion from the endothelium may be detrimental via NOS pathway. Further studies are needed to confirm this. Studies have shown that over-expression of eNOS in the vasculature of brain regions which control blood pressure such as nucleus tractus solitarius (NTS) and rostral ventrolateral medulla (RVLM), can lead to hypotension [237,255]. Although plasma nitrate/nitrate levels were not assessed in these HFD-fed mice, these studies provide a suggestive reasoning that there might be dysregulation in production of nitric oxide in *Trail*$^{EC-/-}$ mice experiencing hypotension and up-regulated NOS aortic mRNA expression [237,255]. Lower blood pressure might also be associated with

reduced VCAM-1 mRNA expression observed in this model. Cell adhesion molecules are up-regulated during high sheer stress hypertensive systems [187]. This may be a possible explanation for the reduced blood pressure we observed in this model.

We also observed significant reduction in VCAM-1 expression. Similar changes, though not significant, was also observed in the baseline study. VCAM-1 is expressed exclusively in the luminal side of activated endothelium and is essential for immune surveillance. Cancer studies have shown that reduced VCAM-1 expression enables tumour cells to evade immune-surveillance [256,257]. Also, the inflammatory marker IL-1β was reduced in *Trail*$^{EC-/-}$ mice. Though this result suggests TRAIL potentiates vascular inflammation in the endothelium, recent reports have observed that IL-1β depletion leads to characteristics of an unstable plaque [258]. However, it is important to note that our model is a non-atheroma developing model and my findings may not reflect what occurs during plaque development. Furthermore, mRNA levels measured reflect the whole vascular wall, not just the endothelium, and there may be alternate expression levels between different cell types that contribute to these changes. Given that IL-1β can self-regulate in a paracrine manner [259] and also regulate VCAM-1 [260], suggests the existence of a TRAIL/VCAM-1/IL-1β axis. Additional studies are required to fully understand whether these changes are specific to TRAIL deletion in the endothelium, and whether they have functional consequences in the vessel wall. These are described in greater detail in the future directions (Section 7.2). In combination with our lab's finding that *Trail*$^{-/-}$ *Apoe*$^{-/-}$ mice having accelerated atherosclerosis, increased calcification, IL-1β reduction can indicate an unstable plaque development [173]. These results are suggestive that EC-specific TRAIL deletion has increased percentage of activated endothelium in the vasculature which can attract and tether more circulating monocytes. Furthermore, in Chapter 4, it was shown that TRAIL can mitigate monocyte adhesion following AngII exposure to ECs in an in-vitro setting. In chapter 5, histological analysis of the vasculature examining cell adhesion molecules, pro-

inflammatory cytokines and immune cell infiltartes (e.g. macrophages) at baseline and following 12-weeks of HFD will provide a more comprehensive insight into the effect of EC-expressed TRAIL in the blood vessel wall. These experiments can further be supplemented by analysing the aortic lysates for the above-mentioned molecules via western blotting or ELISA. Also, whilst observing significant differences in aortic mRNA expression of cytokines and cell adhesions molecules following an HFD, it is important to consider the impact of baseline changes such as those observed for MCP-1 and IL-18 mRNA expression, in its contribution during the HFD treatment. In addition to reduced IL-18 and IL-1β in both naive and 12-week HFD $Trail^{EC-/-}$ mice, my lab has recently shown that circulating IL-18 levels were reduced in $Trail^{-/-}$ mice. Indeed IL-18 can attenuate TRAIL mRNA expression in macrophages under certain conditions [261]. These suggests that there is a correlation between immune regulation and EC homeostasis, modulated in part via TRAIL.

In summary, this chapter establishes the importance of TRAIL originating from the endothelium and its systemic effect in a murine model. EC-specific TRAIL deletion had dysregulated cholesterol metabolism and blood pressure control implicating a critical function in vascular disease.

Chapter 6: **VSMC-specific TRAIL knockout mice characterisation**

6.1 INTRODUCTION

VSMCs possesses remarkable phenotypic plasticity that allows them to change phenotype based on environmental cues during vessel development, angiogenesis and vascular diseases [262]. At homeostasis, VSMCs are mostly contractile in their phenotype and autoregulate blood vessel lumen, blood pressure and blood flow distribution. These VSMCs exhibit contractile cell markers such as α-SMA, α-tropomyosin, myosin heavy chain (MYH) 10 and 11, along with maintaining minimal proliferation and synthetic activity. These cells are able to adapt to changes such as biomechanical stress, and vasoactive physiological and pathological molecules [263]. Also, at homeostasis, VSMCs can respond to NO produced by the endothelial layer, which can limit their proliferation, maintain their contractile state and modulate vaso-constriction and vaso-relaxation.

In atherosclerosis, following endothelial dysfunction and leukocyte recruitment, VSMCs undergo proliferation and migration into the sub-endothelial space leading to plaque progression. During this process, these cells undergo phenotypic switching with the help of transcription factors such as Krüppel-like factor (KLF) 4 and 5. Though phenotypic switching is a transient process, during atherosclerosis, most of the VSMCs are in their synthetic phenotype creating an inflammatory environment along with proliferation and migration of VSMCs.

Our lab was the first to establish the non-apoptotic role of TRAIL in VSMCs at physiological concentrations. We have also shown that *Trail*$^{-/-}$ mice had reduced neo-intimal formation following injury and VSMCs obtained from *Trail*$^{-/-}$ mice had reduced proliferative activity [184,194]. These experiments suggest that TRAIL plays an important proliferative role

in VSMCs enabling intimal thickening after a vascular injury. However, the role of TRAIL in VSMCs during atherosclerosis is unknown. VSMC's phenotypic markers along with their systemic physiological impact due to TRAIL is not fully understood.

In this chapter we aim to characterise the role of TRAIL in VSMCs *in vivo* under physiological and pathological conditions using VSMC-specific TRAIL deleted mice.

6.2 BRIEF METHODS

6.2.1 **Animals**

In this chapter $Trail^{VSMC-/-}$ and $Trail^{VSMC+/+}$ male mice were generated as described in method section 2.4.4 and characterised at baseline and following 12 w HFD as described in method section 2.4.5. Animal ethics were obtained from Sydney Local Animal Welfare Committee (2017-020, 2014-027).

6.2.2 **Mouse aortic RNA extraction**

Aortas obtained from mice at baseline and 12 w HFD were extracted for RNA as described in method section 2.4.8 and PCR analysis was done with primers listed in method section 2.4.9.

6.2.3 **Plasma biochemistry**

Plasma extracted from mice at baseline and following 12 w HFD were measured for cholesterol, insulin and nitrate/nitrite as described in method section 2.4.12, 2.4.13 and 2.4.14.

6.2.4 **Glucose and insulin tolerance test**

GTT and ITT were carried out in 12 w HFD fed mice according to method section 2.4.7.

6.2.5 **Blood pressure**

Blood pressure was measured at week 10-12 in HFD fed mice according to method section 2.4.6.

6.3 RESULTS

6.3.1 Baseline characterisation *Trail*$^{VSMC-/-}$ showed changes in contractile and synthetic gene mRNA expression

Mice aged between 6 to 14 weeks were euthanised and thoracic aortas were collected. RNA was extracted and analysed for gene expression markers for contractile and synthetic phenotypes. Investigation of contractile makers showed α-tropomyosin was reduced in *Trail*$^{VSMC-/-}$ mice, yet this did not reach significance. No difference was observed with smooth muscle α-actin (SMα-A), myosin heavy chain -10 (MYH-10) and myosin heavy chain-11 (MYH-11) (**Figure 6.1a-d**). Krüppel-like factor (KLF), an important transcriptional factor of VSMCs is important in identifying the pathological condition of the vasculature [264]. Synthetic markers KLF-4 and KLF-5 were significantly reduced in *Trail*$^{VSMC-/-}$ mice compared to the control (**Figure 6.1e-f**). This suggests that TRAIL gene deletion from VSMCs affects phenotypic switching in the vasculature.

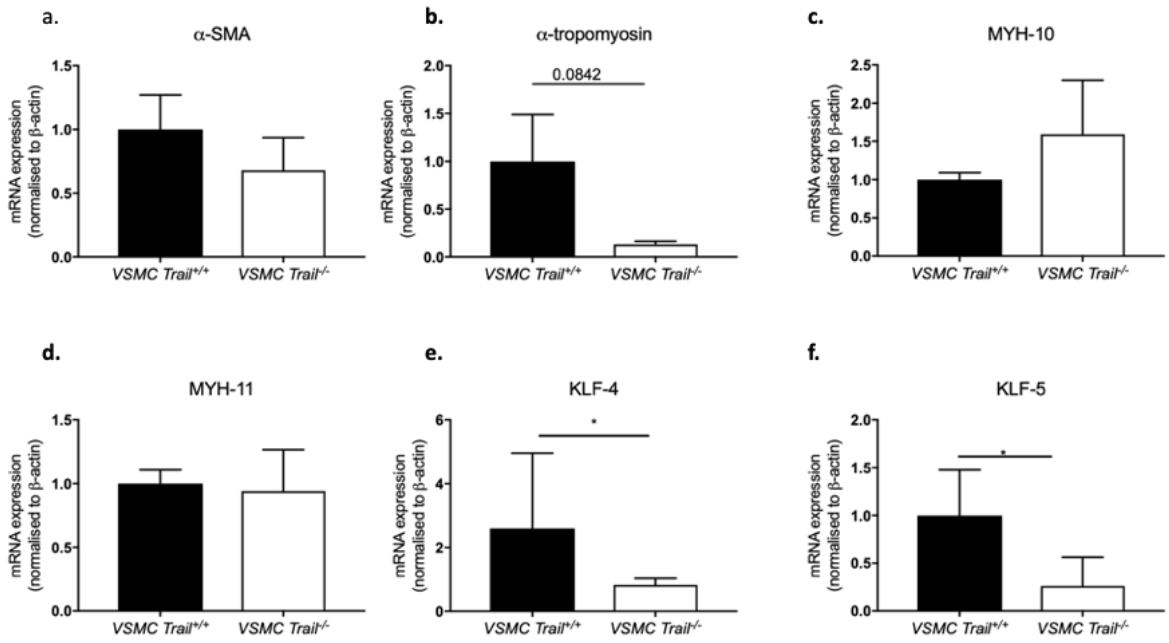

Figure 6.1 Baseline characterisation of *Trail*$^{VSMC-/-}$ and *Trail*$^{VSMC+/+}$ showed changes in contractile and synthetic gene mRNA expression. Aortae from 6 - 14-week-old *Trail*$^{VSMC+/+}$ and *Trail*$^{VSMC-/-}$ were collected a and quantified for gene expression using qPCR. Contractile markers **(a)** α-tropomyosin was down-regulated in *Trail*$^{VSMC-/-}$ compared the control. However, there was no significant changes with other contractile markers **(b)** SMα-A, **(c)** MYH-10 and **(d)** MYH-11. On the other hand, transcription factors such as **(e)** KLF-4 and **(f)** KLF-5 were significantly reduced in *Trail*$^{VSMC-/-}$ mice compared to the control *Trail*$^{VSMC+/+}$ mice. mRNA expression was normalized to β-actin. n = 4 – 5/group. Results were expressed as mean ± SEM; *p < 0.05; Student *t-test*.

6.3.2 **Baseline characterisation of *Trail*$^{VSMC-/-}$ mice showed reduced VCAM-1 and IL-1β mRNA expression**

Several research have indicated cross-talk between VSMCs and ECs. This cross-talk regulates vascular functionality and sustains homeostasis. Thus identification of inflammation and endothelial specific markers are important in *Trail*$^{VSMC-/-}$ mice [265]. Though there was no difference between cell adhesion molecules ICAM-1, VCAM-1 was significantly reduced in *Trail*$^{VSMC-/-}$ compared to the control (**Figure 6.2a-b**). There was no change observed with VE-cadherin, an important endothelial permeability marker (**Figure 6.2c**). Furthermore, inflammatory marker IL-1β was reduced in *Trail*$^{VSMC-/-}$ mice (**Figure 6.2d**). These changes prove a cross-talk between ECs and VSMCs, as well as provide a directionality for future research.

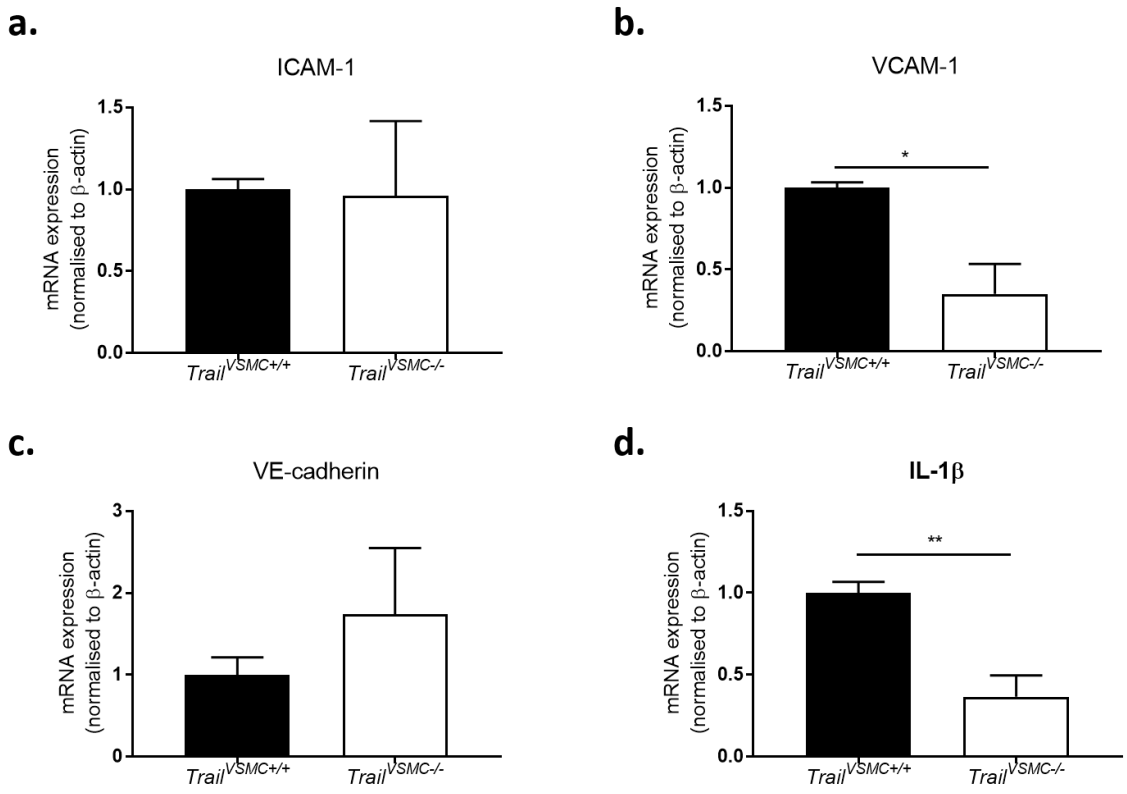

Figure 6.2 Baseline characterisation of Trail$^{VSMC-/-}$ showed reduced VCAM-1 and IL-1β mRNA expression. See changes above 6 - 14-week-old *Trail$^{VSMC+/+}$* and *Trail$^{VSMC-/-}$* aorta were collected and RNA was extracted and quantified for gene expression using qPCR. Endothelial specific gene expression such as **(a)** ICAM-1 showed no significant difference, but **(b)** VCAM-1 mRNA expression was reduced in *Trail$^{VSMC-/-}$* compared to the control and **(c)** VE-cadherin did not exhibit any difference between the two groups. Inflammatory marker **(d)** IL-1β showed significant reduction in *Trail$^{VSMC-/-}$* mice compared to the control *Trail$^{VSMC+/+}$*. n = 4 – 5/group. Results were expressed as mean ± SEM; *p < 0.05, **p < 0.01; Student *t-test*.

6.3.3 **TRAIL deletion in VSMC has no effect on plasma chemistries at baseline**

To analyse the metabolic state of baseline *Trail*$^{VSMC-/-}$ mice, plasma biochemistry analysis was done. Mice were fasted before euthanasia and blood was collected through cardiac puncture. Plasma was extracted and analysed. There were no difference observed with plasma cholesterol, insulin and Nitrate/nitrite between *Trail*$^{VSMC-/-}$ and *Trail*$^{VSMC+/+}$ mice (**Figure 6.3a-c**).

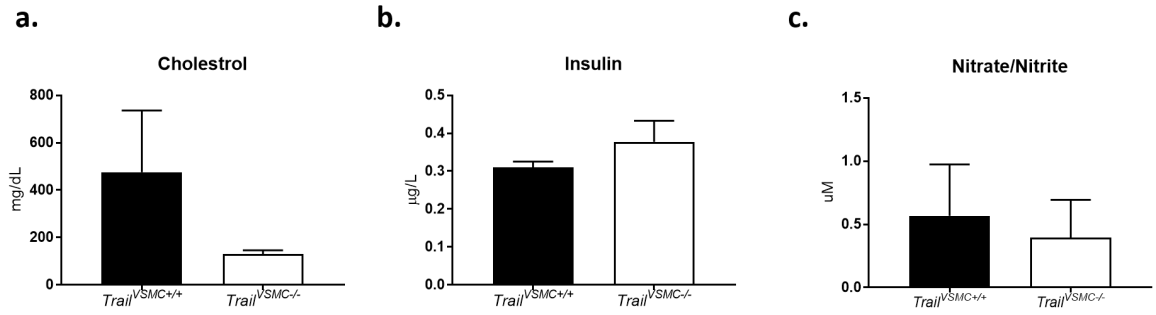

Figure 6.3 No significant difference was observed in plasma biochemistry in baseline VSMC-specific TRAIL knockout mice see title above. Blood was collected from mice by cardiac puncture and plasma isolated. Plasma was used to analyze **(a)** cholesterol, **(b)** insulin and **(c)** nitrate/nitrite level, which showed no significant difference between *Trail*$^{VSMC-/-}$ and the control *Trail*$^{VSMC+/+}$ at baseline. n = 4 - 5/group. Results were expressed as mean ± SEM, Mann-Whitney test.

6.3.4 **Baseline characterisation of *Trail*$^{VSMC-/-}$ mice showed no difference in the physical structure of the vasculature**

Thoracic aorta collected from 6 to 14-week old mice were fixed in paraffin for histology and cut into 5μm sections. 20x magnification of aortic sections were taken. ECM proteins such as collagen and elastin which provides structural integrity to vessel wall was observed [73]. There were no difference observed with elastin and collagen content (**Figure 6.4a-b**). H&E staining was performed to observe the vessel wall's thickness, which showed no difference between *Trail*$^{VSMC-/-}$ and its control *Trail*$^{VSMC+/+}$mice **(Figure 6.4c**).

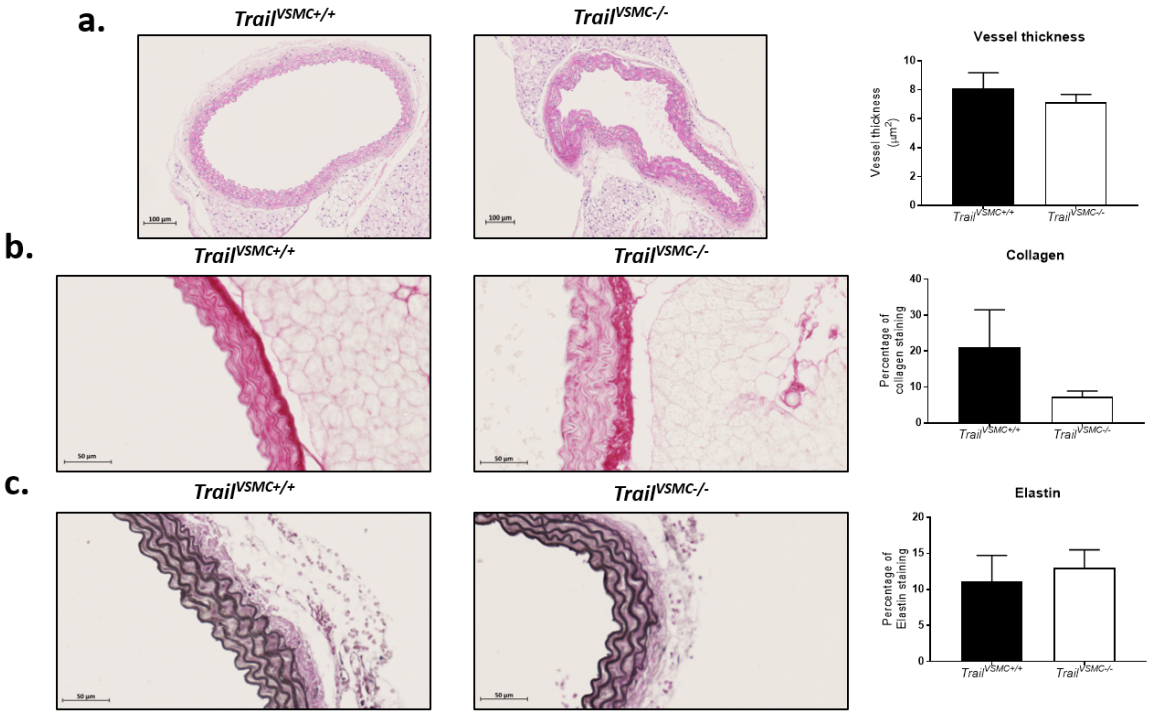

Figure 6.4 No significant difference at baseline in physical characteristic of vessel wall between *Trail*$^{VSMC-/-}$ and *Trail*$^{VSMC+/+}$ mice. 5μm histological sections of thoracic aorta stained for **(a)** *Left* – H&E staining of *Trail*$^{VSMC+/+}$ and *Trail*$^{VSMC-/-}$ and measured for vessel thickness; *Right* – Quantification of aortic wall thickens between the two groups showed no significant difference. **(b)** *Left* – 20x magnification of *Trail*$^{VSMC+/+}$ and *Trail*$^{VSMC-/-}$ stained for collagen content; *Right* – quantification of collagen (dark red) staining between the two groups showed no significant difference. **(c)** *Left* – 20x magnification of *Trail*$^{VSMC+/+}$ and *Trail*$^{VSMC-/-}$ stained for elastin content; *Right* – quantification of elastin (dark purple) staining between the two groups showed no significant difference. n = 3 - 4/group. Results were expressed as mean ± SEM, Student *t-test*.

6.3.5 **Liver weights were significantly increased in *Trail*$^{VSMC-/-}$ mice after 12 w HFD**

Because we observed little changes in gene expression and no changes in plasma biochemistry or vessel structure of 6-week old *Trail*$^{VSMC-/-}$ and *Trail*$^{VSMC+/+}$ mice, we next wanted to examine whether challenging these mice by feeding them an HFD for 12 weeks would affect any of these parameter. Mice were fasted over-night before sacrifice. Following euthanasia of mice placed on a 12-week HFD, organs were collected and weighted. No difference in weight was observed between the two groups throughout the 12-weeks of HFD (**Figure 6.5a**) *Trail*$^{VSMC-/-}$ mice had significantly larger liver than the control *Trail*$^{VSMC+/+}$ (**Figure 6.5b**). However, there was no difference in other organ weights such as spleen, fat, retro-fat and kidney between the two groups (**Figure 6.5c-f**).

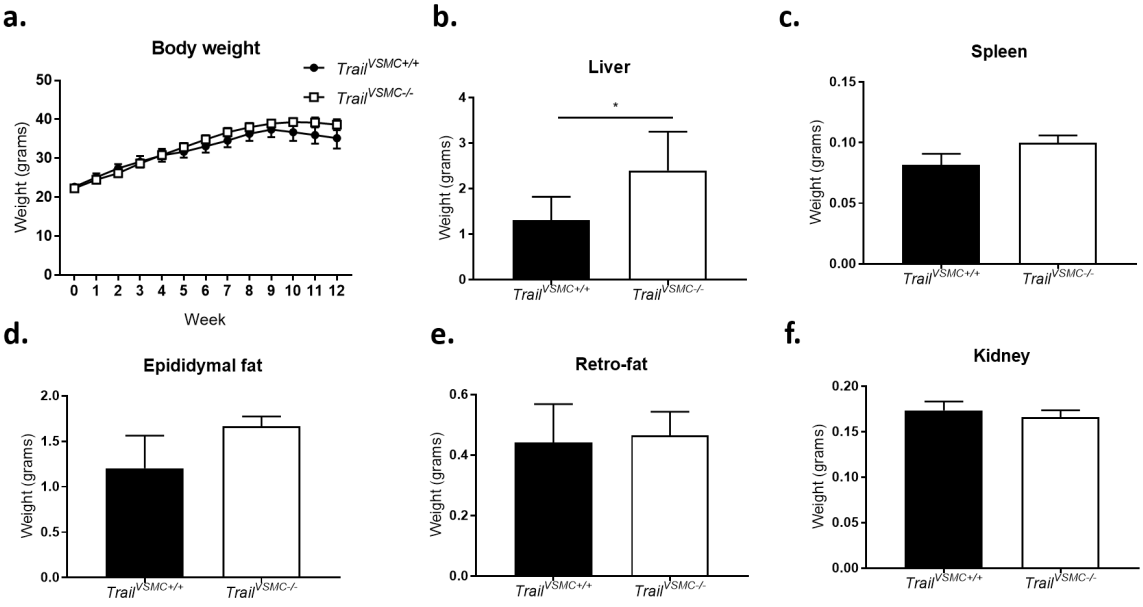

Figure 6.5 Liver weight was significantly increased in *Trail*$^{VSMC-/-}$ compared to VSMC Trail$^{+/+}$ mice on a 12-week HFD. 6-week old mice were placed on a 12-week HFD. **(a)** Body weight was measured weekly with no significant difference. Following 12-weeks HFD, over-night fasted mice were euthanised via cardiac puncture and organs were extracted and weighted. **(b)** There was a significant up-regulation in liver mass in *Trail*$^{VSMC-/-}$ mice compared to the control *Trail*$^{VSMC+/+}$. Other organs such as **(c)** spleen, **(d)** epididymal fat **(e)** retro-fat and **(f)** kidney showed no significant difference between the two groups. n = 10 - 11/group. Results were expressed as mean ± SEM; *p < 0.05; Student *t-test*.

6.3.6 **12-week HFD mice showed no difference in body weight, glucose and insulin tolerance test between *Trail*$^{VSMC+/+}$ and *Trail*$^{VSMC-/-}$**

Ince HFD Trail$^{-/-}$ mice displayed glucose intolerance and insulin resistance compared to Trail$^{+/+}$ mice [170], we also examined glucose and insulin tolerance at week 10 and week 11 of HFD in *Trail*$^{VSMC+/+}$ and *Trail*$^{VSMC-/-}$ mice respectively. Glucose and insulin tolerance test were performed at week 10 and week 11 of HFD respectively. A bolus of glucose or insulin was given to over-night fasted and non-fasted mice, for GTT and ITT respectively. No difference difference was observed with GTT or ITT between *Trail*$^{VSMC-/-}$ and its control *Trail*$^{VSMC+/+}$ mice (**Figure 6.5a-b**). The large variation in ITT data is potentially due to animal stress, animal handling and probable variation in response to insulin between animals from the same genotype [266]

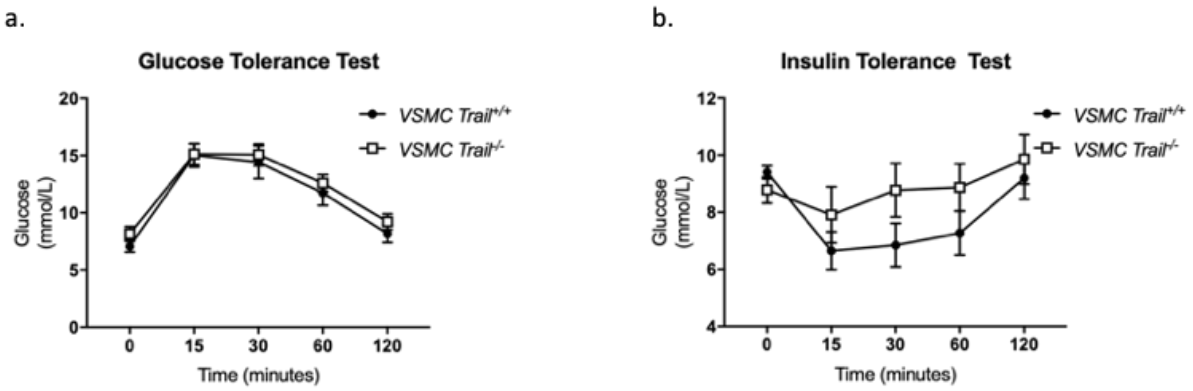

Figure 6.6 12-week HFD mice showed no difference **difference in glucose and insulin tolerance test between *Trail*$^{VSMC+/+}$and *Trail*$^{VSMC-/-}$. (a)** Over-night fasted mice were given a bolus of glucose (1 g/kg) and blood glucose level measured at baseline, 15, 30, 60 and 120 minutes after glucose administration and showed no significant difference. **(b)** Non-fasted mice were given a bolus of insulin (1 U/kg) and blood glucose level measured at baseline, 15, 30, 60 and 120 minutes after insulin administration and showed no significant difference. n = 10 -11/group. Results were expressed as mean ± SEM, ANOVA, Sidak's multiple comparison test.

6.3.7 **No changes in blood pressure in *Trail*$^{VSMC-/-}$ mice and its control in a 12-week HFD model**

Because TRAIL is protective of EC dysfunction and vascular inflammation (chapter 3), which can regulate blood pressure, tail-cuff blood pressure measurements were taken from *Trail*$^{VSMC-/-}$ and *Trail*$^{VSMC+/+}$ mice between 10 to 12 weeks of HFD feeding. These animals were analysed for systolic and diastolic blood pressure, mean arterial pressure and heart rate. There were no difference observed in any of the mentioned parameters between *Trail*$^{VSMC-/-}$ and *Trail*$^{VSMC+/+}$ mice (**Figure 6.7a-d**).

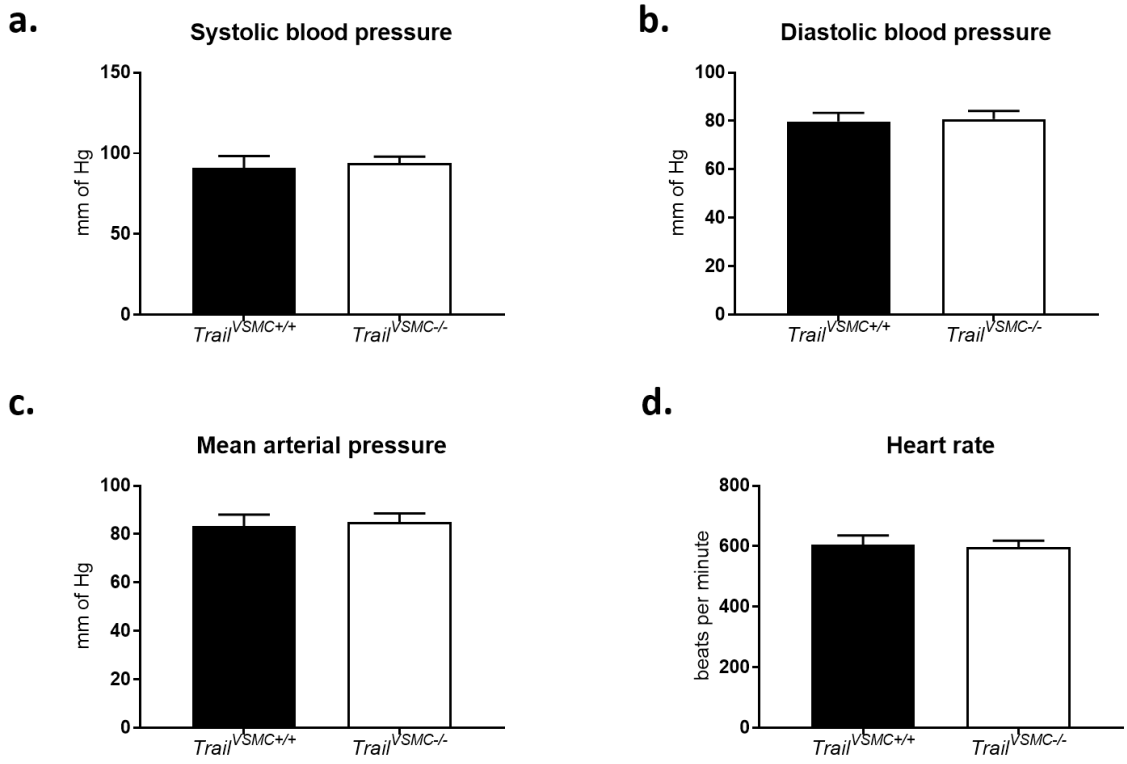

Figure 6.7 No significant changes between *Trail*$^{VSMC-/-}$ and *Trail*$^{VSMC+/+}$on a 12-week HFD. Tail-cuff blood pressure was measured between the two groups between 10 – 12 weeks of HFD. There were no significant changes between **(a)** systolic blood pressure, **(b)** diastolic blood pressure, **(c)** mean arterial pressure and **(d)** heart rate between *Trail*$^{VSMC-/-}$ and *Trail*$^{VSMC+/+}$n = 4 - 8/group. Results were expressed as mean ± SEM; Student *t-test*.

6.3.8 **No changes in plasma biochemistry of VSMC-specific TRAIL knockout mice following 12-week HFD**

As in baseline characterisation (section 6.2.4), plasma chemistries, specifically, blood glucose, insulin and cholesterol were assessed. There were no difference observed with plasma glucose, insulin and cholesterol concentrations in $Trail^{VSMC-/-}$ and $Trail^{VSMC+/+}$ mice on a 12-week HFD (**Figure 6.8a-d**).

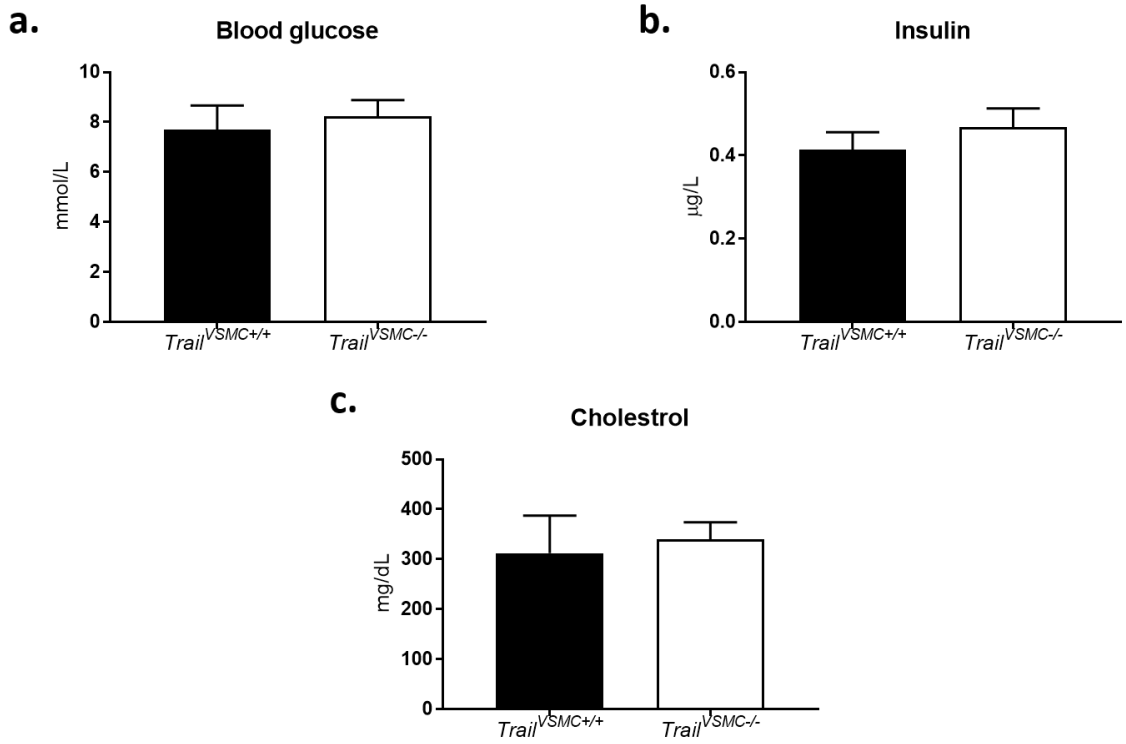

Figure 6.8 No changes in plasma biochemistry of VSMC-specific TRAIL deleted mice on a 12-week HFD. Blood was extracted from mice during euthanasia through cardiac puncture. Plasma was used to analyze **(a)** blood glucose, **(b)** insulin and **(c)** cholesterol levels showed no significant difference between $Trail^{VSMC-/-}$ mice compared to its control $Trail^{VSMC+/+}$. n = 6/group. Results were expressed as mean ± SEM; *$p < 0.05$; Student *t-test*.

6.3.9 **No difference difference in vessel structure was observed in 12-week HFD *Trail*$^{VSMC-/-}$ mice**

To analyse aortic wall structure and its structural integrity after a 12-week HFD challenge, similar to baseline analysis (section 6.2.4), H&E, collagen and elastin staining were performed. Thoracic aortas were collected from 12-week HFD fed *Trail*$^{VSMC+/+}$ and *Trail*$^{VSMC-/-}$ mice and fixed for histological analysis and cut into 5µm section for analysis. No difference was observed between *Trail*$^{VSMC-/-}$ mice and control (**Figure 6.9a-b**). Measurement of aortic vessel wall thickness of sections stained with H&E staining showed no difference between *Trail*$^{VSMC-/-}$ and control *Trail*$^{VSMC+/+}$ mice (**Figure 6.9c**). This suggests that there was no difference in physical characterisation of the vessel wall when TRAIL is deleted from the endothelium.

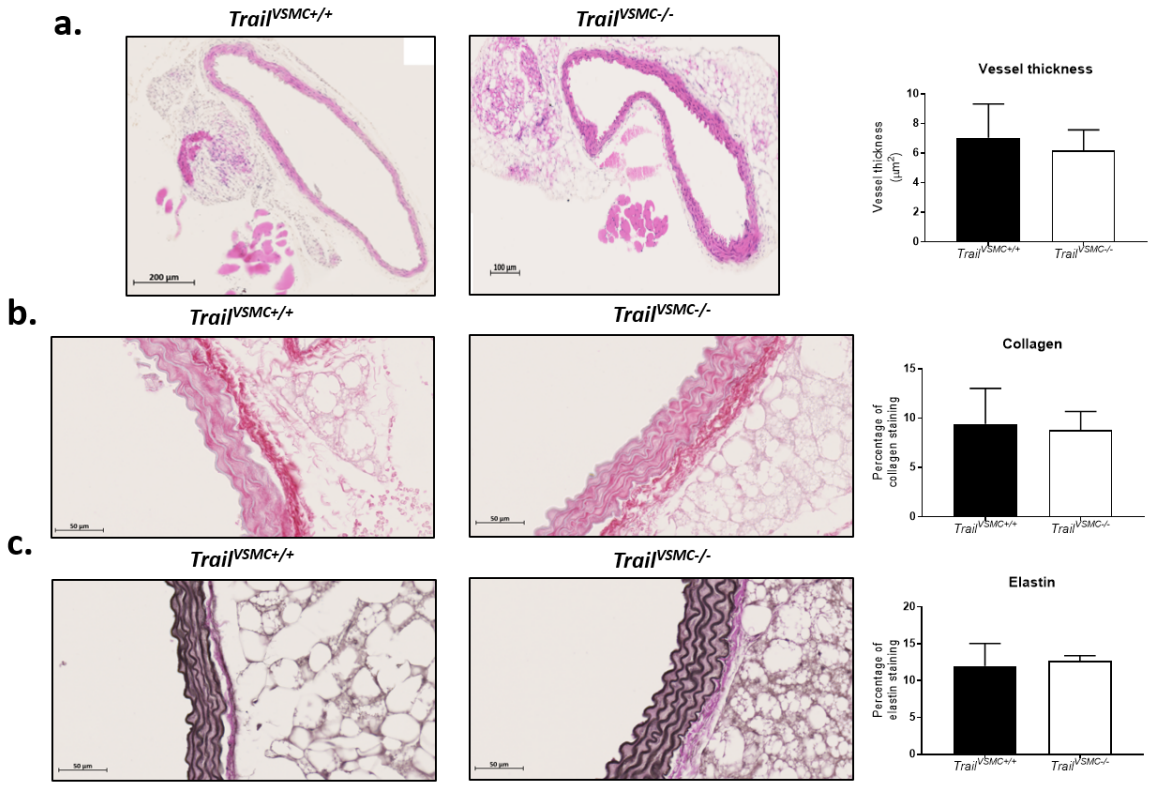

Figure 6.9 No significant difference in physical characteristic of vessel wall between *Trail*$^{VSMC-/-}$ and *Trail*$^{VSMC+/+}$ mice on a 12-week HFD. 5µm histological sections of thoracis aorta stained for **(a)** *Left* – H&E staining of *Trail*$^{VSMC+/+}$ and *Trail*$^{VSMC-/-}$ and measured for vessel thickness; *Right* – Quantification of aortic wall thickens between the two groups showed no significant difference. **(b)** *Left* – 20x magnification of *Trail*$^{VSMC+/+}$ and *Trail*$^{VSMC-/-}$ stained for collagen (dark red) content; *Right* – quantification of collagen staining between the two groups showed no significant difference. **(c)** *Left* – 20x magnification of *Trail*$^{VSMC+/+}$ and *Trail*$^{VSMC-/-}$ stained for elastin content; *Right* – quantification of elastin (dark purple) staining between the two groups showed no significant difference. n = 4 - 6/group. Results were expressed as mean ± SEM, Student *t-test*.

6.3.10 **α-tropomyosin mRNA expression was increased in *Trail*$^{VSMC-/-}$ mice in a 12-week HFD model**

Similar to baseline aortic mRNA analysis of *Trail*$^{VSMC-/-}$, thoracic aortas were collected from 12-week HFD fed *Trail*$^{VSMC+/+}$ and *Trail*$^{VSMC-/-}$ mice and RNA w0as extracted analysed through qPCR. Contractile marker α-tropomyosin was significantly elevated in *Trail*$^{VSMC-/-}$ mice compared to the control (**Figure 6.10a**). However, other contractile and synthetic markers such as SMα-A, MYH-10, MYH-11, KLF-4 and KLF-5 showed no difference between *Trail*$^{VSMC-/-}$ and its control (**Figure 6.10b-f**).

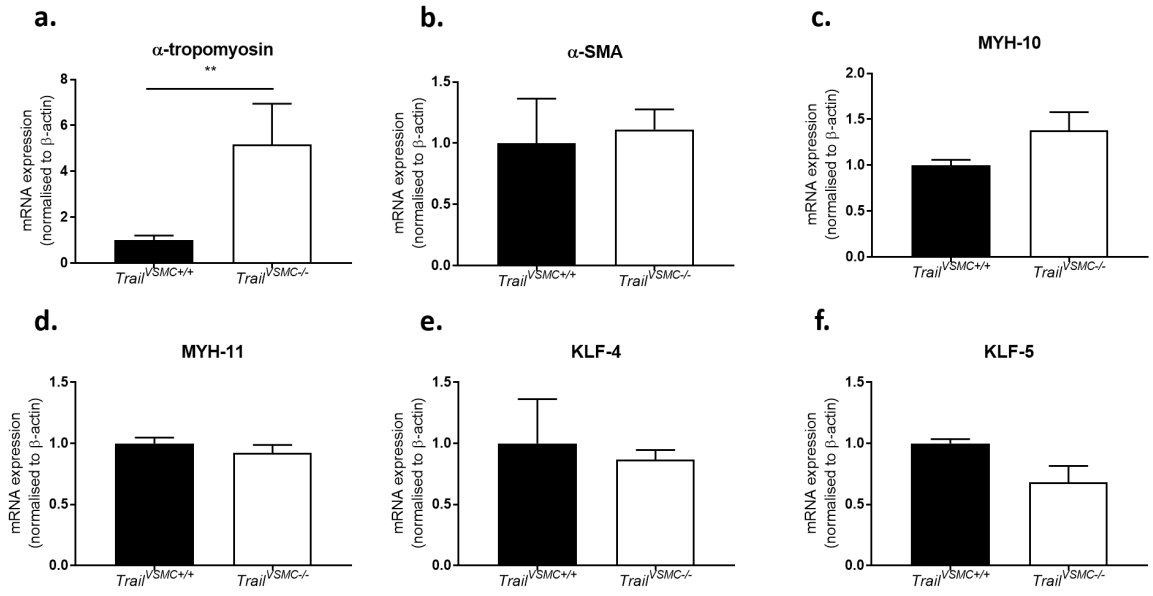

Figure 6.10 Baseline characterisation of *Trail*$^{VSMC-/-}$ and *Trail*$^{VSMC+/+}$showed an increase in α-tropomyosin mRNA gene expression. 12-week HFD, *Trail*$^{VSMC+/+}$ and *Trail*$^{VSMC-/-}$ mice aorta was collected, and RNA was extracted and quantified for gene expression using qPCR. To analyse phenotypic switching of VSMC in this model, contractile and synthetic mRNA gene expression were analysed. Contractile marker **(a)** α-tropomyosin mRNA expression was significantly increased in *Trail*$^{VSMC-/-}$ mice compared to the control *Trail*$^{VSMC+/+}$. Other contractile markers such as **(b)** SMα-A, **(c)** MYH-10 and **(d)** MYH-11 showed no significant difference between the two groups. Synthetic marker **(e)** KLF-4 and **(f)** KLF-5 also showed no significant reduction between the two groups. mRNA expression was normalized to β-actin. n = 6/group. Results were expressed as mean ± SEM; **p < 0.01; Student *t-test*.

6.3.11 **VE-cadherin mRNA expression was increased in *Trail*$^{VSMC-/-}$ mice in a 12-week HFD model**

12-week HFD mice aortic RNA was also analysed for endothelial specific gene markers and inflammatory gene. There were no difference in cell adhesion markers such as ICAM-1 and VCAM-1 (**Figure 6.11a-b**). However, VE-cadherin mRNA expression was significantly elevated in *Trail*$^{VSMC-/-}$ mice compared to the control *Trail*$^{VSMC+/+}$ (**Figure 6.11c**). Also, there was no difference with the inflammatory marker IL-1β (**Figure 6.11d**).

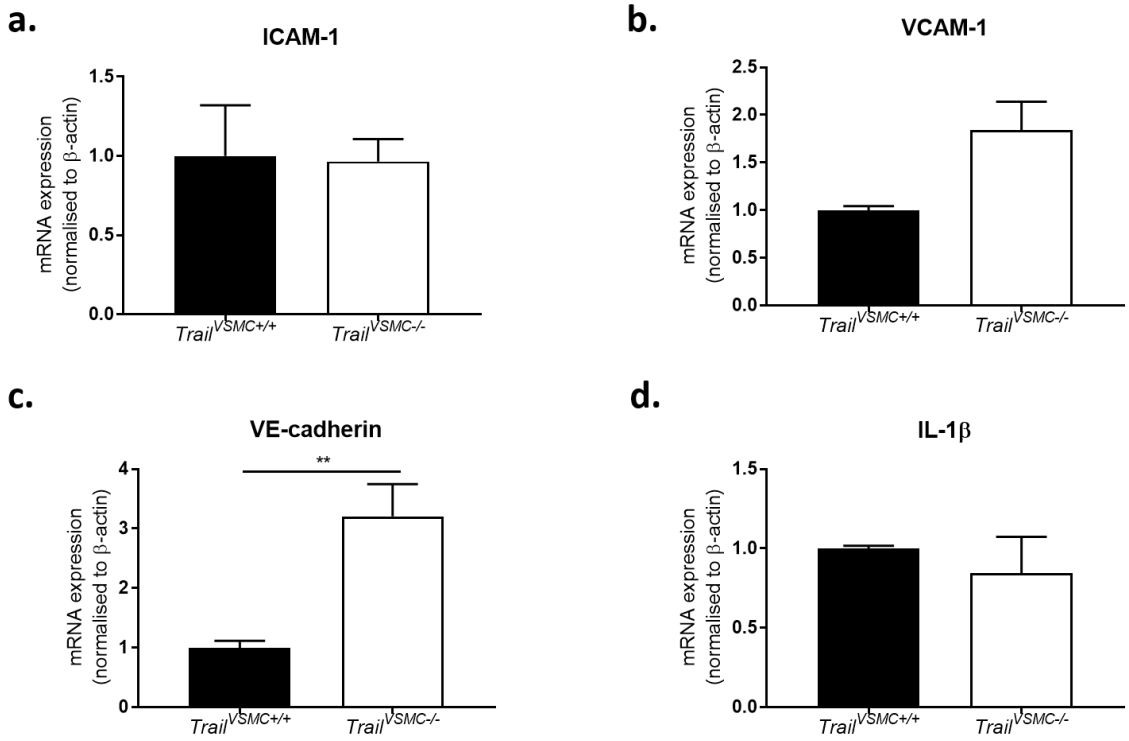

Figure 6.11 VE-cadherin mRNA expression was increased in *Trail*$^{VSMC-/-}$ 12-week HFD mice. 12-week HFD, *Trail*$^{VSMC+/+}$ and *Trail*$^{VSMC-/-}$ mice aorta was collected, and RNA was extracted and quantified for gene expression using qPCR. Endothelial specific markers such as **(a)** ICAM-1 and **(b)** VCAM-1 showed no significant changes between the two groups. **(c)** VE-cadherin mRNA expression was significantly elevated in *Trail*$^{VSMC-/-}$ mice compared to the control *Trail*$^{VSMC+/+}$. Inflammatory marker **(d)** IL-1β showed no significant difference. mRNA expression was normalized to β-actin. n = 6/group. Results were expressed as mean ± SEM; **p < 0.01; Student *t-test*.

6.4 DISCUSSION

In this chapter we investigated the effect of VSMC-specific TRAIL deletion in in the aorta, at baseline and after a 12-week HFD challenge. At baseline, *Trail*$^{VSMC-/-}$ mice showed a reduction in contractile markers α-tropomyosin and a reduction in phenotypic transcription factors such as KLF-4 and KLF-5. There was also a reduction in endothelial specific marker VCAM-1 and inflammatory gene expression IL-1β in the thoracic aortas of *Trail*$^{VSMC-/-}$ mice. After 12-week HFD feeding, there was up-regulation of contractile marker α-tropomyosin and endothelial specific marker VE-cadherin in *Trail*$^{VSMC-/-}$ mice compared to the control. We also observed an increase in liver mass in *Trail*$^{VSMC-/-}$ mice.

Over-all TRAIL deletion specifically in the VSMCs at baseline resulted in changes in phenotypic modulatory genes. α-tropomyosin, a contractile gene marker that is an important structural protein in the cytoskeleton of VSMCs [65,267]. A reduction of this gene expression in the vasculature of a VSMC-specific TRAIL deleted mice suggests that it has a poor contractile phenotype which can lead to stiffening of arterial walls and structural damage to the vessel wall due to changes in blood pressure [268]. Measurement of transcription activator Krüppel-like factors advised the phenotypic state of VSMCs. Both KLF-4 and KLF-5 were significantly reduced in *Trail*$^{VSMC-/-}$ mice compared to the control. In recent times research have shown the function of KLF-4 to be contradictory in VSMCs. Certain studies have shown that the increased accumulation of KLF-4 leads to inhibition of DNA synthesis and cell-cycle arrest suggesting an anti-proliferative role in VSMCs [269,270]. On the other hand, other research have shown KLF-4 to play an important role in pathogenesis of atherosclerosis by induction of a synthetic phenotype in VSMCs [271,272]. The directionality of VSMC phenotype due to KLF-4 needs further investigation by looking at KLF-4 induced down-stream targets such as NFκB and SMAD pathways which have the ability to induce pro and anti-inflammatory effect on

the vessel wall [273,274]. However, KLF-5 reduction in *Trail*$^{VSMC-/-}$ mice indicate a reduced synthetic phenotype. KLF-5 has been implicated in pulmonary arterial hypertension and breast cancer due to its induction of synthetic phenotype in VSMCs [275,276]. They do so by increasing cell-cycle progression and increasing VSMC proliferation and being a major inducer of vascular hyperplastic diseases [277]. These differences observed with phenotypic modulatory genes needs to be studied further for their respective protein translation and their impact on the vasculature. *Trail*$^{VSMC-/-}$ mice also showed reduced VCAM-1 expression compared to the control. VCAM-1 is expressed on the luminal surface of ECs play an important role in leukocyte attraction and immune surveillance. Similar to the discussion in chapter 5 (section 5.3), reduction in VCAM-1 expression is suggestive of vascular cells evading immune cell intervention which can promote vascular disease. However, VCAM-1 detection via western blotting or immune-histochemistry is essential to confirm the role of endothelial TRAIL in immune-surveillance. We also found a significant reduction in IL-1β mRNA expression in *Trail*$^{VSMC-/-}$ mice compared to the control. This could indicate a reduction in inflammation, however recent research established that, IL-1β might protect against advanced atherosclerotic progression [258]. This could mean, TRAIL deletion VSMC might accelerate advanced atherosclerotic plaque progression.

To investigate the effect of diet induced changes in the vasculature of VSMC-specific TRAIL deletion, *Trail*$^{VSMC-/-}$ and *Trail*$^{VSMC+/+}$ mice were placed on an HFD for 12-weeks. Vascular mRNA gene expression revealed an increase in α-tropomyosin and VE-cadherin expression in *Trail*$^{VSMC-/-}$ mice compared to the control. Expression of α-tropomyosin was significantly reduced at baseline in *Trail*$^{VSMC-/-}$ mice, however, when these animals were challenged to a 12-week HFD, opposite result was observed. This suggests that the phenotypic switching is affected with VSMC-specific TRAIL deletion

in mice. Though these animals were not obese or insulin resistant, studies have shown that baseline phenotypic characterisation of VSMCs can change with the induction of an HFD [278,279]. The increase in endothelial specific marker VE-cadherin mRNA expression in *Trail*$^{VSMC-/-}$ mice compared to the control is suggestive that, VSMC-specific TRAIL deletion, affects the endothelium. VE-cadherin is regarded as an important molecule responsible for vessel permeability. Results from Chapter 4 revealed reduced VE-cadherin mRNA expression in *Trail*$^{-/-}$ and *Trail*$^{-/-}$*Apoe*$^{-/-}$ vasculature, however, in the current model up-regulation of this gene expression is suggestive of feed-back mechanisms or alternative activation of VE-cadherin, which needs to be explored further.

We also noticed an increase in liver weight in *Trail*$^{VSMC-/-}$ compared to the control, with no difference observed in overall body weight. This can be an indication of hepatic hypertrophy, fatty liver or dysfunctional cholesterol metabolism. Studies have shown that, an enlarged liver usually indicates inflammation [280]. While no physical evidence of inflammation was observed, an enlarged liver can generate key inflammatory components which are pro-atherogenic. They cause an up-regulation in liver derived inflammatory markers such as C-reactive protein (CRP) [281]. Previous findings from our lab have shown that global TRAIL deleted mice on an HFD had increased liver lipid content, inflammation and fibrosis. This could be a possibility with the enlarged liver of *Trail*$^{VSMC-/-}$ mice. Furthermore, from Chapter 5 it was evident that EC-specific TRAIL deletion led to a substantial increase in plasma cholesterol level. In the current model with enlarged liver in *Trail*$^{VSMC-/-}$ mice, there is again the possibility of damaged sinusoidal capillaries of the liver and dysfunctional cholesterol metabolism resulting in an enlarged liver. Further studies on *Trail*$^{VSMC-/-}$ liver is essential to pinpoint the cause of an enlarged liver.

In summary, this chapter establishes the importance of TRAIL originating in VSMCs and its systemic effect in the murine model. VSMC-specific TRAIL deletion had changes with phenotypic gene expression markers and resulted in an enlarged liver following an HFD. We also need to consider that in this chapter mRNA was obtained from the entire aorta consisting of ECs, VSMCs and other vascular cells. This can be regarded as a limitation whilst studying the impact of VSMC-specific TRAIL effect. Future experiments of extracting VSMCs from these animals and performing ex-vivo analysis is essential.

Chapter 7: **Discussion**

7.1 DISCUSSION

CVD affects nearly 66% of Australians over the age of 75, thus accounting for the largest share of health expenditure of any disease group (Heart Foundation Australia; https://www.heartfoundation.org.au). Atherosclerosis is the main cause. It is a chronic condition spanning decades and can lead to fatal events such as myocardial infarction or stroke [282]. Initiation of atherosclerosis begins with vascular damage, promoting a pro-inflammatory, pro-atherogenic and pro-thrombotic state in the vessel wall. The initial insult to ECs is usually caused by oxidative stress produced by various sources including mitochondrial electron transport chain, NOX system and eNOS uncoupling [283]. Identifying novel stimuli that protect the vascular endothelium against oxidative stress in atherosclerosis may be attractive strategy for development of new therapeutics.

TRAIL is a cytokine discovered and named for its ability to promote cancer cell death [284]. However, we and others have shown that TRAIL stimulates EC proliferation and migration *in vitro* and *in vivo* [194-196], and plays an overall protective role in CVD. For example, patients with CVD [163] and its complications [168,197] have reduced circulating TRAIL concentrations, and mice lacking TRAIL exhibit accelerated atherogenesis [172]. The mechanisms by which TRAIL regulates EC function and protects against atherosclerosis are unclear. The aim of this thesis was to (i) investigate the role of TRAIL against oxidative stress in clinical, pre-clinical and EC *in-vitro* models, (ii) observe the role of TRAIL in the endothelium *in vivo* at baseline and following 12-week HFD and (iii) observe the role of TRAIL in VSMCs *in vivo* at baseline and following 12-week HFD. The major findings of this thesis were: (i) A protective association was established with TRAIL against oxidative stress

in people with CAD, pre-clinical models of atherosclerosis, as well as in ECs *in-vitro*; (ii) TRAIL deletion from the endothelium in mice modulated cholesterol metabolism such that $Trail^{EC-/-}$ mice had 7-fold more plasma cholesterol than wildtype mice in response to an HFD. EC-dependent TRAIL expression was also crucial in blood pressure control, since these mice were hypotensive. Furthermore, these mice had altered gene expression profiles for inflammatory markers; (iii) TRAIL expression specifically coming from VSMCs were found to modulate phenotypic gene expression of VSMCs. $Trail^{VSMC-/-}$ mice also were found to have enlarged liver following an HFD.

We first explored the relationship between TRAIL and oxidative stress in clinical and pre-clinical models. A negative correlation between TRAIL and oxidative stress in coronary artery disease (CAD) patients was the first report suggesting that circulating TRAIL levels may be a determinant of oxidative stress in CAD. This finding is supported in other inflammatory diseases which also have elevated levels of oxidative stress including diabetes and kidney disease [163,168,171]. Furthermore, the pre-clinical models in this thesis provided mechanistic insight into how TRAIL may protect against CVD, describing the impact of TRAIL on different forms of endothelial dysfunction, namely, increased vascular oxidative stress, impaired endothelial-dependent vasorelaxation, increased endothelial permeability and endothelial-leukocyte adhesion.

Because oxidative stress is an important factor leading to endothelial dysfunction and plaque progression [285,286], we used AngII, which produces endothelial ROS via multiple sources [221,287]. In this thesis, we confirmed that HMEC-1 cells exposed to AngII produced ROS via NOX, and specifically NOX-4, eNOS coupling and via the mitochondrial electron transport chain. Importantly, this thesis identified that TRAIL protects against AngII-induced oxidative stress in ECs. These results are supported by Liu *et al*. (2014), where TRAIL was used as an

effective treatment against high glucose induced oxidative stress in both *in vivo* and *in-vitro* models [288].

Several cell processes known to promote atherogenesis were also observed in our *in vitro* models in response to AngII. For example, up-regulation of cell adhesion molecules, monocyte adhesion and increased endothelial permeability, more importantly, these processes were brought back to baseline with TRAIL pre-treatment of ECs. Previous studies of HFD *Trail*$^{-/-}$ *Apoe*$^{-/-}$ mice showed accelerated atherosclerosis [172,173,289]. The accelerated atherosclerosis observed in these animals may be due to increased monocyte recruitment, commonly observed when the endothelium is damaged and activated [290]. Also, increased vessel permeability can aid in monocyte migration into the sub-endothelial space [291], leading to bigger plaques as observed in the *Trail*$^{-/-}$*Apoe*$^{-/-}$ mice [173]. These findings indicate that increasing TRAIL levels under these circumstances could combat many of these initial changes in the vasculature to prevent accelerated atherosclerosis. These findings also contribute to our understanding as to how TRAIL may protect against oxidative stress in the endothelium.

ECs are the first point of contact to any systemic circulatory changes as well as the initial cell type to be damaged during atherosclerosis. Identification of TRAIL's protective role in the endothelium raised several question as to its *in vivo* impact on endothelial function, vascular homeostasis and its systemic effect. Our lab created *Trail*$^{EC-/-}$ mice to investigate the effect of TRAIL deletion only in the endothelium. We found that *Trail*$^{EC-/-}$ mice challenged on a 12-week HFD, had high circulating plasma cholesterol in the blood; a finding also observed with global TRAIL deletion mice [170]. This indicates the potential role of TRAIL from the endothelium in cholesterol metabolism. In clinical studies, patients with EC dysfunction are known to have hypercholesterolemia [292]. Unlike VSMCs and macrophages, ECs do not accumulate cholesterol or transform into foam cells, they can up-regulate efflux of cholesterol through RCT thereby affecting plasma cholesterol levels during atherosclerosis [293].

Importantly, the role of the endothelium in cholesterol metabolism has been described for other genes. For example, endothelial-specific deletion of lipoprotein receptor-related protein 1 (LPR1) or NOTCH1 increased systemic cholesterol concentrations [294,295]. Deletion of these receptors from ECs were shown to have similar phenotypes to its deletion in hepatocytes and adipocytes suggesting a regulatory role of EC in cholesterol metabolism. Both LPR1 and NOTCH1 were shown to be transactional activators of cholesterol metabolism in ECs. This can be indicative that TRAIL can be transcriptional regulator of cholesterol metabolism genes in the endothelium. Further analysis of various cholesterol genes and its transcriptional regulators can provide answers to the role of TRAIL in cholesterol metabolism in ECs.

Hypertension is a common sign of arterial stiffening and its inability to contract and relax to systolic and diastolic pressures [296]; high expression of NOS is usually associated with hypotension [237,255]. Over-expression of eNOS leads to an increase in NO production whereby there is a reduction in blood-pressure due to vaso-relaxation of the vasculature. In humans, chronic hypotension is usually a sign of the body's inability to maintain fluid balance in kidney disease [297,298]. HFD challenged $Trail^{EC-/-}$ mice exhibited hypotension and dysregulated NOS expression. Low-blood pressure in these animals can be an indication of vascular damage leading to the inability to change vessel diameter, changes in blood volume/cardiac output and dysregulation of blood pressure controlling hormones such as AngII [299]. In particular to the endothelium, a clinical study has shown that endothelial activation markers such as E-selectin can lead to hypotension in sepsis patients [300]. Furthermore, in animal studies involving EC-specific deletion of blood pressure related genes such as guanylyl cyclase-A (GC-A), a receptor of atrial natriuretic peptide (ANP) a potent vasodilator causes systemic vasorelaxation [301]. These results suggest that EC's play a major role in blood pressure regulation and TRAIL from the endothelium can potentially regulate endothelial NO and control systemic blood pressure.

IL-1β is a cytokine important in inflammation. Circulating levels of this cytokine are significantly elevated in CVDs. The CANTOS (Canakinumab Anti-Inflammatory Thrombosis Outcome Study) trial, used canakinumab, an inhibitor of IL-1β in patients with CAD, which lead to significantly reduced recurrence of cardiovascular events due to its anti-inflammatory properties [302]. Though blockage of IL-1β was thought to bring about infection, IL-1β knockout mice responded normally to systemic injection of LPS compared to the control, suggesting its possible usage in clinical trials [303]. This thesis identified that *Trail*$^{EC-/-}$ mice had significantly reduced vascular IL-1β gene expression in response to an HFD, contrasting to the findings indicated above. However, a recent study by Gomez *et al.* (2018) provided compelling evidence to the critical role of IL-1β signalling in late stage atherosclerosis. It showed *Apoe*$^{-/-}$ mice treated to neutralising antibody of IL-1β had reduced VSMCs and collagen, whilst increased macrophage content in the plaque making it unstable [258]. Hence, low IL-1β expression in *Trail*$^{EC-/-}$ mice can indicate an unstable plaque phenotype, similar to what was observed in *Trail*$^{-/-}$*Apoe*$^{-/-}$ mice placed on an HFD diet [177].

Trail$^{EC-/-}$ mice also had reduced vascular VCAM-1 gene expression in response to an HFD challenge. Cancer models have shown that tumours have reduced VCAM-1 expression, enabling them to escape immunological attack. VCAM-1 down-regulation may be a strategy for reduced immune-surveillance [256]. Thus, reduced VCAM-1 expression in *Trail*$^{EC-/-}$ mice, might be an indication of defective immune system, preventing clearance of accumulated monocytes and other inflammatory cytokines on the endothelium, leading to progression of atherosclerosis and CVDs. This result indicates the possible role of endothelial TRAIL in immune-surveillance. However, VCAM-1 detection via western blotting or immune-histochemistry is essential to confirm the role of endothelial TRAIL in immune-surveillance.

Because we are interested in the effects of TRAIL on vascular cells, my lab also produced VSMC-specific TRAIL knockout mice. VSMCs form the second layer of the blood vessel, playing a crucial role in blood pressure regulation by controlling the vessel diameter [304]. These cells play a major role in plaque progression in atherosclerosis by modulating their phenotype. Previously my lab and others have shown that TRAIL stimulates VSMC proliferation, migration and differentiation [184,194] and stimulates a stable plaque phenotype [177].

VSMCs are plastic cells capable of switching from contractile to a synthetic phenotype. Contractile VSMCs express specific markers such as SMα-A, α-tropomyosin, MYH-10/11 [65], whereas synthetic VSMCs express predominantly KLF-4 and -5 [272,305]. Importantly, during atherosclerosis, VSMCs are synthetic, which aid in proliferation and migration of these cells, leading to plaque progression [69].

Trail$^{VSMC-/-}$ mice on both baseline and HFD challenge showed differences in both contractile and synthetic gene expressions. A conclusive result to the phenotypic state of VSMCs in this model wasn't established, however, these gene expression changes signify the potential role of TRAIL in phenotypic switching of VSMCs. This work is preliminary, and more studies are required to fully delineate TRAIL's effect in VSMCs *in vivo*.

In conclusion, my thesis identified the protective role of TRAIL in the endothelium during oxidative stress and enabled us to uncover new molecular pathways in the vasculature indicating TRAIL dependence in CVD. Thus, comprehension of TRAIL signals may help us to develop more effective treatment for debilitating conditions associated with CVDs and its complications.

7.2 FUTURE DIRECTIONS

This thesis provided insight into TRAIL's protective stature in the vasculature under physiological and pathological conditions.

While my work established that TRAIL inhibits AngII-induced ROS production, an understanding of the precise molecular mechanism(s) by which it acts requires more extensive studies. This is because our data indicate that the production of ROS by ECs in response to AngII is complex, involving the interaction of several enzyme sources including NOX-4, mitochondria and uncoupled eNOS [191]. This complexity has been noted by others with recent work reporting that redox cross-talk between NOX, mitochondria and uncoupled eNOS is required to achieve maximal ROS production by ECs treated with AngII [306-308]. Interestingly, our data showing that TRAIL limits NOX4-derived ROS in AngII-stimulated ECs contrasts with our prior work [177] where TRAIL stimulated NOX-4 expression and H_2O_2 under basal conditions. TRAIL's role on NOX-4 expression and down-stream effects may differ under normal vs. pathogenic conditions, such as in AngII stimulation and warrants further study. Though $Trail^{-/-}Apoe^{-/-}$ vasculature have been shown to have increased ROS damage, this project in future will warrant an interventional study to see if antioxidant treatment will improve endothelial function in mice. Furthermore, in Chapter 4, I showed that TRAIL can mitigate monocyte adhesion following AngII exposure in ECs. To confirm this, additional studies detecting monocyte adhesion in vivo (either via flow cytometry or intravital microscopy) will validate the role of TRAIL in leukocyte adhesion and support the in-vitro data.

My lab is world-first to generate EC and VSMC-specific TRAIL knockout mice, and work from this thesis raised several questions. First, why would TRAIL deletion specifically from ECs increase plasma cholesterol 7-fold compared to wildtype mice. Liver histology and gene/protein expression along with analysis of reverse cholesterol transport gene expression

both in the vasculature and the liver can provide mechanism of action of endothelial TRAIL in cholesterol metabolism.

The second question relates to why this animal model exhibited hypotension along with dysregulated NOS expression. Performing myography which analyse endothelial dependant vaso-relaxation against various drugs such as Ach and SNP can conclusively prove endothelial damage in *Trail*$^{EC-/-}$ mice and indicate the importance of TRAIL in the homeostasis of a healthy endothelium.

The final question relates to why *Trail*$^{VSMC-/-}$ mice showed changes in contractile and transcription factor gene expression at both baseline and following an HFD. Though these changes indicate the role of TRAIL in phenotypic switching of VSMCs, protein expression of these gene in the vasculature can provide a definite answer to the state of VSMC in *Trail*$^{VSMC-/-}$ mice. Also, changes in liver weight in *Trail*$^{VSMC-/-}$ mice can be analysed further by liver histology and gene/protein expression to identify the cause.

Both EC and VSMC-specific TRAIL deleted mice models require further characterisation under various pathological models such as hind-limb ischaemia, peri-arterial cuff and wound healing models. These models are currently been carried out in our lab and promises novel findings which will aid in discovering TRAIL's mechanism of action. The experiments performed in Chapters 5 and 6 were pilot studies. Even though I observed significant changes, it is necessary to acknowledge that mRNA analysis was obtained from the entire aortae consisting of ECs, VSMCs and other vascular cells. Future experiments using only ECs and VSMCs isolated from these animals and performing ex-vivo analysis is essential. It is also essential to analyse plasma biochemistry such as cholesterol, triglycerides, nitrate/nitrite, glucose and insulin with increased animal numbers. Furthermore, myography will need to be performed to identify the contribution of TRAIL expressed EC or VSMCs to vasorelaxation

and vasoconstriction. Additional experiments to increase animal cohort numbers to reduce variance and increase sample power is essential.

In conclusion, my thesis created the foundation for the role of TRAIL in the vasculature. Several more studies are required to discover the mechanisms of TRAIL in the vascular cells under physiological and pathological conditions. These studies will eventually lead to the use of TRAIL as a therapeutic target against vascular diseases.

Bibliography

1. Azijli, K.; Weyhenmeyer, B.; Peters, G.J.; de Jong, S.; Kruyt, F.A. Non-canonical kinase signaling by the death ligand trail in cancer cells: Discord in the death receptor family. *Cell death and differentiation* **2013**, *20*, 858-868.
2. Davis-Dusenbery, B.N.; Wu, C.; Hata, A. Micromanaging vascular smooth muscle cell differentiation and phenotypic modulation. *Arteriosclerosis, thrombosis, and vascular biology* **2011**, *31*, 2370-2377.
3. Manuneedhi Cholan, P.; Cartland, S.P.; Kavurma, M.M. Nadph oxidases, angiogenesis, and peripheral artery disease. *Antioxidants* **2017**, *6*.
4. Fukai, T. Endothelial gtpch in enos uncoupling and atherosclerosis. *Arteriosclerosis, thrombosis, and vascular biology* **2007**, *27*, 1493-1495.
5. Libby, P.; Ridker, P.M.; Hansson, G.K. Progress and challenges in translating the biology of atherosclerosis. *Nature* **2011**, *473*, 317-325.
6. Tucker, W.D.; Mahajan, K. Anatomy, blood vessels. In *Statpearls*, Treasure Island (FL), 2019.
7. Baldwin, A.L.; Thurston, G. Mechanics of endothelial cell architecture and vascular permeability. *Critical reviews in biomedical engineering* **2001**, *29*, 247-278.
8. Vink, H.; Duling, B.R. Capillary endothelial surface layer selectively reduces plasma solute distribution volume. *American journal of physiology. Heart and circulatory physiology* **2000**, *278*, H285-289.
9. Ludmer, P.L.; Selwyn, A.P.; Shook, T.L.; Wayne, R.R.; Mudge, G.H.; Alexander, R.W.; Ganz, P. Paradoxical vasoconstriction induced by acetylcholine in atherosclerotic coronary arteries. *The New England journal of medicine* **1986**, *315*, 1046-1051.
10. Gimbrone, M.A., Jr.; Topper, J.N.; Nagel, T.; Anderson, K.R.; Garcia-Cardena, G. Endothelial dysfunction, hemodynamic forces, and atherogenesis. *Annals of the New York Academy of Sciences* **2000**, *902*, 230-239; discussion 239-240.
11. Gimbrone, M.A., Jr.; Garcia-Cardena, G. Vascular endothelium, hemodynamics, and the pathobiology of atherosclerosis. *Cardiovascular pathology : the official journal of the Society for Cardiovascular Pathology* **2013**, *22*, 9-15.
12. Pamukcu, B.; Lip, G.Y.; Shantsila, E. The nuclear factor--kappa b pathway in atherosclerosis: A potential therapeutic target for atherothrombotic vascular disease. *Thrombosis research* **2011**, *128*, 117-123.
13. Napoli, C.; Ignarro, L.J. Nitric oxide and atherosclerosis. *Nitric oxide : biology and chemistry* **2001**, *5*, 88-97.
14. Tedgui, A.; Mallat, Z. Anti-inflammatory mechanisms in the vascular wall. *Circulation research* **2001**, *88*, 877-887.
15. Park, S.K.; Yang, W.S.; Lee, S.K.; Ahn, H.; Park, J.S.; Hwang, O.; Lee, J.D. Tgf-beta(1) down-regulates inflammatory cytokine-induced vcam-1 expression in cultured human glomerular endothelial cells. *Nephrology, dialysis, transplantation : official publication of the European Dialysis and Transplant Association - European Renal Association* **2000**, *15*, 596-604.

16. Noble, K.E.; Harkness, D.; Yong, K.L. Interleukin 10 regulates cellular responses in monocyte/endothelial cell co-cultures. *British journal of haematology* **2000**, *108*, 497-504.
17. Ashby, D.T.; Rye, K.A.; Clay, M.A.; Vadas, M.A.; Gamble, J.R.; Barter, P.J. Factors influencing the ability of hdl to inhibit expression of vascular cell adhesion molecule-1 in endothelial cells. *Arteriosclerosis, thrombosis, and vascular biology* **1998**, *18*, 1450-1455.
18. Elhage, R.; Maret, A.; Pieraggi, M.T.; Thiers, J.C.; Arnal, J.F.; Bayard, F. Differential effects of interleukin-1 receptor antagonist and tumor necrosis factor binding protein on fatty-streak formation in apolipoprotein e-deficient mice. *Circulation* **1998**, *97*, 242-244.
19. Jiang, R.; Teng, Y.; Huang, Y.; Gu, J.; Li, M. Protein kinase c-alpha activation induces nf-kb-dependent vcam-1 expression in cultured human umbilical vein endothelial cells treated with sera from preeclamptic patients. *Gynecologic and obstetric investigation* **2010**, *69*, 101-108.
20. Jia, Z.; Nallasamy, P.; Liu, D.; Shah, H.; Li, J.Z.; Chitrakar, R.; Si, H.; McCormick, J.; Zhu, H.; Zhen, W.*, et al.* Luteolin protects against vascular inflammation in mice and tnf-alpha-induced monocyte adhesion to endothelial cells via suppressing ikappabalpha/nf-kappab signaling pathway. *The Journal of nutritional biochemistry* **2015**, *26*, 293-302.
21. Yang, L.; Froio, R.M.; Sciuto, T.E.; Dvorak, A.M.; Alon, R.; Luscinskas, F.W. Icam-1 regulates neutrophil adhesion and transcellular migration of tnf-alpha-activated vascular endothelium under flow. *Blood* **2005**, *106*, 584-592.
22. Kim, J.J.; Lee, S.B.; Park, J.K.; Yoo, Y.D. Tnf-alpha-induced ros production triggering apoptosis is directly linked to romo1 and bcl-x(l). *Cell death and differentiation* **2010**, *17*, 1420-1434.
23. Lin, J.; Kakkar, V.; Lu, X. Impact of mcp-1 in atherosclerosis. *Current pharmaceutical design* **2014**, *20*, 4580-4588.
24. Badimon, L. Interleukin-18: A potent pro-inflammatory cytokine in atherosclerosis. *Cardiovascular research* **2012**, *96*, 172-175; discussion 176-180.
25. Dewberry, R.; Holden, H.; Crossman, D.; Francis, S. Interleukin-1 receptor antagonist expression in human endothelial cells and atherosclerosis. *Arteriosclerosis, thrombosis, and vascular biology* **2000**, *20*, 2394-2400.
26. van der Vorst, E.P.; Doring, Y.; Weber, C. Chemokines and their receptors in atherosclerosis. *Journal of molecular medicine* **2015**, *93*, 963-971.
27. Tacke, F.; Alvarez, D.; Kaplan, T.J.; Jakubzick, C.; Spanbroek, R.; Llodra, J.; Garin, A.; Liu, J.; Mack, M.; van Rooijen, N.*, et al.* Monocyte subsets differentially employ ccr2, ccr5, and cx3cr1 to accumulate within atherosclerotic plaques. *The Journal of clinical investigation* **2007**, *117*, 185-194.
28. Frank, P.G.; Lisanti, M.P. Icam-1: Role in inflammation and in the regulation of vascular permeability. *American journal of physiology. Heart and circulatory physiology* **2008**, *295*, H926-H927.
29. Dong, Z.M.; Wagner, D.D. Leukocyte-endothelium adhesion molecules in atherosclerosis. *The Journal of laboratory and clinical medicine* **1998**, *132*, 369-375.
30. Poston, R.N.; Haskard, D.O.; Coucher, J.R.; Gall, N.P.; Johnson-Tidey, R.R. Expression of intercellular adhesion molecule-1 in atherosclerotic plaques. *The American journal of pathology* **1992**, *140*, 665-673.
31. Hwang, S.J.; Ballantyne, C.M.; Sharrett, A.R.; Smith, L.C.; Davis, C.E.; Gotto, A.M., Jr.; Boerwinkle, E. Circulating adhesion molecules vcam-1, icam-1, and e-selectin in

carotid atherosclerosis and incident coronary heart disease cases: The atherosclerosis risk in communities (aric) study. *Circulation* **1997**, *96*, 4219-4225.
32. Nakashima, Y.; Raines, E.W.; Plump, A.S.; Breslow, J.L.; Ross, R. Upregulation of vcam-1 and icam-1 at atherosclerosis-prone sites on the endothelium in the apoe-deficient mouse. *Arteriosclerosis, thrombosis, and vascular biology* **1998**, *18*, 842-851.
33. O'Brien, K.D.; Allen, M.D.; McDonald, T.O.; Chait, A.; Harlan, J.M.; Fishbein, D.; McCarty, J.; Ferguson, M.; Hudkins, K.; Benjamin, C.D.*, et al.* Vascular cell adhesion molecule-1 is expressed in human coronary atherosclerotic plaques. Implications for the mode of progression of advanced coronary atherosclerosis. *The Journal of clinical investigation* **1993**, *92*, 945-951.
34. Dong, Z.M.; Brown, A.A.; Wagner, D.D. Prominent role of p-selectin in the development of advanced atherosclerosis in apoe-deficient mice. *Circulation* **2000**, *101*, 2290-2295.
35. Collins, R.G.; Velji, R.; Guevara, N.V.; Hicks, M.J.; Chan, L.; Beaudet, A.L. P-selectin or intercellular adhesion molecule (icam)-1 deficiency substantially protects against atherosclerosis in apolipoprotein e-deficient mice. *The Journal of experimental medicine* **2000**, *191*, 189-194.
36. Dunlop, L.C.; Skinner, M.P.; Bendall, L.J.; Favaloro, E.J.; Castaldi, P.A.; Gorman, J.J.; Gamble, J.R.; Vadas, M.A.; Berndt, M.C. Characterization of gmp-140 (p-selectin) as a circulating plasma protein. *The Journal of experimental medicine* **1992**, *175*, 1147-1150.
37. Blann, A.D.; Lip, G.Y. Hypothesis: Is soluble p-selectin a new marker of platelet activation? *Atherosclerosis* **1997**, *128*, 135-138.
38. Davies, M.J.; Gordon, J.L.; Gearing, A.J.; Pigott, R.; Woolf, N.; Katz, D.; Kyriakopoulos, A. The expression of the adhesion molecules icam-1, vcam-1, pecam, and e-selectin in human atherosclerosis. *The Journal of pathology* **1993**, *171*, 223-229.
39. Wood, K.M.; Cadogan, M.D.; Ramshaw, A.L.; Parums, D.V. The distribution of adhesion molecules in human atherosclerosis. *Histopathology* **1993**, *22*, 437-444.
40. Dong, Z.M.; Chapman, S.M.; Brown, A.A.; Frenette, P.S.; Hynes, R.O.; Wagner, D.D. The combined role of p- and e-selectins in atherosclerosis. *The Journal of clinical investigation* **1998**, *102*, 145-152.
41. Ley, K.; Miller, Y.I.; Hedrick, C.C. Monocyte and macrophage dynamics during atherogenesis. *Arteriosclerosis, thrombosis, and vascular biology* **2011**, *31*, 1506-1516.
42. Rosenfeld, M.E.; Yla-Herttuala, S.; Lipton, B.A.; Ord, V.A.; Witztum, J.L.; Steinberg, D. Macrophage colony-stimulating factor mrna and protein in atherosclerotic lesions of rabbits and humans. *The American journal of pathology* **1992**, *140*, 291-300.
43. Jones, N.L.; Reagan, J.W.; Willingham, M.C. The pathogenesis of foam cell formation: Modified ldl stimulates uptake of co-incubated ldl via macropinocytosis. *Arteriosclerosis, thrombosis, and vascular biology* **2000**, *20*, 773-781.
44. Li, Q.; Park, K.; Li, C.; Rask-Madsen, C.; Mima, A.; Qi, W.; Mizutani, K.; Huang, P.; King, G.L. Induction of vascular insulin resistance and endothelin-1 expression and acceleration of atherosclerosis by the overexpression of protein kinase c-beta isoform in the endothelium. *Circulation research* **2013**, *113*, 418-427.
45. Pucci, M.L.; Miller, K.B.; Dick, L.B.; Guan, H.; Lin, L.; Nasjletti, A. Vascular responsiveness to nitric oxide synthesis inhibition in hypertensive rats. *Hypertension* **1994**, *23*, 744-751.
46. Selwyn, A.P. Prothrombotic and antithrombotic pathways in acute coronary syndromes. *The American journal of cardiology* **2003**, *91*, 3H-11H.
47. Chistiakov, D.A.; Orekhov, A.N.; Bobryshev, Y.V. Effects of shear stress on endothelial cells: Go with the flow. *Acta physiologica* **2017**, *219*, 382-408.

48. Lefer, D.J.; Jones, S.P.; Girod, W.G.; Baines, A.; Grisham, M.B.; Cockrell, A.S.; Huang, P.L.; Scalia, R. Leukocyte-endothelial cell interactions in nitric oxide synthase-deficient mice. *The American journal of physiology* **1999**, *276*, H1943-1950.
49. Marletta, M.A. Nitric oxide synthase: Aspects concerning structure and catalysis. *Cell* **1994**, *78*, 927-930.
50. Ignarro, L.J.; Napoli, C. Novel features of nitric oxide, endothelial nitric oxide synthase, and atherosclerosis. *Current diabetes reports* **2005**, *5*, 17-23.
51. Kolluru, G.K.; Siamwala, J.H.; Chatterjee, S. Enos phosphorylation in health and disease. *Biochimie* **2010**, *92*, 1186-1198.
52. Wallerath, T.; Deckert, G.; Ternes, T.; Anderson, H.; Li, H.; Witte, K.; Forstermann, U. Resveratrol, a polyphenolic phytoalexin present in red wine, enhances expression and activity of endothelial nitric oxide synthase. *Circulation* **2002**, *106*, 1652-1658.
53. Feron, O.; Dessy, C.; Desager, J.P.; Balligand, J.L. Hydroxy-methylglutaryl-coenzyme a reductase inhibition promotes endothelial nitric oxide synthase activation through a decrease in caveolin abundance. *Circulation* **2001**, *103*, 113-118.
54. Kubes, P.; Suzuki, M.; Granger, D.N. Nitric oxide: An endogenous modulator of leukocyte adhesion. *Proceedings of the National Academy of Sciences of the United States of America* **1991**, *88*, 4651-4655.
55. Radomski, M.W.; Palmer, R.M.; Moncada, S. The anti-aggregating properties of vascular endothelium: Interactions between prostacyclin and nitric oxide. *British journal of pharmacology* **1987**, *92*, 639-646.
56. Garg, U.C.; Hassid, A. Nitric oxide-generating vasodilators and 8-bromo-cyclic guanosine monophosphate inhibit mitogenesis and proliferation of cultured rat vascular smooth muscle cells. *The Journal of clinical investigation* **1989**, *83*, 1774-1777.
57. Wallez, Y.; Huber, P. Endothelial adherens and tight junctions in vascular homeostasis, inflammation and angiogenesis. *Biochimica et biophysica acta* **2008**, *1778*, 794-809.
58. Vestweber, D. Ve-cadherin: The major endothelial adhesion molecule controlling cellular junctions and blood vessel formation. *Arteriosclerosis, thrombosis, and vascular biology* **2008**, *28*, 223-232.
59. Wallez, Y.; Vilgrain, I.; Huber, P. Angiogenesis: The ve-cadherin switch. *Trends in cardiovascular medicine* **2006**, *16*, 55-59.
60. Miyazaki, T.; Taketomi, Y.; Takimoto, M.; Lei, X.F.; Arita, S.; Kim-Kaneyama, J.R.; Arata, S.; Ohata, H.; Ota, H.; Murakami, M.*, et al.* M-calpain induction in vascular endothelial cells on human and mouse atheromas and its roles in ve-cadherin disorganization and atherosclerosis. *Circulation* **2011**, *124*, 2522-2532.
61. Yau, J.W.; Teoh, H.; Verma, S. Endothelial cell control of thrombosis. *BMC cardiovascular disorders* **2015**, *15*, 130.
62. Pearson, J.D. Endothelial cell function and thrombosis. *Bailliere's best practice & research. Clinical haematology* **1999**, *12*, 329-341.
63. Gimbrone, M.A., Jr.; Garcia-Cardena, G. Endothelial cell dysfunction and the pathobiology of atherosclerosis. *Circulation research* **2016**, *118*, 620-636.
64. Owens, G.K. Regulation of differentiation of vascular smooth muscle cells. *Physiological reviews* **1995**, *75*, 487-517.
65. Rensen, S.S.; Doevendans, P.A.; van Eys, G.J. Regulation and characteristics of vascular smooth muscle cell phenotypic diversity. *Netherlands heart journal : monthly journal of the Netherlands Society of Cardiology and the Netherlands Heart Foundation* **2007**, *15*, 100-108.
66. Guo, X.; Chen, S.Y. Transforming growth factor-beta and smooth muscle differentiation. *World journal of biological chemistry* **2012**, *3*, 41-52.

67. Pahk, K.; Joung, C.; Jung, S.M.; Young Song, H.; Yong Park, J.; Woo Byun, J.; Lee, Y.S.; Chul Paeng, J.; Kim, C.; Kim, S.*, et al.* Visualization of synthetic vascular smooth muscle cells in atherosclerotic carotid rat arteries by f-18 fdg pet. *Scientific reports* **2017**, *7*, 6989.
68. Aksoy, I.; Giudice, V.; Delahaye, E.; Wianny, F.; Aubry, M.; Mure, M.; Chen, J.; Jauch, R.; Bogu, G.K.; Nolden, T.*, et al.* Klf4 and klf5 differentially inhibit mesoderm and endoderm differentiation in embryonic stem cells. *Nature communications* **2014**, *5*, 3719.
69. Gomez, D.; Owens, G.K. Smooth muscle cell phenotypic switching in atherosclerosis. *Cardiovascular research* **2012**, *95*, 156-164.
70. Fogelstrand, P.; Feral, C.C.; Zargham, R.; Ginsberg, M.H. Dependence of proliferative vascular smooth muscle cells on cd98hc (4f2hc, slc3a2). *The Journal of experimental medicine* **2009**, *206*, 2397-2406.
71. Zhang, L.; Xu, Z.; Wu, Y.; Liao, J.; Zeng, F.; Shi, L. Akt/enos and mapk signaling pathways mediated the phenotypic switching of thoracic aorta vascular smooth muscle cells in aging/hypertensive rats. *Physiological research* **2018**, *67*, 543-553.
72. Sazonova, O.V.; Isenberg, B.C.; Herrmann, J.; Lee, K.L.; Purwada, A.; Valentine, A.D.; Buczek-Thomas, J.A.; Wong, J.Y.; Nugent, M.A. Extracellular matrix presentation modulates vascular smooth muscle cell mechanotransduction. *Matrix biology : journal of the International Society for Matrix Biology* **2015**, *41*, 36-43.
73. Xu, J.; Shi, G.P. Vascular wall extracellular matrix proteins and vascular diseases. *Biochimica et biophysica acta* **2014**, *1842*, 2106-2119.
74. Suwanabol, P.A.; Seedial, S.M.; Shi, X.; Zhang, F.; Yamanouchi, D.; Roenneburg, D.; Liu, B.; Kent, K.C. Transforming growth factor-beta increases vascular smooth muscle cell proliferation through the smad3 and extracellular signal-regulated kinase mitogen-activated protein kinases pathways. *Journal of vascular surgery* **2012**, *56*, 446-454.
75. Rao, V.H.; Kansal, V.; Stoupa, S.; Agrawal, D.K. Mmp-1 and mmp-9 regulate epidermal growth factor-dependent collagen loss in human carotid plaque smooth muscle cells. *Physiological reports* **2014**, *2*, e00224.
76. Wagenseil, J.E.; Mecham, R.P. Elastin in large artery stiffness and hypertension. *Journal of cardiovascular translational research* **2012**, *5*, 264-273.
77. Bennett, M.R.; Sinha, S.; Owens, G.K. Vascular smooth muscle cells in atherosclerosis. *Circulation research* **2016**, *118*, 692-702.
78. Fakhruddin, S.; Alanazi, W.; Jackson, K.E. Diabetes-induced reactive oxygen species: Mechanism of their generation and role in renal injury. *Journal of diabetes research* **2017**, *2017*, 8379327.
79. Lassegue, B.; Griendling, K.K. Reactive oxygen species in hypertension; an update. *American journal of hypertension* **2004**, *17*, 852-860.
80. Tangvarasittichai, S. Oxidative stress, insulin resistance, dyslipidemia and type 2 diabetes mellitus. *World journal of diabetes* **2015**, *6*, 456-480.
81. Magder, S. Reactive oxygen species: Toxic molecules or spark of life? *Critical care* **2006**, *10*, 208.
82. Raman, M.; Chen, W.; Cobb, M.H. Differential regulation and properties of mapks. *Oncogene* **2007**, *26*, 3100-3112.
83. Taniyama, Y.; Griendling, K.K. Reactive oxygen species in the vasculature: Molecular and cellular mechanisms. *Hypertension* **2003**, *42*, 1075-1081.
84. Griendling, K.K.; Ushio-Fukai, M. Redox control of vascular smooth muscle proliferation. *The Journal of laboratory and clinical medicine* **1998**, *132*, 9-15.
85. Coudray, C.; Roussel, A.M.; Mainard, F.; Arnaud, J.; Favier, A. Lipid peroxidation level and antioxidant micronutrient status in a pre-aging population; correlation with

chronic disease prevalence in a french epidemiological study (nantes, france). *Journal of the American College of Nutrition* **1997**, *16*, 584-591.
86. Ito, Y.; Shimizu, H.; Yoshimura, T.; Ross, R.K.; Kabuto, M.; Takatsuka, N.; Tokui, N.; Suzuki, K.; Shinohara, R. Serum concentrations of carotenoids, alpha-tocopherol, fatty acids, and lipid peroxides among japanese in japan, and japanese and caucasians in the us. *International journal for vitamin and nutrition research. Internationale Zeitschrift fur Vitamin- und Ernahrungsforschung. Journal international de vitaminologie et de nutrition* **1999**, *69*, 385-395.
87. Harman, D. Aging: A theory based on free radical and radiation chemistry. *Journal of gerontology* **1956**, *11*, 298-300.
88. Aseervatham, G.S.; Sivasudha, T.; Jeyadevi, R.; Arul Ananth, D. Environmental factors and unhealthy lifestyle influence oxidative stress in humans--an overview. *Environmental science and pollution research international* **2013**, *20*, 4356-4369.
89. Jensen, P.K. Antimycin-insensitive oxidation of succinate and reduced nicotinamide-adenine dinucleotide in electron-transport particles. I. Ph dependency and hydrogen peroxide formation. *Biochimica et biophysica acta* **1966**, *122*, 157-166.
90. Hanna, M.G.; Nelson, I.P. Genetics and molecular pathogenesis of mitochondrial respiratory chain diseases. *Cellular and molecular life sciences : CMLS* **1999**, *55*, 691-706.
91. Hatefi, Y. The mitochondrial electron transport and oxidative phosphorylation system. *Annual review of biochemistry* **1985**, *54*, 1015-1069.
92. Therade-Matharan, S.; Laemmel, E.; Carpentier, S.; Obata, Y.; Levade, T.; Duranteau, J.; Vicaut, E. Reactive oxygen species production by mitochondria in endothelial cells exposed to reoxygenation after hypoxia and glucose depletion is mediated by ceramide. *American journal of physiology. Regulatory, integrative and comparative physiology* **2005**, *289*, R1756-1762.
93. Murphy, M.P. How mitochondria produce reactive oxygen species. *The Biochemical journal* **2009**, *417*, 1-13.
94. Wispe, J.R.; Clark, J.C.; Burhans, M.S.; Kropp, K.E.; Korfhagen, T.R.; Whitsett, J.A. Synthesis and processing of the precursor for human mangano-superoxide dismutase. *Biochimica et biophysica acta* **1989**, *994*, 30-36.
95. Ohashi, M.; Runge, M.S.; Faraci, F.M.; Heistad, D.D. Mnsod deficiency increases endothelial dysfunction in apoe-deficient mice. *Arteriosclerosis, thrombosis, and vascular biology* **2006**, *26*, 2331-2336.
96. Munoz, M.; Martinez, M.P.; Lopez-Oliva, M.E.; Rodriguez, C.; Corbacho, C.; Carballido, J.; Garcia-Sacristan, A.; Hernandez, M.; Rivera, L.; Saenz-Medina, J.*, et al.* Hydrogen peroxide derived from nadph oxidase 4- and 2 contributes to the endothelium-dependent vasodilatation of intrarenal arteries. *Redox biology* **2018**, *19*, 92-104.
97. Paneni, F.; Cosentino, F. P66 shc as the engine of vascular aging. *Current vascular pharmacology* **2012**, *10*, 697-699.
98. Paneni, F.; Mocharla, P.; Akhmedov, A.; Costantino, S.; Osto, E.; Volpe, M.; Luscher, T.F.; Cosentino, F. Gene silencing of the mitochondrial adaptor p66(shc) suppresses vascular hyperglycemic memory in diabetes. *Circulation research* **2012**, *111*, 278-289.
99. Camici, G.G.; Schiavoni, M.; Francia, P.; Bachschmid, M.; Martin-Padura, I.; Hersberger, M.; Tanner, F.C.; Pelicci, P.; Volpe, M.; Anversa, P.*, et al.* Genetic deletion of p66(shc) adaptor protein prevents hyperglycemia-induced endothelial dysfunction and oxidative stress. *Proceedings of the National Academy of Sciences of the United States of America* **2007**, *104*, 5217-5222.

100. Basta, G.; Lazzerini, G.; Del Turco, S.; Ratto, G.M.; Schmidt, A.M.; De Caterina, R. At least 2 distinct pathways generating reactive oxygen species mediate vascular cell adhesion molecule-1 induction by advanced glycation end products. *Arteriosclerosis, thrombosis, and vascular biology* **2005**, *25*, 1401-1407.
101. Srinivasan, S.; Yeh, M.; Danziger, E.C.; Hatley, M.E.; Riggan, A.E.; Leitinger, N.; Berliner, J.A.; Hedrick, C.C. Glucose regulates monocyte adhesion through endothelial production of interleukin-8. *Circulation research* **2003**, *92*, 371-377.
102. Yu, T.; Robotham, J.L.; Yoon, Y. Increased production of reactive oxygen species in hyperglycemic conditions requires dynamic change of mitochondrial morphology. *Proceedings of the National Academy of Sciences of the United States of America* **2006**, *103*, 2653-2658.
103. Virag, L. Structure and function of poly(adp-ribose) polymerase-1: Role in oxidative stress-related pathologies. *Current vascular pharmacology* **2005**, *3*, 209-214.
104. Ballinger, S.W.; Patterson, C.; Knight-Lozano, C.A.; Burow, D.L.; Conklin, C.A.; Hu, Z.; Reuf, J.; Horaist, C.; Lebovitz, R.; Hunter, G.C.*, et al.* Mitochondrial integrity and function in atherogenesis. *Circulation* **2002**, *106*, 544-549.
105. Manea, S.A.; Constantin, A.; Manda, G.; Sasson, S.; Manea, A. Regulation of nox enzymes expression in vascular pathophysiology: Focusing on transcription factors and epigenetic mechanisms. *Redox biology* **2015**, *5*, 358-366.
106. de Oliveira-Junior, E.B.; Bustamante, J.; Newburger, P.E.; Condino-Neto, A. The human nadph oxidase: Primary and secondary defects impairing the respiratory burst function and the microbicidal ability of phagocytes. *Scandinavian journal of immunology* **2011**, *73*, 420-427.
107. Lambeth, J.D.; Neish, A.S. Nox enzymes and new thinking on reactive oxygen: A double-edged sword revisited. *Annual review of pathology* **2014**, *9*, 119-145.
108. Suh, Y.A.; Arnold, R.S.; Lassegue, B.; Shi, J.; Xu, X.; Sorescu, D.; Chung, A.B.; Griendling, K.K.; Lambeth, J.D. Cell transformation by the superoxide-generating oxidase mox1. *Nature* **1999**, *401*, 79-82.
109. Honjo, T.; Otsui, K.; Shiraki, R.; Kawashima, S.; Sawamura, T.; Yokoyama, M.; Inoue, N. Essential role of noxa1 in generation of reactive oxygen species induced by oxidized low-density lipoprotein in human vascular endothelial cells. *Endothelium : journal of endothelial cell research* **2008**, *15*, 137-141.
110. Shin, H.K.; Kim, Y.K.; Kim, K.Y.; Lee, J.H.; Hong, K.W. Remnant lipoprotein particles induce apoptosis in endothelial cells by nad(p)h oxidase-mediated production of superoxide and cytokines via lectin-like oxidized low-density lipoprotein receptor-1 activation: Prevention by cilostazol. *Circulation* **2004**, *109*, 1022-1028.
111. Zhao, R.; Ma, X.; Xie, X.; Shen, G.X. Involvement of nadph oxidase in oxidized ldl-induced upregulation of heat shock factor-1 and plasminogen activator inhibitor-1 in vascular endothelial cells. *American journal of physiology. Endocrinology and metabolism* **2009**, *297*, E104-111.
112. Rouhanizadeh, M.; Hwang, J.; Clempus, R.E.; Marcu, L.; Lassegue, B.; Sevanian, A.; Hsiai, T.K. Oxidized-1-palmitoyl-2-arachidonoyl-sn-glycero-3-phosphorylcholine induces vascular endothelial superoxide production: Implication of nadph oxidase. *Free radical biology & medicine* **2005**, *39*, 1512-1522.
113. Bismuth, J.; Chai, H.; Lin, P.H.; Yao, Q.; Chen, C. Lactosylceramide causes endothelial dysfunction in porcine coronary arteries and human coronary artery endothelial cells. *Medical science monitor : international medical journal of experimental and clinical research* **2009**, *15*, BR270-274.
114. Murdoch, C.E.; Alom-Ruiz, S.P.; Wang, M.; Zhang, M.; Walker, S.; Yu, B.; Brewer, A.; Shah, A.M. Role of endothelial nox2 nadph oxidase in angiotensin ii-induced

hypertension and vasomotor dysfunction. *Basic research in cardiology* **2011**, *106*, 527-538.
115. Matsuno, K.; Yamada, H.; Iwata, K.; Jin, D.; Katsuyama, M.; Matsuki, M.; Takai, S.; Yamanishi, K.; Miyazaki, M.; Matsubara, H.*, et al.* Nox1 is involved in angiotensin ii-mediated hypertension: A study in nox1-deficient mice. *Circulation* **2005**, *112*, 2677-2685.
116. Youn, J.Y.; Gao, L.; Cai, H. The p47phox- and nadph oxidase organiser 1 (noxo1)-dependent activation of nadph oxidase 1 (nox1) mediates endothelial nitric oxide synthase (enos) uncoupling and endothelial dysfunction in a streptozotocin-induced murine model of diabetes. *Diabetologia* **2012**, *55*, 2069-2079.
117. Schroder, K.; Zhang, M.; Benkhoff, S.; Mieth, A.; Pliquett, R.; Kosowski, J.; Kruse, C.; Luedike, P.; Michaelis, U.R.; Weissmann, N.*, et al.* Nox4 is a protective reactive oxygen species generating vascular nadph oxidase. *Circulation research* **2012**, *110*, 1217-1225.
118. Mayr, M.; Xu, Q. Smooth muscle cell apoptosis in arteriosclerosis. *Experimental gerontology* **2001**, *36*, 969-987.
119. Lee, M.Y.; San Martin, A.; Mehta, P.K.; Dikalova, A.E.; Garrido, A.M.; Datla, S.R.; Lyons, E.; Krause, K.H.; Banfi, B.; Lambeth, J.D.*, et al.* Mechanisms of vascular smooth muscle nadph oxidase 1 (nox1) contribution to injury-induced neointimal formation. *Arteriosclerosis, thrombosis, and vascular biology* **2009**, *29*, 480-487.
120. Deliri, H.; McNamara, C.A. Nox 4 regulation of vascular smooth muscle cell differentiation marker gene expression. *Arteriosclerosis, thrombosis, and vascular biology* **2007**, *27*, 12-14.
121. Przybylska, D.; Janiszewska, D.; Gozdzik, A.; Bielak-Zmijewska, A.; Sunderland, P.; Sikora, E.; Mosieniak, G. Nox4 downregulation leads to senescence of human vascular smooth muscle cells. *Oncotarget* **2016**, *7*, 66429-66443.
122. Montenegro, M.F.; Valdivia, A.; Smolensky, A.; Verma, K.; Taylor, W.R.; San Martin, A. Nox4-dependent activation of cofilin mediates vsmc reorientation in response to cyclic stretching. *Free radical biology & medicine* **2015**, *85*, 288-294.
123. Forstermann, U.; Sessa, W.C. Nitric oxide synthases: Regulation and function. *European heart journal* **2012**, *33*, 829-837, 837a-837d.
124. Chen, W.; Xiao, H.; Rizzo, A.N.; Zhang, W.; Mai, Y.; Ye, M. Endothelial nitric oxide synthase dimerization is regulated by heat shock protein 90 rather than by phosphorylation. *PloS one* **2014**, *9*, e105479.
125. Rafikov, R.; Fonseca, F.V.; Kumar, S.; Pardo, D.; Darragh, C.; Elms, S.; Fulton, D.; Black, S.M. Enos activation and no function: Structural motifs responsible for the posttranslational control of endothelial nitric oxide synthase activity. *The Journal of endocrinology* **2011**, *210*, 271-284.
126. Taddei, S.; Virdis, A.; Ghiadoni, L.; Salvetti, G.; Bernini, G.; Magagna, A.; Salvetti, A. Age-related reduction of no availability and oxidative stress in humans. *Hypertension* **2001**, *38*, 274-279.
127. Matsubara, K.; Higaki, T.; Matsubara, Y.; Nawa, A. Nitric oxide and reactive oxygen species in the pathogenesis of preeclampsia. *International journal of molecular sciences* **2015**, *16*, 4600-4614.
128. Gielis, J.F.; Lin, J.Y.; Wingler, K.; Van Schil, P.E.; Schmidt, H.H.; Moens, A.L. Pathogenetic role of enos uncoupling in cardiopulmonary disorders. *Free radical biology & medicine* **2011**, *50*, 765-776.
129. Harrison, D.G.; Chen, W.; Dikalov, S.; Li, L. Regulation of endothelial cell tetrahydrobiopterin pathophysiological and therapeutic implications. *Advances in pharmacology* **2010**, *60*, 107-132.

130. Maier, W.; Cosentino, F.; Lutolf, R.B.; Fleisch, M.; Seiler, C.; Hess, O.M.; Meier, B.; Luscher, T.F. Tetrahydrobiopterin improves endothelial function in patients with coronary artery disease. *Journal of cardiovascular pharmacology* **2000**, *35*, 173-178.
131. Bitar, M.S.; Wahid, S.; Mustafa, S.; Al-Saleh, E.; Dhaunsi, G.S.; Al-Mulla, F. Nitric oxide dynamics and endothelial dysfunction in type ii model of genetic diabetes. *European journal of pharmacology* **2005**, *511*, 53-64.
132. Heitzer, T.; Krohn, K.; Albers, S.; Meinertz, T. Tetrahydrobiopterin improves endothelium-dependent vasodilation by increasing nitric oxide activity in patients with type ii diabetes mellitus. *Diabetologia* **2000**, *43*, 1435-1438.
133. Suvorava, T.; Nagy, N.; Pick, S.; Lieven, O.; Ruther, U.; Dao, V.T.; Fischer, J.W.; Weber, M.; Kojda, G. Impact of enos-dependent oxidative stress on endothelial function and neointima formation. *Antioxidants & redox signaling* **2015**, *23*, 711-723.
134. Tsihlis, N.D.; Oustwani, C.S.; Vavra, A.K.; Jiang, Q.; Keefer, L.K.; Kibbe, M.R. Nitric oxide inhibits vascular smooth muscle cell proliferation and neointimal hyperplasia by increasing the ubiquitination and degradation of ubch10. *Cell biochemistry and biophysics* **2011**, *60*, 89-97.
135. Kattoor, A.J.; Pothineni, N.V.K.; Palagiri, D.; Mehta, J.L. Oxidative stress in atherosclerosis. *Current atherosclerosis reports* **2017**, *19*, 42.
136. Singh, U.; Jialal, I. Oxidative stress and atherosclerosis. *Pathophysiology : the official journal of the International Society for Pathophysiology* **2006**, *13*, 129-142.
137. Madamanchi, N.R.; Runge, M.S. Mitochondrial dysfunction in atherosclerosis. *Circulation research* **2007**, *100*, 460-473.
138. Chomyn, A.; Attardi, G. Mtdna mutations in aging and apoptosis. *Biochemical and biophysical research communications* **2003**, *304*, 519-529.
139. Leonarduzzi, G.; Chiarpotto, E.; Biasi, F.; Poli, G. 4-hydroxynonenal and cholesterol oxidation products in atherosclerosis. *Molecular nutrition & food research* **2005**, *49*, 1044-1049.
140. Chapple, S.J.; Cheng, X.; Mann, G.E. Effects of 4-hydroxynonenal on vascular endothelial and smooth muscle cell redox signaling and function in health and disease. *Redox biology* **2013**, *1*, 319-331.
141. Niu, X.L.; Madamanchi, N.R.; Vendrov, A.E.; Tchivilev, I.; Rojas, M.; Madamanchi, C.; Brandes, R.P.; Krause, K.H.; Humphries, J.; Smith, A.*, et al.* Nox activator 1: A potential target for modulation of vascular reactive oxygen species in atherosclerotic arteries. *Circulation* **2010**, *121*, 549-559.
142. Gavazzi, G.; Banfi, B.; Deffert, C.; Fiette, L.; Schappi, M.; Herrmann, F.; Krause, K.H. Decreased blood pressure in nox1-deficient mice. *FEBS letters* **2006**, *580*, 497-504.
143. Madamanchi, N.R.; Runge, M.S. Nadph oxidases and atherosclerosis: Unraveling the details. *American journal of physiology. Heart and circulatory physiology* **2010**, *298*, H1-2.
144. Harrison, D.G. Cellular and molecular mechanisms of endothelial cell dysfunction. *The Journal of clinical investigation* **1997**, *100*, 2153-2157.
145. Vanhoutte, P.M.; Boulanger, C.M. Endothelium-dependent responses in hypertension. *Hypertension research : official journal of the Japanese Society of Hypertension* **1995**, *18*, 87-98.
146. Kuhlencordt, P.J.; Gyurko, R.; Han, F.; Scherrer-Crosbie, M.; Aretz, T.H.; Hajjar, R.; Picard, M.H.; Huang, P.L. Accelerated atherosclerosis, aortic aneurysm formation, and ischemic heart disease in apolipoprotein e/endothelial nitric oxide synthase double-knockout mice. *Circulation* **2001**, *104*, 448-454.
147. Sanz, M.J.; Hickey, M.J.; Johnston, B.; McCafferty, D.M.; Raharjo, E.; Huang, P.L.; Kubes, P. Neuronal nitric oxide synthase (nos) regulates leukocyte-endothelial cell

interactions in endothelial nos deficient mice. *British journal of pharmacology* **2001**, *134*, 305-312.
148. Kanazawa, K.; Kawashima, S.; Mikami, S.; Miwa, Y.; Hirata, K.; Suematsu, M.; Hayashi, Y.; Itoh, H.; Yokoyama, M. Endothelial constitutive nitric oxide synthase protein and mrna increased in rabbit atherosclerotic aorta despite impaired endothelium-dependent vascular relaxation. *The American journal of pathology* **1996**, *148*, 1949-1956.
149. d'Uscio, L.V.; Smith, L.A.; Katusic, Z.S. Hypercholesterolemia impairs endothelium-dependent relaxations in common carotid arteries of apolipoprotein e-deficient mice. *Stroke* **2001**, *32*, 2658-2664.
150. Ozaki, M.; Kawashima, S.; Yamashita, T.; Hirase, T.; Namiki, M.; Inoue, N.; Hirata, K.; Yasui, H.; Sakurai, H.; Yoshida, Y.*, et al.* Overexpression of endothelial nitric oxide synthase accelerates atherosclerotic lesion formation in apoe-deficient mice. *The Journal of clinical investigation* **2002**, *110*, 331-340.
151. Thorburn, A. Tumor necrosis factor-related apoptosis-inducing ligand (trail) pathway signaling. *Journal of thoracic oncology : official publication of the International Association for the Study of Lung Cancer* **2007**, *2*, 461-465.
152. Wiley, S.R.; Schooley, K.; Smolak, P.J.; Din, W.S.; Huang, C.P.; Nicholl, J.K.; Sutherland, G.R.; Smith, T.D.; Rauch, C.; Smith, C.A.*, et al.* Identification and characterization of a new member of the tnf family that induces apoptosis. *Immunity* **1995**, *3*, 673-682.
153. Mongkolsapaya, J.; Grimes, J.M.; Chen, N.; Xu, X.N.; Stuart, D.I.; Jones, E.Y.; Screaton, G.R. Structure of the trail-dr5 complex reveals mechanisms conferring specificity in apoptotic initiation. *Nature structural biology* **1999**, *6*, 1048-1053.
154. Perri, P.; Zauli, G.; Gonelli, A.; Milani, D.; Celeghini, C.; Lamberti, G.; Secchiero, P. Tnf-related apoptosis inducing ligand in ocular cancers and ocular diabetic complications. *BioMed research international* **2015**, *2015*, 424019.
155. Vigneswaran, N.; Baucum, D.C.; Wu, J.; Lou, Y.; Bouquot, J.; Muller, S.; Zacharias, W. Repression of tumor necrosis factor-related apoptosis-inducing ligand (trail) but not its receptors during oral cancer progression. *BMC cancer* **2007**, *7*, 108.
156. Cretney, E.; Shanker, A.; Yagita, H.; Smyth, M.J.; Sayers, T.J. Tnf-related apoptosis-inducing ligand as a therapeutic agent in autoimmunity and cancer. *Immunol Cell Biol* **2006**, *84*, 87-98.
157. McGrath, E.E. The tumor necrosis factor-related apoptosis-inducing ligand and lung cancer: Still following the right trail? *Journal of thoracic oncology : official publication of the International Association for the Study of Lung Cancer* **2011**, *6*, 983-987.
158. Secchiero, P.; Gonelli, A.; Carnevale, E.; Milani, D.; Pandolfi, A.; Zella, D.; Zauli, G. Trail promotes the survival and proliferation of primary human vascular endothelial cells by activating the akt and erk pathways. *Circulation* **2003**, *107*, 2250-2256.
159. Gonzalvez, F.; Ashkenazi, A. New insights into apoptosis signaling by apo2l/trail. *Oncogene* **2010**, *29*, 4752-4765.
160. Volpato, S.; Ferrucci, L.; Secchiero, P.; Corallini, F.; Zuliani, G.; Fellin, R.; Guralnik, J.M.; Bandinelli, S.; Zauli, G. Association of tumor necrosis factor-related apoptosis-inducing ligand with total and cardiovascular mortality in older adults. *Atherosclerosis* **2011**, *215*, 452-458.
161. Mori, K.; Ikari, Y.; Jono, S.; Shioi, A.; Ishimura, E.; Emoto, M.; Inaba, M.; Hara, K.; Nishizawa, Y. Association of serum trail level with coronary artery disease. *Thrombosis research* **2010**, *125*, 322-325.

162. Osmancik, P.; Teringova, E.; Tousek, P.; Paulu, P.; Widimsky, P. Prognostic value of tnf-related apoptosis inducing ligand (trail) in acute coronary syndrome patients. *PloS one* **2013**, *8*, e53860.
163. Dessein, P.H.; Lopez-Mejias, R.; Ubilla, B.; Genre, F.; Corrales, A.; Hernandez, J.L.; Ferraz-Amaro, I.; Tsang, L.; Pina, T.; Llorca, J.*, et al.* Tnf-related apoptosis-inducing ligand and cardiovascular disease in rheumatoid arthritis. *Clinical and experimental rheumatology* **2015**, *33*, 491-497.
164. Pott, J.; Burkhardt, R.; Beutner, F.; Horn, K.; Teren, A.; Kirsten, H.; Holdt, L.M.; Schuler, G.; Teupser, D.; Loeffler, M.*, et al.* Genome-wide meta-analysis identifies novel loci of plaque burden in carotid artery. *Atherosclerosis* **2017**, *259*, 32-40.
165. Ashley, D.T.; O'Sullivan, E.P.; Davenport, C.; Devlin, N.; Crowley, R.K.; McCaffrey, N.; Moyna, N.M.; Smith, D.; O'Gorman, D.J. Similar to adiponectin, serum levels of osteoprotegerin are associated with obesity in healthy subjects. *Metabolism: clinical and experimental* **2011**, *60*, 994-1000.
166. O'Sullivan, E.P.; Ashley, D.T.; Davenport, C.; Devlin, N.; Crowley, R.; Agha, A.; Thompson, C.J.; O'Gorman, D.; Smith, D. Osteoprotegerin and biomarkers of vascular inflammation in type 2 diabetes. *Diabetes/metabolism research and reviews* **2010**, *26*, 496-502.
167. Chang, Y.H.; Lin, K.D.; He, S.R.; Hsieh, M.C.; Hsiao, J.Y.; Shin, S.J. Serum osteoprotegerin and tumor necrosis factor related apoptosis inducing-ligand (trail) are elevated in type 2 diabetic patients with albuminuria and serum osteoprotegerin is independently associated with the severity of diabetic nephropathy. *Metabolism: clinical and experimental* **2011**, *60*, 1064-1069.
168. Xiang, G.; Zhang, J.; Ling, Y.; Zhao, L. Circulating level of trail concentration is positively associated with endothelial function and increased by diabetic therapy in the newly diagnosed type 2 diabetic patients. *Clinical endocrinology* **2014**, *80*, 228-234.
169. Hirsova, P.; Gores, G.J. Death receptor-mediated cell death and proinflammatory signaling in nonalcoholic steatohepatitis. *Cellular and molecular gastroenterology and hepatology* **2015**, *1*, 17-27.
170. Cartland, S.P.; Harith, H.H.; Genner, S.W.; Dang, L.; Cogger, V.C.; Vellozzi, M.; Di Bartolo, B.A.; Thomas, S.R.; Adams, L.A.; Kavurma, M.M. Non-alcoholic fatty liver disease, vascular inflammation and insulin resistance are exacerbated by trail deletion in mice. *Scientific reports* **2017**, *7*, 1898.
171. Malyszko, J.; Przybylowski, P.; Malyszko, J.; Koc-Zorawska, E.; Mysliwiec, M. Tumor necrosis factor-related apoptosis-inducing ligand is a marker of kidney function and inflammation in heart and kidney transplant recipients. *Transplantation proceedings* **2011**, *43*, 1877-1880.
172. Di Bartolo, B.A.; Chan, J.; Bennett, M.R.; Cartland, S.; Bao, S.; Tuch, B.E.; Kavurma, M.M. Tnf-related apoptosis-inducing ligand (trail) protects against diabetes and atherosclerosis in apoe (-)/(-) mice. *Diabetologia* **2011**, *54*, 3157-3167.
173. Di Bartolo, B.A.; Cartland, S.P.; Harith, H.H.; Bobryshev, Y.V.; Schoppet, M.; Kavurma, M.M. Trail-deficiency accelerates vascular calcification in atherosclerosis via modulation of rankl. *PloS one* **2013**, *8*, e74211.
174. Cartland, S.P.; Erlich, J.H.; Kavurma, M.M. Trail deficiency contributes to diabetic nephropathy in fat-fed apoe-/- mice. *PloS one* **2014**, *9*, e92952.
175. Schulman, I.H.; Zhou, M.S. Vascular insulin resistance: A potential link between cardiovascular and metabolic diseases. *Current hypertension reports* **2009**, *11*, 48-55.
176. Lamhamedi-Cherradi, S.E.; Zheng, S.; Tisch, R.M.; Chen, Y.H. Critical roles of tumor necrosis factor-related apoptosis-inducing ligand in type 1 diabetes. *Diabetes* **2003**, *52*, 2274-2278.

177. Di Bartolo, B.A.; Cartland, S.P.; Prado-Lourenco, L.; Griffith, T.S.; Gentile, C.; Ravindran, J.; Azahri, N.S.; Thai, T.; Yeung, A.W.; Thomas, S.R.*, et al.* Tumor necrosis factor-related apoptosis-inducing ligand (trail) promotes angiogenesis and ischemia-induced neovascularization via nadph oxidase 4 (nox4) and nitric oxide-dependent mechanisms. *Journal of the American Heart Association* **2015**, *4*.
178. Secchiero, P.; Candido, R.; Corallini, F.; Zacchigna, S.; Toffoli, B.; Rimondi, E.; Fabris, B.; Giacca, M.; Zauli, G. Systemic tumor necrosis factor-related apoptosis-inducing ligand delivery shows antiatherosclerotic activity in apolipoprotein e-null diabetic mice. *Circulation* **2006**, *114*, 1522-1530.
179. Li, J.H.; Kirkiles-Smith, N.C.; McNiff, J.M.; Pober, J.S. Trail induces apoptosis and inflammatory gene expression in human endothelial cells. *Journal of immunology* **2003**, *171*, 1526-1533.
180. Cartland, S.P.; Genner, S.W.; Zahoor, A.; Kavurma, M.M. Comparative evaluation of trail, fgf-2 and vegf-a-induced angiogenesis in vitro and in vivo. *International journal of molecular sciences* **2016**, *17*.
181. Cantarella, G.; Di Benedetto, G.; Ribatti, D.; Saccani-Jotti, G.; Bernardini, R. Involvement of caspase 8 and c-flipl in the proangiogenic effects of the tumour necrosis factor-related apoptosis-inducing ligand (trail). *The FEBS journal* **2014**, *281*, 1505-1513.
182. Zauli, G.; Pandolfi, A.; Gonelli, A.; Di Pietro, R.; Guarnieri, S.; Ciabattoni, G.; Rana, R.; Vitale, M.; Secchiero, P. Tumor necrosis factor-related apoptosis-inducing ligand (trail) sequentially upregulates nitric oxide and prostanoid production in primary human endothelial cells. *Circulation research* **2003**, *92*, 732-740.
183. Rajaram, R.D.; Dissard, R.; Jaquet, V.; de Seigneux, S. Potential benefits and harms of nadph oxidase type 4 in the kidneys and cardiovascular system. *Nephrology, dialysis, transplantation : official publication of the European Dialysis and Transplant Association - European Renal Association* **2019**, *34*, 567-576.
184. Kavurma, M.M.; Schoppet, M.; Bobryshev, Y.V.; Khachigian, L.M.; Bennett, M.R. Trail stimulates proliferation of vascular smooth muscle cells via activation of nf-kappab and induction of insulin-like growth factor-1 receptor. *The Journal of biological chemistry* **2008**, *283*, 7754-7762.
185. Azahri, N.S.; Di Bartolo, B.A.; Khachigian, L.M.; Kavurma, M.M. Sp1, acetylated histone-3 and p300 regulate trail transcription: Mechanisms of pdgf-bb-mediated vsmc proliferation and migration. *Journal of cellular biochemistry* **2012**, *113*, 2597-2606.
186. Ades, E.W.; Candal, F.J.; Swerlick, R.A.; George, V.G.; Summers, S.; Bosse, D.C.; Lawley, T.J. Hmec-1: Establishment of an immortalized human microvascular endothelial cell line. *The Journal of investigative dermatology* **1992**, *99*, 683-690.
187. Robertson, S.; Martinez, G.J.; Payet, C.A.; Barraclough, J.Y.; Celermajer, D.S.; Bursill, C.; Patel, S. Colchicine therapy in acute coronary syndrome patients acts on caspase-1 to suppress nlrp3 inflammasome monocyte activation. *Clinical science* **2016**, *130*, 1237-1246.
188. Radu, M.; Chernoff, J. An in vivo assay to test blood vessel permeability. *Journal of visualized experiments : JoVE* **2013**, e50062.
189. Lattouf, R.; Younes, R.; Lutomski, D.; Naaman, N.; Godeau, G.; Senni, K.; Changotade, S. Picrosirius red staining: A useful tool to appraise collagen networks in normal and pathological tissues. *The journal of histochemistry and cytochemistry : official journal of the Histochemistry Society* **2014**, *62*, 751-758.
190. Manuneedhi Cholan, P.; Cartland, S.P.; Dang, L.; Rayner, B.S.; Patel, S.; Thomas, S.R.; Kavurma, M.M. Trail protects against endothelial dysfunction in vivo and inhibits

angiotensin-ii-induced oxidative stress in vascular endothelial cells in vitro. *Free radical biology & medicine* **2018**, *126*, 341-349.
191. Thomas, S.R.; Witting, P.K.; Drummond, G.R. Redox control of endothelial function and dysfunction: Molecular mechanisms and therapeutic opportunities. *Antioxidants & redox signaling* **2008**, *10*, 1713-1765.
192. Vita, J.A.; Keaney, J.F., Jr. Endothelial function: A barometer for cardiovascular risk? *Circulation* **2002**, *106*, 640-642.
193. Wang, S.; El-Deiry, W.S. Trail and apoptosis induction by tnf-family death receptors. *Oncogene* **2003**, *22*, 8628-8633.
194. Chan, J.; Prado-Lourenco, L.; Khachigian, L.M.; Bennett, M.R.; Di Bartolo, B.A.; Kavurma, M.M. Trail promotes vsmc proliferation and neointima formation in a fgf-2-, sp1 phosphorylation-, and nfkappab-dependent manner. *Circulation research* **2010**, *106*, 1061-1071.
195. Kavurma, M.M.; Schoppet, M.; Bobryshev, Y.V.; Khachigian, L.M.; Bennett, M.R. Trail stimulates proliferation of vascular smooth muscle cells via activation of nf-kappa b and induction of insulin-like growth factor-1 receptor. *J Biol Chem* **2008**, *283*, 7754-7762.
196. Azahri, N.S.; Di Bartolo, B.A.; Khachigian, L.M.; Kavurma, M.M. Sp1, acetylated histone-3 and p300 regulate trail transcription: Mechanisms for pdgf-bb-mediated vsmc proliferation and migration. *J Cell Biochem* **2012**, *13*, 2597-2606.
197. Liabeuf, S.; Barreto, D.V.; Barreto, F.C.; Chasseraud, M.; Brazier, M.; Choukroun, G.; Kamel, S.; Massy, Z.A. The circulating soluble trail is a negative marker for inflammation inversely associated with the mortality risk in chronic kidney disease patients. *Nephrology, dialysis, transplantation : official publication of the European Dialysis and Transplant Association - European Renal Association* **2010**, *25*, 2596-2602.
198. Roberts, L.J.; Morrow, J.D. Measurement of f(2)-isoprostanes as an index of oxidative stress in vivo. *Free radical biology & medicine* **2000**, *28*, 505-513.
199. Rajendran, P.; Rengarajan, T.; Thangavel, J.; Nishigaki, Y.; Sakthisekaran, D.; Sethi, G.; Nishigaki, I. The vascular endothelium and human diseases. *Int J Biol Sci* **2013**, *9*, 1057-1069.
200. Giannotta, M.; Trani, M.; Dejana, E. Ve-cadherin and endothelial adherens junctions: Active guardians of vascular integrity. *Dev Cell* **2013**, *26*, 441-454.
201. Cai, H.; Harrison, D.G. Endothelial dysfunction in cardiovascular diseases: The role of oxidant stress. *Circulation research* **2000**, *87*, 840-844.
202. Cervantes Gracia, K.; Llanas-Cornejo, D.; Husi, H. Cvd and oxidative stress. *Journal of clinical medicine* **2017**, *6*.
203. Dhalla, N.S.; Temsah, R.M.; Netticadan, T. Role of oxidative stress in cardiovascular diseases. *Journal of hypertension* **2000**, *18*, 655-673.
204. Hadi, H.A.; Carr, C.S.; Al Suwaidi, J. Endothelial dysfunction: Cardiovascular risk factors, therapy, and outcome. *Vascular health and risk management* **2005**, *1*, 183-198.
205. Li, H.; Horke, S.; Forstermann, U. Vascular oxidative stress, nitric oxide and atherosclerosis. *Atherosclerosis* **2014**, *237*, 208-219.
206. Davignon, J.; Ganz, P. Role of endothelial dysfunction in atherosclerosis. *Circulation* **2004**, *109*, III27-32.
207. Sukriti, S.; Tauseef, M.; Yazbeck, P.; Mehta, D. Mechanisms regulating endothelial permeability. *Pulmonary circulation* **2014**, *4*, 535-551.
208. Dejana, E.; Orsenigo, F.; Lampugnani, M.G. The role of adherens junctions and ve-cadherin in the control of vascular permeability. *Journal of cell science* **2008**, *121*, 2115-2122.

209. Muller, W.A. Mechanisms of leukocyte transendothelial migration. *Annual review of pathology* **2011**, *6*, 323-344.
210. Hofmann, S.; Grasberger, H.; Jung, P.; Bidlingmaier, M.; Vlotides, J.; Janssen, O.E.; Landgraf, R. The tumour necrosis factor-alpha induced vascular permeability is associated with a reduction of ve-cadherin expression. *Eur J Med Res* **2002**, *7*, 171-176.
211. Yang, J.; Jones, S.P.; Suhara, T.; Greer, J.J.; Ware, P.D.; Nguyen, N.P.; Perlman, H.; Nelson, D.P.; Lefer, D.J.; Walsh, K. Endothelial cell overexpression of fas ligand attenuates ischemia-reperfusion injury in the heart. *J Biol Chem* **2003**, *278*, 15185-15191.
212. Betteridge, D.J. What is oxidative stress? *Metabolism: clinical and experimental* **2000**, *49*, 3-8.
213. Panth, N.; Paudel, K.R.; Parajuli, K. Reactive oxygen species: A key hallmark of cardiovascular disease. *Advances in medicine* **2016**, *2016*, 9152732.
214. He, F.; Zuo, L. Redox roles of reactive oxygen species in cardiovascular diseases. *International journal of molecular sciences* **2015**, *16*, 27770-27780.
215. Hitomi, H.; Kiyomoto, H.; Nishiyama, A. Angiotensin ii and oxidative stress. *Current opinion in cardiology* **2007**, *22*, 311-315.
216. Wen, H.; Gwathmey, J.K.; Xie, L.H. Oxidative stress-mediated effects of angiotensin ii in the cardiovascular system. *World journal of hypertension* **2012**, *2*, 34-44.
217. Nakashima, H.; Suzuki, H.; Ohtsu, H.; Chao, J.Y.; Utsunomiya, H.; Frank, G.D.; Eguchi, S. Angiotensin ii regulates vascular and endothelial dysfunction: Recent topics of angiotensin ii type-1 receptor signaling in the vasculature. *Current vascular pharmacology* **2006**, *4*, 67-78.
218. Gomolak, J.R.; Didion, S.P. Angiotensin ii-induced endothelial dysfunction is temporally linked with increases in interleukin-6 and vascular macrophage accumulation. *Frontiers in physiology* **2014**, *5*, 396.
219. Starkov, A.A. The role of mitochondria in reactive oxygen species metabolism and signaling. *Annals of the New York Academy of Sciences* **2008**, *1147*, 37-52.
220. Schulz, A.; Jankowski, J.; Zidek, W.; Jankowski, V. Absolute quantification of endogenous angiotensin ii levels in human plasma using esi-lc-ms/ms. *Clinical proteomics* **2014**, *11*, 37.
221. Touyz, R.M. Reactive oxygen species and angiotensin ii signaling in vascular cells -- implications in cardiovascular disease. *Brazilian journal of medical and biological research = Revista brasileira de pesquisas medicas e biologicas* **2004**, *37*, 1263-1273.
222. Dikalov, S.I.; Nazarewicz, R.R. Angiotensin ii-induced production of mitochondrial reactive oxygen species: Potential mechanisms and relevance for cardiovascular disease. *Antioxidants & redox signaling* **2013**, *19*, 1085-1094.
223. Nisimoto, Y.; Diebold, B.A.; Cosentino-Gomes, D.; Lambeth, J.D. Nox4: A hydrogen peroxide-generating oxygen sensor. *Biochemistry* **2014**, *53*, 5111-5120.
224. Lee, D.Y.; Wauquier, F.; Eid, A.A.; Roman, L.J.; Ghosh-Choudhury, G.; Khazim, K.; Block, K.; Gorin, Y. Nox4 nadph oxidase mediates peroxynitrite-dependent uncoupling of endothelial nitric-oxide synthase and fibronectin expression in response to angiotensin ii: Role of mitochondrial reactive oxygen species. *The Journal of biological chemistry* **2013**, *288*, 28668-28686.
225. Montezano, A.C.; Touyz, R.M. Reactive oxygen species and endothelial function--role of nitric oxide synthase uncoupling and nox family nicotinamide adenine dinucleotide phosphate oxidases. *Basic & clinical pharmacology & toxicology* **2012**, *110*, 87-94.
226. Crowley, S.D.; Gurley, S.B.; Herrera, M.J.; Ruiz, P.; Griffiths, R.; Kumar, A.P.; Kim, H.S.; Smithies, O.; Le, T.H.; Coffman, T.M. Angiotensin ii causes hypertension and

cardiac hypertrophy through its receptors in the kidney. *Proceedings of the National Academy of Sciences of the United States of America* **2006**, *103*, 17985-17990.
227. Welch, W.J. Angiotensin ii-dependent superoxide: Effects on hypertension and vascular dysfunction. *Hypertension* **2008**, *52*, 51-56.
228. Li, X.; Han, W.Q.; Boini, K.M.; Xia, M.; Zhang, Y.; Li, P.L. Trail death receptor 4 signaling via lysosome fusion and membrane raft clustering in coronary arterial endothelial cells: Evidence from asm knockout mice. *Journal of molecular medicine* **2013**, *91*, 25-36.
229. Gorin, Y.; Ricono, J.M.; Kim, N.H.; Bhandari, B.; Choudhury, G.G.; Abboud, H.E. Nox4 mediates angiotensin ii-induced activation of akt/protein kinase b in mesangial cells. *American journal of physiology. Renal physiology* **2003**, *285*, F219-229.
230. Kim, S.M.; Kim, Y.G.; Jeong, K.H.; Lee, S.H.; Lee, T.W.; Ihm, C.G.; Moon, J.Y. Angiotensin ii-induced mitochondrial nox4 is a major endogenous source of oxidative stress in kidney tubular cells. *PloS one* **2012**, *7*, e39739.
231. Sfriso, R.; Bongoni, A.; Banz, Y.; Klymiuk, N.; Wolf, E.; Rieben, R. Assessment of the anticoagulant and anti-inflammatory properties of endothelial cells using 3d cell culture and non-anticoagulated whole blood. *Journal of visualized experiments : JoVE* **2017**.
232. Kim, C.W.; Song, H.; Kumar, S.; Nam, D.; Kwon, H.S.; Chang, K.H.; Son, D.J.; Kang, D.W.; Brodie, S.A.; Weiss, D.*, et al.* Anti-inflammatory and antiatherogenic role of bmp receptor ii in endothelial cells. *Arteriosclerosis, thrombosis, and vascular biology* **2013**, *33*, 1350-1359.
233. Tousoulis, D.; Kampoli, A.M.; Tentolouris, C.; Papageorgiou, N.; Stefanadis, C. The role of nitric oxide on endothelial function. *Current vascular pharmacology* **2012**, *10*, 4-18.
234. Silva, B.R.; Pernomian, L.; Bendhack, L.M. Contribution of oxidative stress to endothelial dysfunction in hypertension. *Frontiers in physiology* **2012**, *3*, 441.
235. Schulz, E.; Jansen, T.; Wenzel, P.; Daiber, A.; Munzel, T. Nitric oxide, tetrahydrobiopterin, oxidative stress, and endothelial dysfunction in hypertension. *Antioxidants & redox signaling* **2008**, *10*, 1115-1126.
236. Friedman, D.I.; Jankovic, J.; McCrary, J.A., 3rd. Neuro-ophthalmic findings in progressive supranuclear palsy. *Journal of clinical neuro-ophthalmology* **1992**, *12*, 104-109.
237. Sakai, K.; Hirooka, Y.; Matsuo, I.; Eshima, K.; Shigematsu, H.; Shimokawa, H.; Takeshita, A. Overexpression of enos in nts causes hypotension and bradycardia in vivo. *Hypertension* **2000**, *36*, 1023-1028.
238. Cox, R.A.; Garcia-Palmieri, M.R. Cholesterol, triglycerides, and associated lipoproteins. In *Clinical methods: The history, physical, and laboratory examinations*, rd; Walker, H.K.; Hall, W.D.; Hurst, J.W., Eds. Boston, 1990.
239. Kanter, M.M.; Kris-Etherton, P.M.; Fernandez, M.L.; Vickers, K.C.; Katz, D.L. Exploring the factors that affect blood cholesterol and heart disease risk: Is dietary cholesterol as bad for you as history leads us to believe? *Advances in nutrition* **2012**, *3*, 711-717.
240. Kalaivanisailaja, J.; Manju, V.; Nalini, N. Lipid profile in mice fed a high-fat diet after exogenous leptin administration. *Polish journal of pharmacology* **2003**, *55*, 763-769.
241. Podrini, C.; Cambridge, E.L.; Lelliott, C.J.; Carragher, D.M.; Estabel, J.; Gerdin, A.K.; Karp, N.A.; Scudamore, C.L.; Sanger Mouse Genetics, P.; Ramirez-Solis, R.*, et al.* High-fat feeding rapidly induces obesity and lipid derangements in c57bl/6n mice. *Mammalian genome : official journal of the International Mammalian Genome Society* **2013**, *24*, 240-251.

242. Lin, D.S.; Connor, W.E. The long term effects of dietary cholesterol upon the plasma lipids, lipoproteins, cholesterol absorption, and the sterol balance in man: The demonstration of feedback inhibition of cholesterol biosynthesis and increased bile acid excretion. *Journal of lipid research* **1980**, *21*, 1042-1052.
243. Chung, S.; Cuffe, H.; Marshall, S.M.; McDaniel, A.L.; Ha, J.H.; Kavanagh, K.; Hong, C.; Tontonoz, P.; Temel, R.E.; Parks, J.S. Dietary cholesterol promotes adipocyte hypertrophy and adipose tissue inflammation in visceral, but not in subcutaneous, fat in monkeys. *Arteriosclerosis, thrombosis, and vascular biology* **2014**, *34*, 1880-1887.
244. Hill, S.A.; McQueen, M.J. Reverse cholesterol transport--a review of the process and its clinical implications. *Clinical biochemistry* **1997**, *30*, 517-525.
245. Westerterp, M.; Murphy, A.J.; Wang, M.; Pagler, T.A.; Vengrenyuk, Y.; Kappus, M.S.; Gorman, D.J.; Nagareddy, P.R.; Zhu, X.; Abramowicz, S.*, et al.* Deficiency of atp-binding cassette transporters a1 and g1 in macrophages increases inflammation and accelerates atherosclerosis in mice. *Circulation research* **2013**, *112*, 1456-1465.
246. Soumian, S.; Albrecht, C.; Davies, A.H.; Gibbs, R.G. Abca1 and atherosclerosis. *Vascular medicine* **2005**, *10*, 109-119.
247. Nahmias, Y.; Casali, M.; Barbe, L.; Berthiaume, F.; Yarmush, M.L. Liver endothelial cells promote ldl-r expression and the uptake of hcv-like particles in primary rat and human hepatocytes. *Hepatology* **2006**, *43*, 257-265.
248. Teratani, T.; Tomita, K.; Suzuki, T.; Furuhashi, H.; Irie, R.; Hida, S.; Okada, Y.; Kurihara, C.; Ebinuma, H.; Nakamoto, N.*, et al.* Free cholesterol accumulation in liver sinusoidal endothelial cells exacerbates acetaminophen hepatotoxicity via tlr9 signaling. *Journal of hepatology* **2017**, *67*, 780-790.
249. Fraser, R.; Dobbs, B.R.; Rogers, G.W. Lipoproteins and the liver sieve: The role of the fenestrated sinusoidal endothelium in lipoprotein metabolism, atherosclerosis, and cirrhosis. *Hepatology* **1995**, *21*, 863-874.
250. Magalhaes, A.; Matias, I.; Palmela, I.; Brito, M.A.; Dias, S. Ldl-cholesterol increases the transcytosis of molecules through endothelial monolayers. *PloS one* **2016**, *11*, e0163988.
251. Kareinen, I.; Cedo, L.; Silvennoinen, R.; Laurila, P.P.; Jauhiainen, M.; Julve, J.; Blanco-Vaca, F.; Escola-Gil, J.C.; Kovanen, P.T.; Lee-Rueckert, M. Enhanced vascular permeability facilitates entry of plasma hdl and promotes macrophage-reverse cholesterol transport from skin in mice. *Journal of lipid research* **2015**, *56*, 241-253.
252. Gamboa, A.; Shibao, C.; Diedrich, A.; Paranjape, S.Y.; Farley, G.; Christman, B.; Raj, S.R.; Robertson, D.; Biaggioni, I. Excessive nitric oxide function and blood pressure regulation in patients with autonomic failure. *Hypertension* **2008**, *51*, 1531-1536.
253. Zhen, J.; Lu, H.; Wang, X.Q.; Vaziri, N.D.; Zhou, X.J. Upregulation of endothelial and inducible nitric oxide synthase expression by reactive oxygen species. *American journal of hypertension* **2008**, *21*, 28-34.
254. Heiss, E.H.; Dirsch, V.M. Regulation of enos enzyme activity by posttranslational modification. *Current pharmaceutical design* **2014**, *20*, 3503-3513.
255. Kishi, T.; Hirooka, Y.; Sakai, K.; Shigematsu, H.; Shimokawa, H.; Takeshita, A. Overexpression of enos in the rvlm causes hypotension and bradycardia via gaba release. *Hypertension* **2001**, *38*, 896-901.
256. Piali, L.; Fichtel, A.; Terpe, H.J.; Imhof, B.A.; Gisler, R.H. Endothelial vascular cell adhesion molecule 1 expression is suppressed by melanoma and carcinoma. *The Journal of experimental medicine* **1995**, *181*, 811-816.
257. Griffioen, A.W.; Tromp, S.C.; Hillen, H.F. Angiogenesis modulates the tumour immune response. *International journal of experimental pathology* **1998**, *79*, 363-368.

258. Gomez, D.; Baylis, R.A.; Durgin, B.G.; Newman, A.A.C.; Alencar, G.F.; Mahan, S.; St Hilaire, C.; Muller, W.; Waisman, A.; Francis, S.E., *et al.* Interleukin-1beta has atheroprotective effects in advanced atherosclerotic lesions of mice. *Nature medicine* **2018**, *24*, 1418-1429.
259. Yang, Y.; Bin, W.; Aksoy, M.O.; Kelsen, S.G. Regulation of interleukin-1beta and interleukin-1beta inhibitor release by human airway epithelial cells. *The European respiratory journal* **2004**, *24*, 360-366.
260. Wang, X.; Feuerstein, G.Z.; Gu, J.L.; Lysko, P.G.; Yue, T.L. Interleukin-1 beta induces expression of adhesion molecules in human vascular smooth muscle cells and enhances adhesion of leukocytes to smooth muscle cells. *Atherosclerosis* **1995**, *115*, 89-98.
261. Cartland, S.P.; Genner, S.W.; Martinez, G.J.; Robertson, S.; Kockx, M.; Lin, R.C.; O'Sullivan, J.F.; Koay, Y.C.; Manuneedhi Cholan, P.; Kebede, M.A., *et al.* Trail-expressing monocyte/macrophages are critical for reducing inflammation and atherosclerosis. *iScience* **2019**, *12*, 41-52.
262. Iyemere, V.P.; Proudfoot, D.; Weissberg, P.L.; Shanahan, C.M. Vascular smooth muscle cell phenotypic plasticity and the regulation of vascular calcification. *Journal of internal medicine* **2006**, *260*, 192-210.
263. Brozovich, F.V.; Nicholson, C.J.; Degen, C.V.; Gao, Y.Z.; Aggarwal, M.; Morgan, K.G. Mechanisms of vascular smooth muscle contraction and the basis for pharmacologic treatment of smooth muscle disorders. *Pharmacological reviews* **2016**, *68*, 476-532.
264. Sweet, D.R.; Fan, L.; Hsieh, P.N.; Jain, M.K. Kruppel-like factors in vascular inflammation: Mechanistic insights and therapeutic potential. *Frontiers in cardiovascular medicine* **2018**, *5*, 6.
265. Li, M.; Qian, M.; Kyler, K.; Xu, J. Endothelial-vascular smooth muscle cells interactions in atherosclerosis. *Frontiers in cardiovascular medicine* **2018**, *5*, 151.
266. Ghosal, S.; Nunley, A.; Mahbod, P.; Lewis, A.G.; Smith, E.P.; Tong, J.; D'Alessio, D.A.; Herman, J.P. Mouse handling limits the impact of stress on metabolic endpoints. *Physiology & behavior* **2015**, *150*, 31-37.
267. Zhang, Y.N.; Xie, B.D.; Sun, L.; Chen, W.; Jiang, S.L.; Liu, W.; Bian, F.; Tian, H.; Li, R.K. Phenotypic switching of vascular smooth muscle cells in the 'normal region' of aorta from atherosclerosis patients is regulated by mir-145. *Journal of cellular and molecular medicine* **2016**, *20*, 1049-1061.
268. Allahverdian, S.; Chaabane, C.; Boukais, K.; Francis, G.A.; Bochaton-Piallat, M.L. Smooth muscle cell fate and plasticity in atherosclerosis. *Cardiovascular research* **2018**, *114*, 540-550.
269. Liu, Y.; Sinha, S.; McDonald, O.G.; Shang, Y.; Hoofnagle, M.H.; Owens, G.K. Kruppel-like factor 4 abrogates myocardin-induced activation of smooth muscle gene expression. *The Journal of biological chemistry* **2005**, *280*, 9719-9727.
270. Wassmann, S.; Wassmann, K.; Jung, A.; Velten, M.; Knuefermann, P.; Petoumenos, V.; Becher, U.; Werner, C.; Mueller, C.; Nickenig, G. Induction of p53 by gklf is essential for inhibition of proliferation of vascular smooth muscle cells. *Journal of molecular and cellular cardiology* **2007**, *43*, 301-307.
271. Wang, C.; Han, M.; Zhao, X.M.; Wen, J.K. Kruppel-like factor 4 is required for the expression of vascular smooth muscle cell differentiation marker genes induced by all-trans retinoic acid. *Journal of biochemistry* **2008**, *144*, 313-321.
272. Zheng, B.; Han, M.; Wen, J.K. Role of kruppel-like factor 4 in phenotypic switching and proliferation of vascular smooth muscle cells. *IUBMB life* **2010**, *62*, 132-139.

273. Feinberg, M.W.; Cao, Z.; Wara, A.K.; Lebedeva, M.A.; Senbanerjee, S.; Jain, M.K. Kruppel-like factor 4 is a mediator of proinflammatory signaling in macrophages. *The Journal of biological chemistry* **2005**, *280*, 38247-38258.
274. Hamik, A.; Lin, Z.; Kumar, A.; Balcells, M.; Sinha, S.; Katz, J.; Feinberg, M.W.; Gerzsten, R.E.; Edelman, E.R.; Jain, M.K. Kruppel-like factor 4 regulates endothelial inflammation. *The Journal of biological chemistry* **2007**, *282*, 13769-13779.
275. Courboulin, A.; Tremblay, V.L.; Barrier, M.; Meloche, J.; Jacob, M.H.; Chapolard, M.; Bisserier, M.; Paulin, R.; Lambert, C.; Provencher, S.*, et al.* Kruppel-like factor 5 contributes to pulmonary artery smooth muscle proliferation and resistance to apoptosis in human pulmonary arterial hypertension. *Respiratory research* **2011**, *12*, 128.
276. Jia, L.; Zhou, Z.; Liang, H.; Wu, J.; Shi, P.; Li, F.; Wang, Z.; Wang, C.; Chen, W.; Zhang, H.*, et al.* Klf5 promotes breast cancer proliferation, migration and invasion in part by upregulating the transcription of tnfaip2. *Oncogene* **2016**, *35*, 2040-2051.
277. Xie, N.; Chen, M.; Dai, R.; Zhang, Y.; Zhao, H.; Song, Z.; Zhang, L.; Li, Z.; Feng, Y.; Gao, H.*, et al.* Srsf1 promotes vascular smooth muscle cell proliferation through a delta133p53/egr1/klf5 pathway. *Nature communications* **2017**, *8*, 16016.
278. Pataky, M.W.; Wang, H.; Yu, C.S.; Arias, E.B.; Ploutz-Snyder, R.J.; Zheng, X.; Cartee, G.D. High-fat diet-induced insulin resistance in single skeletal muscle fibers is fiber type selective. *Scientific reports* **2017**, *7*, 13642.
279. Soares, A.G.; de Carvalho, M.H.C.; Akamine, E. Obesity induces artery-specific alterations: Evaluation of vascular function and inflammatory and smooth muscle phenotypic markers. *BioMed research international* **2017**, *2017*, 5038602.
280. Hall, A.P.; Elcombe, C.R.; Foster, J.R.; Harada, T.; Kaufmann, W.; Knippel, A.; Kuttler, K.; Malarkey, D.E.; Maronpot, R.R.; Nishikawa, A.*, et al.* Liver hypertrophy: A review of adaptive (adverse and non-adverse) changes--conclusions from the 3rd international estp expert workshop. *Toxicologic pathology* **2012**, *40*, 971-994.
281. Kleemann, R.; Verschuren, L.; van Erk, M.J.; Nikolsky, Y.; Cnubben, N.H.; Verheij, E.R.; Smilde, A.K.; Hendriks, H.F.; Zadelaar, S.; Smith, G.J.*, et al.* Atherosclerosis and liver inflammation induced by increased dietary cholesterol intake: A combined transcriptomics and metabolomics analysis. *Genome biology* **2007**, *8*, R200.
282. Lusis, A.J. Atherosclerosis. *Nature* **2000**, *407*, 233-241.
283. Urso, C.; Caimi, G. [oxidative stress and endothelial dysfunction]. *Minerva medica* **2011**, *102*, 59-77.
284. Holoch, P.A.; Griffith, T.S. Tnf-related apoptosis-inducing ligand (trail): A new path to anti-cancer therapies. *European journal of pharmacology* **2009**, *625*, 63-72.
285. Higashi, Y.; Maruhashi, T.; Noma, K.; Kihara, Y. Oxidative stress and endothelial dysfunction: Clinical evidence and therapeutic implications. *Trends in cardiovascular medicine* **2014**, *24*, 165-169.
286. Higashi, Y.; Noma, K.; Yoshizumi, M.; Kihara, Y. Endothelial function and oxidative stress in cardiovascular diseases. *Circulation journal : official journal of the Japanese Circulation Society* **2009**, *73*, 411-418.
287. Yoshimoto, T.; Gochou, N.; Fukai, N.; Sugiyama, T.; Shichiri, M.; Hirata, Y. Adrenomedullin inhibits angiotensin ii-induced oxidative stress and gene expression in rat endothelial cells. *Hypertension research : official journal of the Japanese Society of Hypertension* **2005**, *28*, 165-172.
288. Liu, M.; Xiang, G.; Lu, J.; Xiang, L.; Dong, J.; Mei, W. Trail protects against endothelium injury in diabetes via akt-enos signaling. *Atherosclerosis* **2014**, *237*, 718-724.
289. Bernardi, S.; Zauli, G.; Tikellis, C.; Candido, R.; Fabris, B.; Secchiero, P.; Cooper, M.E.; Thomas, M.C. Tnf-related apoptosis-inducing ligand significantly attenuates

metabolic abnormalities in high-fat-fed mice reducing adiposity and systemic inflammation. *Clinical science* **2012**, *123*, 547-555.
290. Mestas, J.; Ley, K. Monocyte-endothelial cell interactions in the development of atherosclerosis. *Trends in cardiovascular medicine* **2008**, *18*, 228-232.
291. Gerhardt, T.; Ley, K. Monocyte trafficking across the vessel wall. *Cardiovascular research* **2015**, *107*, 321-330.
292. Landmesser, U.; Hornig, B.; Drexler, H. Endothelial dysfunction in hypercholesterolemia: Mechanisms, pathophysiological importance, and therapeutic interventions. *Seminars in thrombosis and hemostasis* **2000**, *26*, 529-537.
293. Hassan, H.H.; Denis, M.; Krimbou, L.; Marcil, M.; Genest, J. Cellular cholesterol homeostasis in vascular endothelial cells. *The Canadian journal of cardiology* **2006**, *22 Suppl B*, 35B-40B.
294. Briot, A.; Civelek, M.; Seki, A.; Hoi, K.; Mack, J.J.; Lee, S.D.; Kim, J.; Hong, C.; Yu, J.; Fishbein, G.A*., et al.* Endothelial notch1 is suppressed by circulating lipids and antagonizes inflammation during atherosclerosis. *The Journal of experimental medicine* **2015**, *212*, 2147-2163.
295. Mao, H.; Lockyer, P.; Li, L.; Ballantyne, C.M.; Patterson, C.; Xie, L.; Pi, X. Endothelial lrp1 regulates metabolic responses by acting as a co-activator of ppargamma. *Nature communications* **2017**, *8*, 14960.
296. Boddaert, J.; Tamim, H.; Verny, M.; Belmin, J. Arterial stiffness is associated with orthostatic hypotension in elderly subjects with history of falls. *Journal of the American Geriatrics Society* **2004**, *52*, 568-572.
297. Franceschini, N.; Rose, K.M.; Astor, B.C.; Couper, D.; Vupputuri, S. Orthostatic hypotension and incident chronic kidney disease: The atherosclerosis risk in communities study. *Hypertension* **2010**, *56*, 1054-1059.
298. Lehman, L.W.; Saeed, M.; Moody, G.; Mark, R. Hypotension as a risk factor for acute kidney injury in icu patients. *Computing in cardiology* **2010**, *37*, 1095-1098.
299. Low, P.A.; Tomalia, V.A. Orthostatic hypotension: Mechanisms, causes, management. *Journal of clinical neurology* **2015**, *11*, 220-226.
300. Schuetz, P.; Jones, A.E.; Aird, W.C.; Shapiro, N.I. Endothelial cell activation in emergency department patients with sepsis-related and non-sepsis-related hypotension. *Shock* **2011**, *36*, 104-108.
301. Sabrane, K.; Kruse, M.N.; Fabritz, L.; Zetsche, B.; Mitko, D.; Skryabin, B.V.; Zwiener, M.; Baba, H.A.; Yanagisawa, M.; Kuhn, M. Vascular endothelium is critically involved in the hypotensive and hypovolemic actions of atrial natriuretic peptide. *The Journal of clinical investigation* **2005**, *115*, 1666-1674.
302. Shah, S.R.; Abbasi, Z.; Fatima, M.; Ochani, R.K.; Shahnawaz, W.; Asim Khan, M.; Shah, S.A. Canakinumab and cardiovascular outcomes: Results of the cantos trial. *Journal of community hospital internal medicine perspectives* **2018**, *8*, 21-22.
303. Fantuzzi, G.; Dinarello, C.A. The inflammatory response in interleukin-1 beta-deficient mice: Comparison with other cytokine-related knock-out mice. *Journal of leukocyte biology* **1996**, *59*, 489-493.
304. Steucke, K.E.; Tracy, P.V.; Hald, E.S.; Hall, J.L.; Alford, P.W. Vascular smooth muscle cell functional contractility depends on extracellular mechanical properties. *Journal of biomechanics* **2015**, *48*, 3044-3051.
305. Suzuki, T.; Sawaki, D.; Aizawa, K.; Munemasa, Y.; Matsumura, T.; Ishida, J.; Nagai, R. Kruppel-like factor 5 shows proliferation-specific roles in vascular remodeling, direct stimulation of cell growth, and inhibition of apoptosis. *The Journal of biological chemistry* **2009**, *284*, 9549-9557.

306. Chalupsky, K.; Cai, H. Endothelial dihydrofolate reductase: Critical for nitric oxide bioavailability and role in angiotensin ii uncoupling of endothelial nitric oxide synthase. *Proceedings of the National Academy of Sciences of the United States of America* **2005**, *102*, 9056-9061.
307. Dikalov, S.I.; Nazarewicz, R.R.; Bikineyeva, A.; Hilenski, L.; Lassegue, B.; Griendling, K.K.; Harrison, D.G.; Dikalova, A.E. Nox2-induced production of mitochondrial superoxide in angiotensin ii-mediated endothelial oxidative stress and hypertension. *Antioxidants & redox signaling* **2014**, *20*, 281-294.
308. Doughan, A.K.; Harrison, D.G.; Dikalov, S.I. Molecular mechanisms of angiotensin ii-mediated mitochondrial dysfunction: Linking mitochondrial oxidative damage and vascular endothelial dysfunction. *Circulation research* **2008**, *102*, 488-496.